# THE CHEMISTRY OF THE CARBON-IN-PULP PROCESS

Michael David Adams

A Thesis submitted to the Faculty of Science
University of the Witwatersrand, Johannesburg
in fulfilment of the requirements for the
degree of Doctor of Philosophy

Johannesburg 1989

## ABSTRACT

Several conflicting theories of the adsorption of aurocyanide onto activated carbon presently exist. To resolve the mechanism, adsorption and elution of aurocyanide are examined by several techniques, including Mössbauer spectroscopy, X-ray photoelectron spectroscopy, X-ray diffractometry, Fourier Transform Infrared spectrophotometry, ultraviolet-visible spectrophotometry and scanning electron microscopy.

The evidence gathered indicates that, under normal plant conditions, aurocyanide is extracted onto activated carbon in the form of an ion pair $M^{n+}[Au(CN)_2^-]_n$, and eluted by hydroxide or cyanide. The hydroxide or cyanide ions react with the carbon surface, rendering it relatively hydrophilic with a decreased affinity for neutral species. Additional adsorption mechanisms are shown to operate under other conditions of ionic strength, pH, and temperature. The poor agreement in the literature regarding the mechanism of adsorption of aurocyanide onto activated carbon is shown to be due to the fact that different mechanisms operate under different experimental conditions. The AuCN produced on the carbon surface by acid treatment is shown to react with hydroxide ion via the reduction of AuCN to metallic gold with formation of $Au(CN)_2^-$, and the oxidation of cyanide to cyanate. Other species, such as $Au(CN)_4^-$ and $Ag(CN)_2^-$ adsorb onto activated carbon by a similar mechanism to that postulated for $Au(CN)_2^-$.

Ion association of $MAu(CN)_2$ salts in aqueous solution is demonstrated by means of potentiometric titration and conductivity measurements, and various associated species of $MAu(CN)_2$ salts are shown to occur in organic

solvents by means of infrared spectrophotometric and distribution measurements.

A kinetic model was developed for elution of aurocyanide from activated carbon and was found to predict gold elution performance successfully using the Zadra procedure.

The influence of the surface chemistry and structure of activated carbon on adsorption of aurocyanide was investigated by characterization of activated carbons that were synthesized or oxidized under various conditions. Synthetic polymeric adsorbents with characteristics similar to activated carbons were also studied. The evidence suggests that a large micropore volume is important in providing suitable active sites for adsorption. Another important factor is the presence of basic functional groups within the micropore, which act as solvating agents for the ion pair.

The aim is to provide a self-consistent adsorption mechanism that accounts for all observations presented in the literature. Interpretation of results in terms of preconceived ideas, and neglect of observations of other authors has greatly contributed to current disagreement in the literature.

**Declaration**

I declare that this Thesis is my own, unaided work. It is being submitted for the degree of Doctor of Philosophy. It has not been submitted before for any degree or examination in any other University.

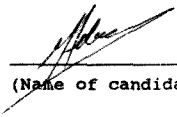

(Name of candidate)

23rd day of October, 1989

**Acknowledgements**

I wish to express my sincere gratitude and appreciation to

my supervisors, Prof R.D. Hancock and Prof R.G. Copperthwaite for their enthusiasm and help;

my wife, Jenni, for her support;

my colleagues, Dr C.A. Fleming, Dr R.L. Paul, Dr M.J. Nicol, Dr B.R. Green, Dr P.J. Harris amongst others, for the many hours of useful discussions;

Prof Dr F.E. Wagner of the Physik-Department, Technische Universität München, for running the Mössbauer spectra and for engaging in a useful collaboration regarding this technique;

Mr P. Ellis and Mrs I. Klingbiel, for their patience with running the Scanning Electron Microscope;

Mr D.E. Innes, for running the X-ray Photoelectron spectra;

Mr P.W. Wade, for his time and help with the Molecular Mechanics calculations;

Mrs M. Arinto, Mrs M.R. Hazell and Ms T. McArthur, for their assistance in the typing of this manuscript;

the Council for Mineral Technology (Mintek), for allowing me to undertake this research during my period of employment with them;

my parents, for their encouragement through the years.

Contents

## List of Symbols

| | |
|---|---|
| $A$ | Onsager constant |
| $a$ | interionic distance |
| $\underline{a}$ | ionic radius in modified Born equation |
| $\alpha$ | degree of dissociation |
| BV | bed-volume of eluant solution |
| $\beta$ | XRD peak width at $\frac{1}{2}$ maximum intensity |
| $\beta_2$ | stability constant of two-coordinate complex |
| C | concentration of gold on the carbon at time t |
| $C_0$ | initial concentration of gold on the carbon |
| c | concentration of gold in the aqueous phase |
| $c_{hv}$ | velocity of light |
| $c_s$ | concentration of gold in the solvent phase |
| D | distribution ratio |
| $D_p$ | pore diameter of adsorbent |
| DN | solvent donor number |
| $\Delta H^o_{hyd}$ | hydration enthalpy |
| $\Delta H^o_s$ | solvation enthalpy |
| $\Delta H^o_e$ | electrostatic contribution to the solvation enthalpy |
| $\Delta H^o_n$ | neutral contribution to the solvation enthalpy |
| $\delta$ | solubility parameter |
| E | single-pass electrowinning efficiency |
| $E_a$ | activation energy |
| $E_b$ | binding energy of electron |
| $E_i$ | energy of incident Mössbauer radiation |
| $E_p$ | kinetic energy of photoelectron |
| $E_{wf}$ | work function |
| $E_\gamma$ | energy of $\gamma$-radiation from stationary Mössbauer source |
| $e_0$ | electronic charge |
| $\epsilon$ | bulk dielectric constant of solvent |
| $\epsilon_1$ | dielectric constant of primary solvation shell |

| | |
|---|---|
| $F$ | Faraday constant |
| $f_s$ | mean activity coefficient in organic phase |
| $f_\pm$ | activity coefficient |
| $K$ | equilibrium constant |
| $K_A$ | association constant |
| $K_{ex}^{ION}$ | ionic extraction constant |
| $K_{ex}^{IP}$ | ion-pair extraction constant |
| $K_{ex}^{TOT}$ | total extraction constant |
| $k$ | intrinsic rate constant |
| $k'$ | measured first order rate constant for gold elution |
| $k_1$ | measured first order rate constant for cyanide decomposition |
| $k_B$ | Boltzmann's constant |
| $\kappa$ | conductivity |
| $L$ | Avogadro's number |
| $L_a$ | microcrystallite diameter |
| $L_c$ | microcrystallite height |
| $\Lambda$ | equivalent conductance |
| $\Lambda_0$ | equivalent conductance at infinite dilution |
| $\lambda$ | wavelength of X-radiation |
| $\lambda_0^+$ | equivalent cationic conductance at infinite dilution |
| $\lambda_0^-$ | equivalent anionic conductance at infinite dilution |
| $M_c$ | mass of carbon in the elution column |
| $M_s$ | mass of solution in the elution column |
| $n$ | aggregation number |
| $\eta$ | solution viscosity |
| $R$ | gas constant |
| $R_m$ | ratio of carbon mass to solution mass in the elution column |
| $r$ | solvent radius |
| $r_c$ | crystallographic ionic radius |
| $r_{eff}$ | effective ionic radius of asymmetrical ion |
| $r_{ij}$ | radial distance from centre of ionic charge |
| $r_s$ | Stokes radius |
| $S_{out}$ | concentration of gold in the eluate solution |

| | |
|---|---|
| | exiting the carbon column or bed at time t |
| $S_{in}$ | concentration of gold in the eluant feed solution to the carbon column or bed at time t |
| $\theta$ | incident angle corresponding to XRD peak maximum |
| $V_s$ | flowrate of eluant |
| $V_1$ | flowrate of eluant solution from carbon bed into simulated electrowinning cell |
| $V_2$ | flowrate of diluent solution into simulated electrowinning cell |
| v | velocity applied to Mössbauer source |
| $X_w$ | mole fraction of water in the organic phase |
| $z_{\pm}$ | ionic charge |

List of Tables

## List of Figures

## CHAPTER 1 INTRODUCTION

The carbon-in-pulp (CIP) process for extraction of gold from cyanide leach liquors, which has undergone widespread application in recent years[1,2], is generally the preferred method for recovery of gold in all new gold plants. However, many aspects of the chemistry involved at various stages of the process remain poorly understood. Even the mechanism of adsorption of the gold species onto activated carbon, the key step in the process, is not fully understood. The aim of this Thesis is to resolve these questions through a fundamental study of these unknown areas.

### 1.1 The Adsorption of Aurocyanide onto Activated Carbon - An Historical Perspective

Carbon has been used as an adsorbent throughout history, with the ancient Hindus using it for water purification[2]. Several centuries ago, it was used extensively in the removal of colours from solutions and for adsorption of gases. It was not until 1847 that its adsorptive properties for gold were first discovered[3]. In 1880, Davis[4] patented a process for recovery of gold from chlorination leach liquors using wood charcoal.

Several years later, in 1890, MacArthur and the Forrest brothers discovered cyanide to be a good lixiviant for gold[5], and soon thereafter, Johnson[6] in 1894 patented the use of wood charcoal for the recovery of gold from cyanide solutions. Cyanidation eventually became the standard technique for leaching gold, which was subsequently recovered by cementation onto zinc. This remained the

process of choice until the 1970's.

During this lengthy period, carbon was never used extensively for gold recovery, except for a brief period[7] at the Yuanmi Mine, Australia, in 1917. The unpopularity of the process during these years is partly due to the poor adsorptive properties of charcoals produced in those days, as compared with the properties of modern activated carbons. Another factor was lack of a suitable method for the elution of gold from the activated carbon after adsorption.

A viable elution process was developed by Zadra[8] in 1952, that paved the way for the first large-scale implementation[9] of carbon-in-pulp (CIP), at the Homestake Mine, U.S.A., in 1971.

Carbon-in-pulp for gold recovery has greatly increased since that time, aided by the advances made[1,10] by Mintek (Council for Mineral Technology) in engineering aspects of the process. Activated carbon has been used for several years for recovery of gold from clear solutions; however, the simplicity of CIP, in which carbon granules are added directly to the cyanided pulp and recovered by screening, has been the most popular new process over the last decade[11].

CIP epitomises the type of innovative technology used in the extractive metallurgy of gold, evidenced by current variations on the conventional process, such as carbon-in leach[11] (CIL), carbon-in-pulp-in-column[12] (CIPIC), and other innovations, such as heap leaching[1] and resin-in-pulp[13,14] (RIP). Engineering and technological aspects of carbon adsorption processes for gold recovery have been successfully developed and, for the most part, commercialized. However, after a hundred years of development, the fundamental chemistry involved in many aspects of the process, remains largely unknown.

## 1.2 The Carbon-in-pulp Process - Process Chemistry and Unknown Areas

CIP relies on one fact - activated carbon exhibits a remarkable ability to adsorb gold as the aurocyanide anion, $Au(CN)_2^-$. This forms the basis of the concentration, separation and recovery of gold on gold plants world wide.

A typical flowsheet for CIP is shown schematically in Figure 1.1. It comprises the following major unit operations:

a) leaching,
b) carbon adsorption,
c) carbon acid-washing and elution,
d) gold electrowinning or precipitation, and
e) carbon reactivation.

A description of each of these unit operations follows, with emphasis on the chemistry involved, and unknown aspects thereof.

### a) *Leaching of Gold from the Ore*

Crushed ore is contacted with a solution of sodium cyanide, typically about 0,01 mol/l, in the presence of oxygen, and for a period of about twenty hours. Gold is dissolved in solution as the soluble aurocyanide ion, $Au(CN)_2^-$, by an electrochemical process described by an anodic dissolution reaction:

$$Au + 2CN^- \rightleftharpoons Au(CN)_2^- + e^- \qquad (1.1)$$

in conjunction with a cathodic reduction of oxygen:

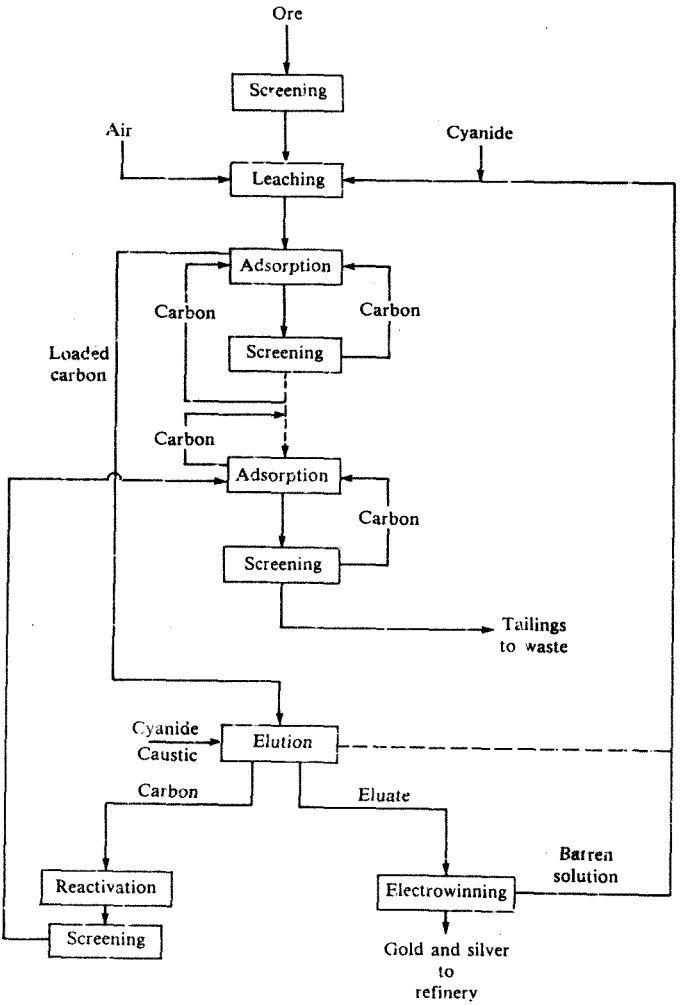


Fig. 1.1 Typical flowsheet of a CIP plant for the recovery of gold (after McDougall and Fleming[11])

$$O_2 + 2H_2O + 4e^- \rightleftharpoons 4OH^- \qquad (1.2)$$

These reactions result in a "mixed potential", $E_m$, at which leaching will occur. this is illustrated schematically in Figure 1.2.

Overall features of the reactions involved here are well established[15]. However, certain details of the reaction mechanisms are uncertain, and the reaction rate can be slowed considerably by a diverse range of factors:

(i) In some instances, this slowing of the leaching rate can be directly attributed to the depletion of cyanide and oxygen in the pulp, due to reaction with various constituents of the pulp.

(ii) Carbonaceous material present in the pulp has been found to adsorb aurocyanide ions. This effect can be eradicated by oxidation with nitric acid[16] or chlorine[17,18]; however, the reason for this effect is not yet clear.

(iii) It is generally accepted that dissolution of gold in cyanide solution occurs via the formation of an adsorbed AuCN species:

$$Au + CN^- \rightleftharpoons AuCN_{ads} + e^- \qquad (1.3)$$

$$AuCN_{ads} + CN^- \rightleftharpoons Au(CN)_2^- \qquad (1.4)$$

A passivating layer of AuCN has been found by several workers[15] to occur at a potential of about -0,4 V, depending on the presence of heavy metal impurities in the solution. Passivation is not normally observed in practice; however, when sulphides are present, it has been postulated to occur. Filmer[19] suggests this to be due to an AuCN layer (Equations 1.3 and 1.4). Fink and Putnam[20] ascribe it to an $Au_2S$ layer. The possibility also exists that sulphide

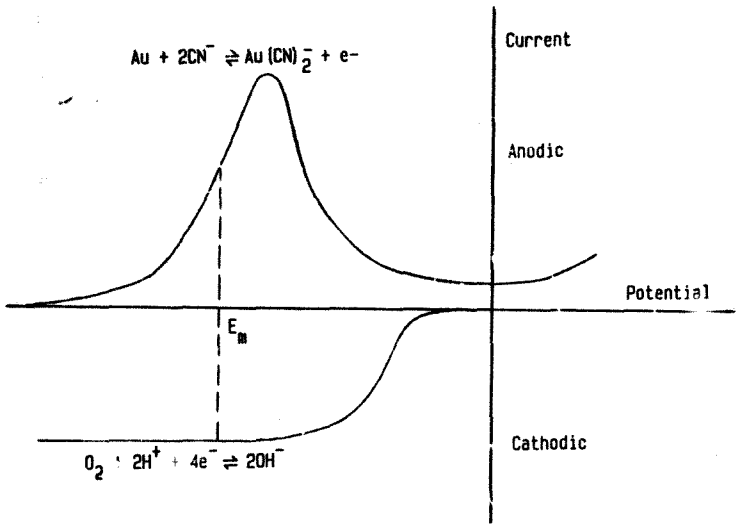


Fig. 1.2 Simplified schema ic diagram of the mixed potential model for the dissolution of gold in cyanide solutions (after Nicol, et al[15])

merely depletes the cyanide concentration in the pulp, via Equation 1.5, for example:

$$2S^{2-} + 2CN^- + O_2 + 2H_2O = 2SCN^- + 4OH^- \qquad (1.5)$$

Several other lixiviants for gold, apart from cyanide, have been considered for specific applications[21]. These reagents include, amongst others, thiourea, thiosulphate, chlorine, bromine and iodine. None of these have yet achieved any widespread use, however.

*b) Adsorption of Aurocyanide onto Activated Carbon*

From the leach tanks, cyanided pulp is pumped to a cascading series of adsorption tanks containing about 25 g/l granular activated carbon, that is retained in the tanks by screens through which pulp passes freely. Carbon is periodically moved countercurrent to the flow of pulp.

Residence time in each stage and number of stages employed are variables that are usually built into the design for a particular target performance of the plant.

The current disagreement regarding the mechanism of adsorption of aurocyanide onto activated carbon is a key issue, and will be dealt with in detail in this Thesis. The chemical nature of the gold cyanide adsorbate has never been unequivocally established, but recent work[22] suggests that the formation of $M^{n+}[Au(CN)_2^-]_n$ ion pairs may be important. Little is known at present regarding the ion association behaviour of aurocyanide, however.

*c) Carbon Acid Washing and Elution*

Gold-loaded carbon from the first adsorption tank is transferred to an elution column, where it is contacted

with a strong caustic cyanide eluant solution of variable composition, depending on the elution procedure employed. The temperature is also dependent on this factor, but in general, high temperatures (> 90°C) are employed. Prior to elution, loaded carbon is often contacted with a hot acid solution (*c.* 10% (m/m) HCl) to remove precipitated $CaCO_3$, fines and slimes from the carbon pores. The chemistry of the elution process has never been addressed in any detail, and no elution mechanism has yet been postulated that can satisfactorily account for all observed facts. Moreover, elution of gold from activated carbon by sodium sulphide solution has been demonstrated[23] to be potentially efficient at room temperature, but a fundamental understanding of this procedure has yet to be reached.

*d) Gold Electrowinning or Precipitation*

Gold recovery from pregnant eluate solution can be achieved by electrowinning, either in a single-pass of eluate through the cell, or in a continuous circuit with the elution column. Alternatively, the gold can be recovered by zinc cementation. Both of these are well established procedures. The chemistry is well known; for example, the cementation of gold onto zinc proceeds via reactions (1.6) and (1.7):

$$Au(CN)_2^- + e^- \rightleftharpoons Au + 2CN^- \qquad (1.6)$$

$$Zn + 4CN^- \rightleftharpoons Zn(CN)_4^{2-} + 2e^- \qquad (1.7)$$

*e) Carbon Reactivation*

In practice, it has been found that activated carbon returning to the adsorption circuit after elution is a poorer adsorbent for gold than the fresh carbon. The reason for this is the poisoning of the carbon by various

organic compounds present in the pulp. Humates, fulvates, hydrocarbons and many other organic compounds exhibit strong adsorption onto activated carbon[24], thereby blocking sites for gold adsorption.

This poisoning has necessitated a thermal reactivation treatment of the carbon when necessary, before being returned to the adsorption circuit. Typically, the carbon is heated to about 750°C in the presence of steam for half an hour, but once again, the parameters used seem to vary depending on the whims of the individual operator. This treatment essentially involves vaporization of volatile adsorbates and burn-off of non-volatile adsorbates.

*f) Other Features of the CIP Process*

Apart from the aspects of the unit operations discussed above, there are various other features of CIP of which little is known regarding the fundamental chemistry involved. These include, amongst others, the chemistry of the decomposition of cyanide throughout the CIP flowsheet, the effect of hot acid treatment on the loaded carbon, and the mechanisms of adsorption of other complexes onto activated carbon, either present in the leach pulp, or useful for elucidation of the aurocyanide adsorption mechanism. The influence of activated carbon surface chemistry and structure on the process is another important aspect. The surface chemistry of activated carbon is complex[24] - even the identities of the surface functional groups are uncertain.

The current commercial success of the carbon-in-pulp process is largely due to decreased capital and operating costs. The improved efficiency of gold recovery by CIP over the zinc precipitation process is most marked when treating calcines and other materials that are difficult to filter. Carbon-in-pulp is by no means the ideal process,

however - the harsh conditions and relatively long times required to elute the gold from the carbon, the need for high-temperature thermal regeneration and the fouling of activated carbon by organic and inorganic materials in the pulp, are some of the more practical factors that could be drastically improved upon.

## 1.3 The Structure and Chemistry of Activated Carbon

Activated carbon is a generic term that encompasses a family of highly porous, amorphous carbonaceous materials, none of which can be characterized by a structural formula or chemical analysis[25]. Modern activated carbons are far superior in terms of abrasion resistance and adsorption activities, as compared with the wood charcoals used in the past. They are used for the adsorption of a range of compounds[24,26,27], both organic and inorganic, gaseous and in solution. Activated carbons also have numerous applications as catalyst supports[28].

### *a) Physical Structure of Activated Carbon*

The single structural factor that results in the adsorptive properties of activated carbon is the extensive pore structure. Most commercial activated carbons have specific surface areas of about 800 to 1200 $m^2/g$, which is predominantly contained within micropores less than 2 nm in diameter. The material contains a complex pore network that is normally categorized as follows:

macropores : $30 < D_p < 10\ 000$ nm
mesopores : $2 < D_p < 30$ nm
micropores : $D_p < 2$ nm,

where $D_p$ is the pore diameter.

The pore size distribution depends on the type of raw material and the conditions of manufacture. Activated carbons can be made from virtually any carbonaceous material, such as coconut shells, peach pits, bituminous coals and peat. The raw material is first carbonized at a temperature not exceeding 700°C, and this charring process is followed by activation at temperatures between 800 and 1100°C in the presence of suitable oxidizing gases, such as steam, air or carbon dioxide. The activation process is responsible for creating the pore structure, by virtue of burn-off of more reactive components of the char. The material also acquires a disordered structure of graphitic platelets known as microcrystallites, shown schematically in Figure 1.3. Also shown is the structure of pure graphite.

*b) Chemical Structure of Activated Carbon*

The edges of the microcrystallites formed during the activation process contain unfilled carbon valencies, that react with the oxidizing gas to form a wide variety of oxygen-containing functional groups. The basal plane of the microcrystallite is relatively inert, so the surface of activated carbon is heterogeneous in nature, with both hydrophilic and hydrophobic domains. This property explains the wide variety of compounds that are strongly adsorbed onto activated carbon.

Activated carbons used for gold recovery are generally prepared by the high-temperature process outlined above. Such carbons are basic in character, by virtue of their ability to strongly adsorb acids, and are popularly classified[29] as H-carbons. Carbons prepared under low temperature conditions are acidic in character, and are classified as L-carbons. These acid-base properties of activated carbons result from the preponderance of functional groups of either acidic or basic character on

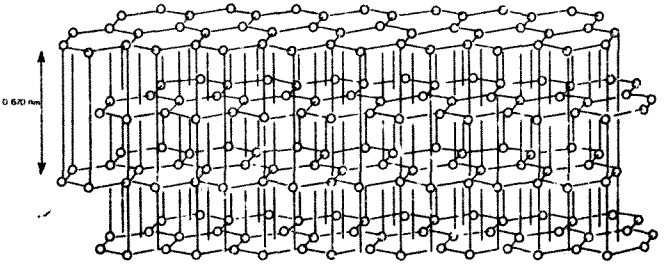


Fig. 1.3a Schematic representation of the structure of graphite. The circles denote the positions of carbon atoms, whereas the horizontal lines represent carbon-to-carbon bonds

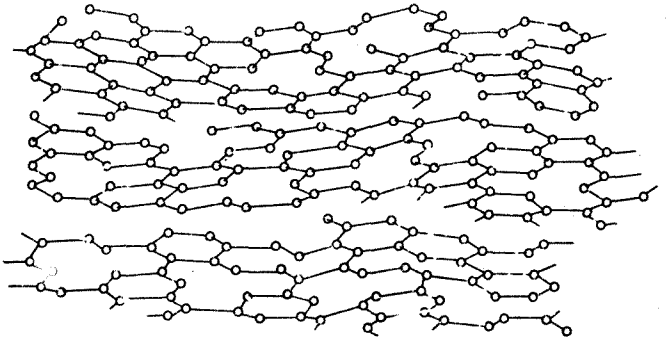

Fig. 1.3b Schematic representation of the structure of activated carbon. Oxygen-containing organic functional groups are located at the edges of broken graphitic ring systems (after Mattson and Mark[24])

the surface. The fact that all carbons adsorb both acids and alkalis to some extent shows that both types of functional groups are normally present.

The precise identities of the functional groups present remain the topic of some debate, but some of the most likely candidates are shown in Figures 1.4 and 1.5.

Activated carbons are known[30] to be electrical conductors, and this property is due to the relatively high degree of condensation of aromatic rings, resulting in an extensive delocalized electron cloud. Electron Spin Resonance (ESR) studies[31] indicate the presence of free radicals. These properties, together with the presence of functional groups that can undergo electrochemical reactions, such as quinones, impart a reduction potential to the activated carbon. Different carbons are found[32] to exhibit a range of different reduction potentials, between +0,06 V and +0,40 V (relative to the Standard Hydrogen Electrode). Hence, activated carbon exhibits both electrochemical and catalytic properties. For example, it can readily effect reduction of $AuCl_4^-$ and $Ag^+$ to the respective metals, and can also act as an oxidation catalyst for $Fe^{2+}$ to $Fe^{3+}$.

## 1 The Chemistry of Gold - An Introduction

The key to the natural occurrence of gold in the metallic form, as well as its many practical uses in jewellery and in industry, is its nobility. It is the only metal that does not corrode in air in the presence of either oxygen or sulphur.

The aqueous chemistry of gold is of great importance to the extractive metallurgist, and an introduction to this is useful in this Thesis. The important oxidation states are the aurous (+1) and the auric (+3). The free uncomplexed ions are thermodynamically unstable in aqueous solution,

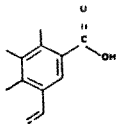

Carboxylic group

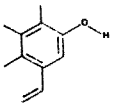

Phenolic hydroxyl group

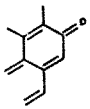

Quinone-type carbonyl group

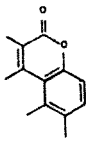

Normal lactone group

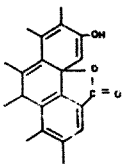

Fluorescein-type lactone group

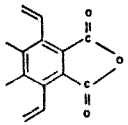

Carboxylic acid anhydride group

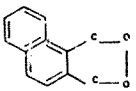

Cyclic peroxide group

Fig. 1.4 Acidic functional groups postulated to be present on the surface of activated carbon (after Cookson[26])

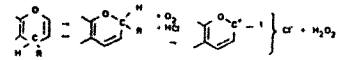

Chromene

Benzopyrylium ion
(Carbonium ion)

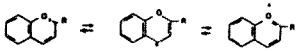

Benzopyrylium derivatives

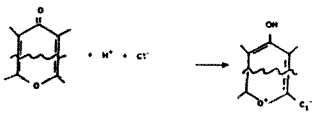

Pyrone-like structures.

Fig. 1.5 Basic functional groups postulated to be present on the surface of activated carbon (after Cookson[26])

and are reduced by water to metallic gold. There are several ligands that form stable complexes with gold, and a few of those of importance in gold metallurgy have already been mentioned. Table 1.1 lists the revelant stability constants of these complexes.

**Table 1.1**
**Stability Constants* for a Selection of Complexes of Gold(I) and Gold(III)**

| Gold(I) | | Gold(III) | |
|---|---|---|---|
| Complex | $\beta_2$ | Complex | $\beta_4$ |
| $Au(CN)_2^-$ | $2 \times 10^{38}$ | $Au(CN)_4^-$ | $10^{56}$ |
| $Au(S_2O_3)_2^{3-}$ | $5 \times 10^{28}$ | $AuI_4^-$ | $5 \times 10^{47}$ |
| $Au(CS(NH_2)_2)_2^+$ | $2 \times 10^{23}$ | $Au(SCN)_4^-$ | $10^{42}$ |
| $AuI_2^-$ | $4 \times 10^{19}$ | $AuBr_4^-$ | $10^{32}$ |
| $Au(SCN)_2^-$ | $1,3 \times 10^{17}$ | $AuCl_4^-$ | $10^{26}$ |
| $AuBr_2^-$ | $10^{12}$ | | |
| $AuCl_2^-$ | $10^{9}$ | | |

*Values are taken from Nicol, *et al*[15].

Gold(I) complexes have the $4f^{14}5d^{10}$ electronic configuration and are diamagnetic. The preferred coordination number of gold(I) is two, forming linear complexes. Very stable complexes are formed[33] with soft ligands, such as cyanide ($Au(CN)_2^-$ ; $\beta_2 = 2x10^{38}$)[5]. In chloride solution, where a hard ligand is involved, the $AuCl_2^-$ species is somewhat unstable, tending to disproportionate according to the following reaction:

$$3AuCl_2^- \rightleftharpoons AuCl_4^- + 2Au^0 + 2\ Cl^- \qquad (1.8)$$

Gold(III) complexes have the $4f^{14}5d^8$ electronic configuration, and are also diamagnetic. In this case,

more stable complexes are formed with hard ligands, such as chloride ($AuCl_4^-$ ; $\beta_4 = 10^{26}$)[5]. The preferred coordination number for gold(III) is four, with square planar complexes usually being formed.

Other aspects of the chemistry of gold, both well known and novel, will be discussed later in this Thesis. It will be shown how these features of the chemistry of gold are important in determining its extractive metallurgical characteristics, and in particular the remarkable selectivity of activated carbon for the adsorption of $Au(CN)_2^-$ over other metal cyanide anions.

## 1.5 Current Processes for the Recovery of Gold

In the past, gold has been collected from placer (surface) deposits by gravity techniques, due to its high specific gravity, sometimes aided by mercury amalgamation. Such processing techniques are relatively unimportant today - in the United States in 1986, 94% of the 3,733 million ounces of gold produced was processed by cyanidation[34].

The two most prevalent gold processes in use today are carbon-in-pulp and zinc cementation, and both of these have been discussed earlier in this chapter. CIP processes are the most popular on all new gold plants; hence the importance of a fundamental study of the processes involved.

There are alternative configurations to the typical CIP process. Carbon-in-leach (CIL) and carbon-in-solution (CIS) are two versions that find many applications. The former involves the placing of carbon in the leach tanks to instil more efficient leaching, and this variation is most appropriate when the pulp contains carbonaceous ("preg-robbing") materials that also have an affinity for gold adsorption. The latter version involves passing a

clarified leach liquor through a bed or column of carbon; this version is most appropriate when treating leach liquors from heap leach operations.

Heap leaching is without doubt the most obvious and simple way to deal with certain lean ores and wastes, and involves the percolation of cyanide solution through a large heap of ore. Pregnant solution is allowed to run out from the bottom of the heap, and the gold is then recovered.

Despite the current popularity of the CIP process, there is much room for improvement, and the search is on for alternative configurations, such as the carbon-in-pulp-in-column (CIPIC) configuration proposed by Mintek researchers[12], and the horizontal flow variation, proposed by Davy-McKee workers[35].

The search is also on for alternative adsorbents to activated carbon. The use of conventional anion-exchange resins in a resin-in-pulp (RIP) variation are reported[36] to be employed in full-scale plants in the Soviet Union. The first reports[13,14] of such an innovation being operated successfully in the western world have recently been made. It is evident that for certain applications, resin-in-pulp is more viable a process than carbon-in-pulp.

The relatively recent advent of carbon-in-pulp on a commercial scale is probably the single most important innovation in gold metallurgy since the introduction of cyanidation in 1890. It is the aim of this Thesis to address the many unknown areas still associated with this process, in particular the mechanism of adsorption of aurocyanide onto activated carbon.

# CHAPTER 2 EXPERIMENTAL PROCEDURE

## 2.1 Reagents and Chemicals

$KAu(CN)_2$ and $KAg(CN)_2$ were supplied by Johnson Matthey (Pty) Limited, $NaAu(CN)_2$ by Engelhard Chemical Division and $AgNO_3$ by Synthon Ltd. All other chemicals were of AR, CP or Spectroscopic grade, and all solutions were made up with de-ionized water. All solvents were washed repeatedly with de-ionized water before use.

Solutions of $HAu(CN)_2$ were prepared by passing a 10 ml aliquot of concentrated $KAu(CN)_2$ solution slowly through a 25 ml column of Dowex 50W-S8 cation exchange resin in the acid form. To convert the resin into this form, 250 ml of 1,0 M HCl solution was slowly passed through the column and subsequently washed with de-ionized water until the conductivity of the solution was less than $1,5 \times 10^{-6}$ S/cm. The $LiAu(CN)_2$ salt was prepared by passing a $KAu(CN)_2$ solution through a Dowex 50W-S8 column in the $Li^+$ form, as above, and evaporating the resultant solution to dryness. The $Li^+$ form of the resin was achieved by reacting resin in the $H^+$ form with 1,0 M LiOH solution and washing to neutrality. $NBu_4Au(CN)_2$ was prepared by adding a concentrated solution of $KAu(CN)_2$ to one of $NBu_4OH$ (20% w/w, supplied by Merck), and washing the resultant precipitate well with de-ionized water.

The activated carbon used was Le Carbone G210, which was purified by continual washing with cold de-ionized water. Additional treatments are described later in the text. Le Carbone G210 was selected because it is used extensively in CIP plants world wide. It is a granular activated carbon

derived from coconut shells, with an average particle diameter of about 2 mm. The surface area as determined by the $N_2$ BET method is 1100 to 1200 $m^2/g$.

The polymeric adsorbents S-761 and S-862 were supplied by Duolite. S-761 is a phenol-formaldehyde matrix , and S-862 a polystyrene matrix. The polymeric adsorbent XAD-8, which comprises an acrylic ester matrix, was supplied by Rohm and Haas. These adsorbents have surface areas of about 450 $m^2/g$.

The soluble poly(oxyethylene) used in this study was the non-ionic surfactant Triton X-100, which has the structure

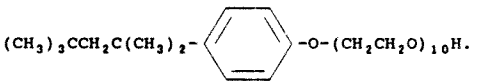

## 2.2 Activated Carbon Adsorption studies

### *a) Equilibrium Adsorption*

For the experiments in section 3.2a, 1,0 g of carbon was equilibrated in a rolling bottle for 3 days with 400 ml of a solution containing 50 to 700 mg of gold, and 0,1 mol of hydrochloric acid or potassium chloride, per litre. Samples of the solution were analysed for gold by atomic-absorption spectrophotometry (AAS). The carbon was analysed for gold by X-ray fluorescence spectroscopy (XRFS), for potassium, by AAS, and for nitrogen by a Heraeus elemental analyser, as well as a LECO nitrogen analyser. The estimated error in all analyses is about 5 per cent.

b) *Elution of the Carbon*

Prior to some elutions 1,0 g of loaded carbon was washed in a rolling bottle with 250 ml of a hydrochloric acid solution (0,1 mol/l) for 24 hours. No gold was detected in the wash solution. In other instances, 1,0 g of loaded carbon was boiled under reflux in 250 ml of solution containing 4 per cent hydrochloric acid (by mass) for varying periods of time. No gold was detected in the pre-treatment solution. The carbon was subsequently washed to neutrality with deionized water.

The carbon was then eluted as follows: approximately 1 g of loaded carbon was placed in an insulated, jacketed column that was heated by hot (90°C) water circulating through the jacket. A fresh solution of sodium hydroxide (0,1 mol/l) was siphoned slowly through the carbon bed until analysis of the eluate solution showed the gold content to be below 0,1 mg/l. The carbon was analysed for gold by XRFS before and after the elution.

Eluates from several of the elutions were analysed for $Au(CN)_2^-$ by UV spectrophotometry. Absorbances were measured at 239,5 nm on a Beckman Acta MIV Spectrophotometer, and were found to follow Beers law, thus yielding a standard curve.

c) *Precipitation of AuCN*

Fresh 250 ml solutions of $KAu(CN)_2$ containing 1000 mg gold per litre, in 0,1 mol/l hydrochloric acid were placed in a magnetically-stirred round-bottomed flask with water-cooled condenser, and heated to the relevant temperature using an oil bath. The solution was analysed periodically for gold by atomic-absorption spectroscopy.

*d) Decomposition of AuCN*

AuCN that was produced in the previous experiment was washed well with ethanol and water and dried under vacuum for twenty four hours. AuCN (0,05 g) was placed either in a rolling bottle or under reflux as above, and contacted with 20 ml of de-ionized water adjusted with hydrochloric acid or sodium hydroxide to pH values in the range 1,0 to 13,0. Solutions were then analysed for gold by atomic absorption spectroscopy, and for cyanide and cyanate by ion chromatography. The solution was further characterized by ultraviolet (UV) spectrophotometry on a Beckman Acta MIV spectrophotometer, and the solid residue by X-ray diffractometry (XRD) using a Philips PW1050 X-ray diffractometer.

*e) Oxygen Effect Experiments*

Typically, 1,0g of carbon was contacted with 250ml of solution containing the appropriate additive. High purity gas (oxygen or nitrogen) was bubbled through the solution vigorously enough to achieve efficient mixing. For each experiment, the temperature was kept at a constant °,5 ± 0,01°C by means of a Hetotherm PF523 thermostat in conjunction with a Grant cooling unit, to minimize evaporation losses. Samples of solution were analysed for gold by atomic absorption spectrophotometry (AAS), and the pH value was measured using a Labion Model 15 pH/mV meter in conjunction with an Orion combination pH electrode. Carbon was analysed for gold by X-ray fluorescence spectroscopy (XRFS), for nitrogen using a Heraeus elemental analyser as well as a LECO nitrogen analyser, and for chloride using silver nitrate turbidity. Solutions were analysed for $NH_4^+$, $HCO_3^-$ and $CNO^-$ by ion chromatography.

*f) Gold(III) Cyanide Experiments*

$KAu(CN)_4$ was prepared by the method of Smith, *et al*[37]. $KAu(CN)_2$ was dissolved in water and reacted with a slight excess of bromine, with the excess being removed by heating to 80°C. The $KAu(CN)_2Br_2$ in the resultant solution was then reacted with a stoichiometric potassium cyanide solution, to yield $KAu(CN)_4$ in solution. In the adsorption experiments, 0,25 g of carbon was equilibrated in a rolling bottle for twenty hours with 100ml of solution containing 300mg of gold per litre (as $KAu(CN)_4$ or $KAu(CN)_2$), as well as potassium chloride, calcium chloride or hydrochloric acid. Samples of solution and carbon were analyzed for gold, potassium and nitrogen as described above. A carbon that was loaded with $KAu(CN)_4$ was also boiled in 250ml of 4% hydrochloric acid for four hours, washed to neutrality and dried in a vacuum desiccator, for subsequent investigation.

*g) Silver and Mercury Experiments*

Carbon (1,0 g) was equilibrated in a rolling bottle for 72 hours with 400 ml of a solution containing 350 mg of silver per litre (as $KAg(CN)_2$), as well as 0,1 mol of potassium chloride or hydrochloric acid per litre. In the case of mercury, the solution contained 700 mg of mercury per litre (as $Hg(CN)_2$) either alone, or with the molar equivalent of $Ca(CN)_2$. The carbon was analysed for silver, mercury, potassium and nitrogen as described above. In a second series of experiments, 0,25 g of carbon was equilibrated in a rolling bottle for 24 hours with 100 ml of a solution containing either 150 mg of silver or 300 mg of mercury, as well as 0 to 1,0 mol of potassium cyanide per litre. The ionic strength was kept at a constant 1,0 mol/kg, by addition of the required amounts of potassium chloride. Samples of solution were analysed for silver by atomic-absorption spectrophotometry (AAS). Silver was also

loaded onto the carbon (0,25 g) from silver nitrate solution (0,0255 M $AgNO_3$, 20 ml) in a rolling bottle for 24 hours, and mercury from a 0,01 M $HgCl_2$ solution.

In the investigation of the effects of acid and base treatment, loaded carbon (0,5 g) was boiled under reflux in 250 ml of solution containing 4 per cent hydrochloric acid (by mass) for five hours. The carbon was subsequently washed to neutrality with deionized water. A portion of the carbon was then boiled in 250 ml of 0,1 M sodium hydroxide for a further five hours. The carbon was then analysed for silver and nitrogen as above.

*h) Miscellaneous Techniques*

(i) X-ray diffractometry

X-ray diffractograms of loaded and treated carbons were obtained using Cu $K_\alpha$ radiation, on a Philips PW1050/25 X-ray diffractometer.

(ii) Scanning electron microscopy

Scanning electron micrographs of loaded and treated carbons were obtained using a Hitachi scanning electron microscope (SEM), as well as a Jeol 840A SEM.

(iii) Fourier Transform Infrared Spectrophotometry

Samples of activated carbon for infrared spectrophotometry were prepared by contacting 0,5 g of carbon with 25 ml of solution containing typically 0,003 moles of gold as $KAu(CN)_2$ and 0,03 moles of either LiCl, KCl, CsCl or $CaCl_2$ in a rolling bottle for 24 hours. In the cases of Ag and Hg

a similar procedure was followed.

Samples were crushed using a mortar and pestle prior to drying. Approximately 0,8 mg of dried carbon powder was mixed with 200 mg of dry KBr by shaking manually. The mixture was made into a disk by placing it under 10 tonnes of pressure for about 10 seconds.

Infrared spectra were obtained using a Perkin-Elmer 1725X Fourier Transform Infrared Spectrophotometer. For each spectrum, 200 scans were made in the transmission mode, at a resolution of 4 $cm^{-1}$. No mathematical smoothing functions were performed on the spectra; however the ordinate of each spectrum was normalized to facilitate comparisons between spectra. All spectra were baseline-flattened to enhance spectral detail.

### (iv) $^{197}$Au Mössbauer spectroscopy

This technique is not commonly used, which necessitates a more detailed discussion of the underlying principles. It is only in the last ten years[38] that sufficient development has been made in the field of $^{197}$Au Mössbauer spectroscopy to facilitate application of the technique to practical problems. The technique is a powerful one, providing information both on oxidation state and chemical environment of the gold atom, provided suitable reference data are available. Recent applications have been some preliminary work[39,40] on the nature of the aurocyanide adsorbate on activated carbon, and a study of the chemical state of gold in gold ores[41].

The principle of the Mössbauer effect is essentially similar to the adsorption of infrared radiation in infrared (IR) spectrophotometry; however in the case of Mössbauer spectroscopy, $\gamma$-rays are used. These $\gamma$-rays are emitted during an isomeric transition of a nucleus in a radioactive

source, and are subsequently absorbed by a nucleus of the same isotope, causing it to undergo a transition from its ground state to the respective excited state, and this phenomenon is called the Mössbauer effect.

To observe a Mössbauer effect in $^{197}$Au, the radioactive source used is $^{197}$Pt, prepared from isotopically enriched $^{196}$Pt that has been irradiated with neutrons in a nuclear reactor. The decay scheme for the $^{197}$Pt isotope is shown in Figure 2.1. The relatively short half-life of 18 hours necessitates prompt measurement of the Mössbauer effect, which may take several days to yield a statistically useful result, depending on the gold concentration in the sample. Some measurements may thus require two or three sources in order to provide a reasonable spectrum. Figure 2.1 shows that 90 percent of the $^{197}$Pt decays to the 77,3 keV excited state of $^{197}$Au, which decays to the ground state with emission of $\gamma$-radiation of energy 77,3 keV. When this radiation reaches the gold sample of interest in the absorber holder, some of the radiation is absorbed by $^{197}$Au atoms in the sample undergoing the transition to the excited state, and measurement of the intensity of the radiation exiting from the absorber yields the percentage transmission, which has a similar meaning to that for IR spectrophotometry.

The resonant absorption of $\gamma$-radiation by $^{197}$Au nuclei can only take place if they do not lose energy due to recoil during emission or absorption, i.e. the atoms must be embedded in a solid matrix. Moreover, the recoil-free fraction, f, decreases with increasing gamma energy and with increasing temperature. The relatively high 77,3 keV gamma energy of $^{197}$Au makes it necessary to cool both source and absorber down to about 4 K in a liquid helium cryostat.

The $\gamma$-radiation produced is very monochromatic[42], and in order to provide a spectrum, a variation in frequency, and hence energy, of the radiation passing through the sample,

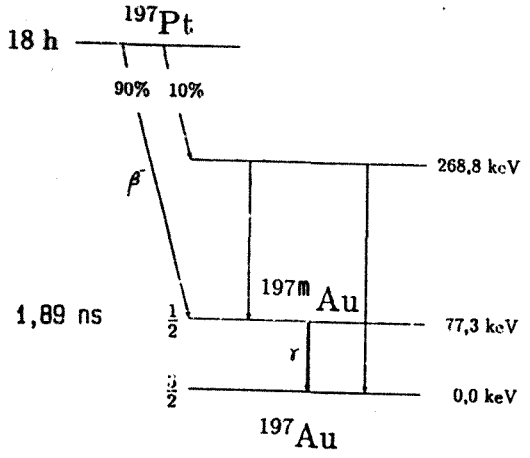


Fig. 2.1 Decay scheme for the $^{197}Pt$ isotope used as a source for $^{197}Au$ Mössbauer spectroscopy

must be produced. This is achieved via the Doppler effect. The source is given a velocity that results in a slight change in energy of the radiation:

$$E_\gamma = E_i(1 + v/c_{h\nu}), \qquad (2.1)$$

where $E_i$ is the energy of incident radiation, $E_\gamma$ is the energy of $\gamma$-radiation from the stationary source, v is the applied velocity, and $c_{h\nu}$ is the velocity of light. Only a small energy range is required for this application. The data are normally plotted in units of velocity.

Mössbauer spectra of gold compounds normally consist of a doublet, or quadrupole, as shown in Figure 2.2, which shows the Mössbauer spectra for the gold cyanide compounds AuCN, $KAu(CN)_2$ and $KAu(CN)_4$. The quadrupole splitting, QS, which is the separation between the two absorption peaks of the doublet, is a measure of the asymmetry of distribution of electronic charge about the gold nucleus. Intermetallic systems usually show zero or very small values of QS, due to the high symmetry of their structures. An example, that of metallic gold, is also shown in Figure 2.2.

Another important parameter in a Mössbauer spectrum is the isomer shift, IS, the position of the centroid of the doublet. The isomer shift is a measure of total electron density at the gold nucleus. An increase in IS is also characteristic of an increase in covalency in bonds to neighbouring atoms. Metallic gold has the lowest electron density of the Au nuclei, and hence exhibits the lowest isomer shift of all known gold compounds and alloys, viz. -1,23 mm/s.

A comparison between the Mössbauer spectra of different gold compounds in Figure 2.2 suggests that identification of unknown gold species is possible, since the IS and QS parameters vary significantly from one gold species to the

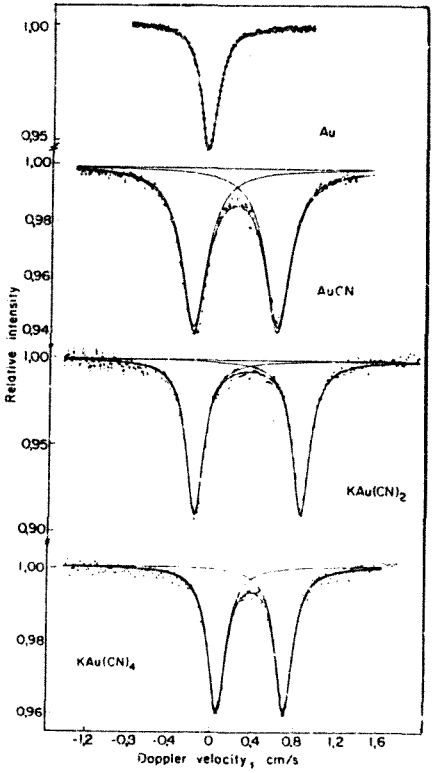


Fig. 2.2 $^{197}$Au Mössbauer spectra of representative gold cyanide compounds. (After Faltens and Shirley[43])

next. Figure 2.3 shows a QS-IS correlation diagram compiled from the spectra of a number of gold(I) and gold(III) compounds. Only a minimal amount of overlap between the Mössbauer parameters of gold(I) and gold(III) species occurs.

Figure 2.4 shows plots of IS and QS against the crystallographic cationic radius for a series of $MAuCl_4$ salts. The data were collected from the literature and are summarized in Table 2.1.

**Table 2.1**
**Mössbauer parameters for $MAuCl_4$ salts**

| Salt | IS mm/s | QS mm/s | Ref. | $r^+$, Å[a] | Ref. |
|---|---|---|---|---|---|
| $HAuCl_4.4H_2O$ | 1,87 | 0,94 | 42 | 0,30 | 45 |
| $KAuCl_4$ | 2,05<br>2,02<br>1,65 | 1,26<br>1,11<br>1,27 | 42<br>44<br>44 | 1,33 | 45 |
| $KAuCl_4.H_2O$ | 2,08 | 1,4 | 44 | | |
| $NH_4AuCl_4.xH_2O$ | 2,07 | 1,7 | 44 | 1,48 | 45 |
| $CsAuCl_4$ | 2,16 | 1,37 | 44 | 1,69 | 45 |
| $Bu_4NAuCl_4$ | 2,23 | 1,31 | 42 | 3,72 | 46 |
| $Ph_4AsAuCl_4$ | 2,30 | 1,88 | 42 | 4,26 | 46 |

[a] Crystallographic cationic radius

The decrease in IS with decreasing cationic radius is attributable to the fact that smaller cations are more polarizing, resulting in a decrease in electron density around the gold atom, and hence a decrease in IS value. The effect of QS is non-linear, probably because change in crystal structure from one compound to the next has a larger influence on the asymmetry of electron density, and hence QS, than does change in cation.

Finally, the intensity of the peak in the Mössbauer spectrum is not only proportional to concentration, i.e. the number of gold atoms present in the cross-sectional area of absorber, but is also proportional to the recoil-

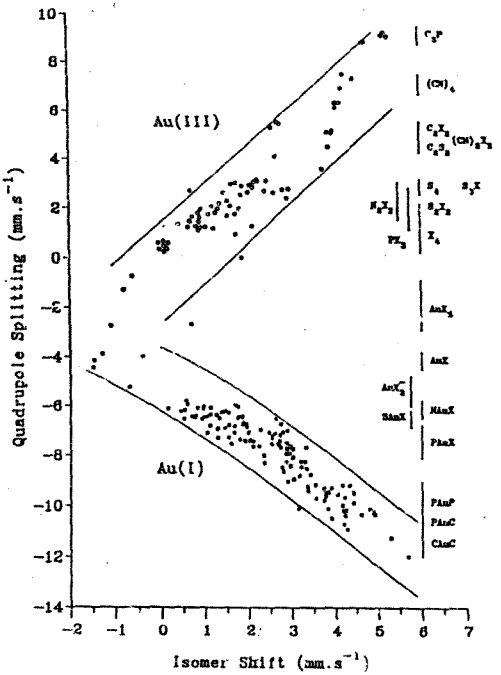


Fig. 2.3 Correlation of isomer shifts and quadrupole splittings for gold(I) and gold(III) compounds, with gold in different chemical environments. Isomer shift values are relative to Au in Pt source. (After Cashion *et al*[39])

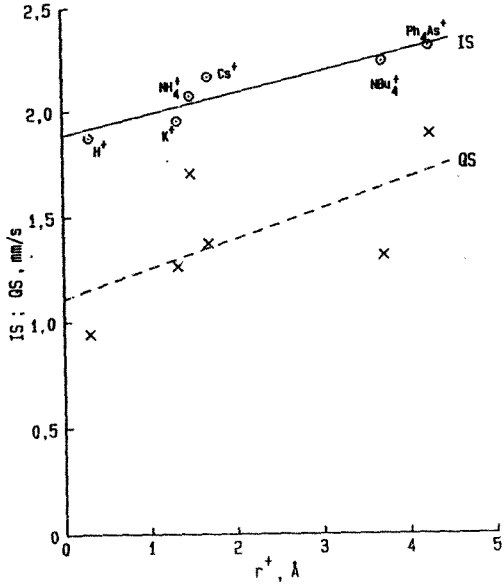


Fig. 2.4 Plot of IS and QS for $^{197}$Au Mössbauer spectra of $MAuCl_4$ salts against cationic radius

free fraction, f, which was mentioned earlier. It is only from a knowledge of the value of f for the relevant species under the experimental conditions, that any quantitative data can be obtained. For example, the value[47] of f (which is sometimes also called the Debye-Waller factor) for metallic gold is 0,19 , whereas that for crystalline $KAu(CN)_2$ is 0,015.

Samples for Mössbauer spectroscopy were prepared by contacting 20g of carbon with 200 ml of solution containing typically 2000 mg of gold per litre, rolling in a bottle for twenty hours and washing with cold de-ionized water. One sample was subsequently boiled for twenty hours in 250 ml of hydrochloric acid solution containing 40% HCl (mm) and washed with cold de-ionized water. Half of this carbon was then boiled in 250 ml of 0,1M NaOH solution for five hours, cooled and washed with cold deionized water. Both fractions were then dried in a vacuum desiccator over silica gel. All Mössbauer spectra were deconvoluted at the Technische Universität München, using computer methods.

(v) X-ray photoelectron spectroscopy (XPS)

In this technique, the surface of the sample is irradiated with X-rays, and the energy distribution of the ejected electrons is measured. The common acronyms for the technique are ESCA (Electron Spectroscopy for Chemical Analysis) and XPS (X-ray Photoelectron Spectroscopy). Analysis of the resultant spectrum of electron counts against photoelectron kinetic energy, can provide useful information regarding chemical and electronic environment of elements in the material, i.e. valence state, binding energies of electrons, etc.

The kinetic energy of the photoelectron produced, $E_p$, is related to the energy of the incident photon, $h\nu$, and the binding energy of the electron in its particular shell, $E_b$,

by the equation

$$E_p = h\nu - E_b - E_{wf} \qquad (2.2,$$

where $E_{wf}$ is the work function, which is the surface potential that each escaping electron must overcome, and is an instrumental constant.

The photoelectron spectrum is characteristic of the material, since the energies of the electronic levels, and hence the binding energies of the electrons, $E_b$, are different for different atoms. A chemical shift in $E_b$ for a given level in an atom is well known[32]. Difficulties in referencing these chemical shifts are discussed in section 3.2f.

XPS measurements are generally performed under ultra-high vacuum (UHV) conditions, to eliminate contamination from stray particles. Electrons are detected with an electron multiplier.

The fact that XPS is a surface technique, combined with its usefulness in determining the valence state and electronic environment of species, make it a suitable choice for studies of adsorbent species, one drawback being the requirement for UHV which may result in the generation of artifacts.

Carbons for investigation were prepared by contacting 0,5 g carbon with a 25 ml solution of $KAu(CN)_2$ containing 4000 mg gold as well as 0,5 moles of either LiCl, NaCl or KCl per litre. One 0,5 g sample of carbon loaded with $KAu(CN)_2$ was boiled in 275 ml of 4 per cent hydrochloric acid for 24 hours. Samples of aurichloride-loaded carbons were produced by contacting 0,5 g carbon with 60 ml of a solution of $HAuCl_4$ containing 1000 mg of gold and 1 mole of HCl per litre. One such carbon was loaded from a similar solution that also contained 30 ml of aqua regia.

Surface analysis was performed in a multitechnique Vacuum Generators "Solar 300" UHV chamber, which was fitted with a VG "CLAM 100" (Combined Lens Analyser Module) comprising XPS and AES facilities. The main chamber was kept at a base pressure of $5 \times 10^{-10}$ mbar with an Edwards E04 oil diffusion pump (running on polyphenyl ether fluid) with a water cooled baffle fitted with a VG CCT150 liquid nitrogen cryostat and an Edwards EDM12 rotary backing-pump. The X-ray source made use of magnesium $K_\alpha$ radiation. Samples for XPS were mounted as powders on double-sided sticky tape. Samples of pure compounds were mixed with powdered activated carbon by physical shaking, and binding energies were referenced against the carbon (1s) peak in activated carbon, which was assigned as 284,4eV. Deconvolution of spectral data was achieved by use of a modified version of PARAFIT[48], a parametric least squares curve-fitting subroutine, on an Apple IIe microcomputer.

## 2.3 Solution Studies

### a) *Potentiometric Titration*

A 50 ml aliquot of 0,005 mol/l $HAu(CN)_2$ which was prepared as described above, was titrated against 0,01062 mol/l NaOH solution previously standardized against 0,0100 mol/l HCl. The titration was monitored using a radiometer PHM 64 research pH meter with an Orion combination pH electrode. The solution was stirred magnetically throughout the titration.

### b) *Conductivity Measurements*

Measurements were made using a Wayne-Kerr B642 Autobalance bridge in conjuction with a Radiometer CDC 344 Immersion

Conductivity cell comprising three non-platinized platinum ring electrodes with a cell constant of 3,318 cm. The temperature was kept at a constant 25,00 ± 0,01°C by means of a Hetotherm 02PF 623 UO thermostat/bath combination in conjunction with a Grant cooling unit.

All solutions were made up using water of conductance lower than $1,5 \times 10^{-6}$ S/cm. Measurements were made by a serial concentration method, starting off with pure water and adding weighed aliquots of the relevant salt solution.

*c) Infrared Spectrophotometry*

Samples of $LiAu(CN)_2$ and $NBu_4(CN)_2$ were placed in pyrex containers and dried in a vacuum oven overnight at 85°C. The containers were subsequently stoppered and allowed to cool in a vacuum desiccator over dried silica gel. The methyl ethyl ketone (MEK) and tetrahydrofuran (THF) solvents used in this study were dried over molecular sieves (4 Å), that had been dried for four days at 140°C and cooled *in vacuo*. Infrared spectra of the dried solvents displayed no bands at ~ 3300 $cm^{-1}$ that would be attributable to the presence of water. Solutions were made up rapidly to ensure the shortest possible exposure time to the atmosphere. Spectra were recorded within a few hours of making up the solutions. Solutions were stored in a desiccator when not in use. IR spectra were recorded on a Beckman IR4260 Research Infrared Spectrophotometer. A cell with $CaF_2$ windows and path-length adjustable to 0,221 mm, supplied by Research and Industrial Instruments Company, England, was used.

*d) Distribution Experiments*

In these experiments, 20 ml of water-saturated organic phase was equilibrated with 20 ml of aqueous phase in a 100

ml separating funnel by shaking for 20 min on a Voss automatic shaker. Efficient mixing was indicated by the milkiness of the solution. Test experiments showed that equilibrium was attained in 2-3 min. Experiments were carried out at 23 ± 1°C. Previous work[45] had shown temperature effects to be small. The aqueous phase in each case contained potassium aurocyanide as well as an excess (0,1 M) of the pertinent chloride salt. Gold concentration in the aqueous phase before and after equilibration was measured by atomic absorption spectrophotometry, and corrected for the effects of the various organics on the absorbance. Appendix 1 shows some physical and chemical properties of the solvents used.

*e) Determination of Chloride Concentration in Organic Phases*

The chloride concentration in the various organic phases was determined by titrating a 10 ml aliquot dissolved in 50 ml ethanol and 10 ml of 1 M $HNO_3$, against a 0,0255 M $AgNO_3$ solution. A 15 min pre-equilibration time was found to be necessary before carrying out the titration. The endpoint was determined potentiometrically with a Labion Model 15 potentiometer, using a platinum electrode in conjunction with a saturated calomel reference electrode.

*f) Determination of Dielectric Constant*

An indication of the dielectric constant of several organic mixtures was obtained by measuring the capacitance of the solution using the Wayne-Kerr bridge/Radiometer conductivity cell apparatus described earlier. A calibration curve was obtained using literature values for the dielectric constant of several pure organic solvents. The high capacitance of the leads connecting the cell to the bridge did not allow very accurate values to be obtained;

however, the results were considered sufficiently accurate for the present purposes.

### g) *Determination of Water Content by Automatic Karl-Fischer Titration*

The solubilities of water in several solvents, mixtures and solutions of Triton X-100 in the solvents, were determined by automatic Karl-Fischer titration. A radiometer TTA 80 automatic titration assembly was linked to an Apple IIe microcomputer. The titration was checked by comparison of the measured solubility of water in nitrobenzene with that reported in the literature[49]. Good agreement was obtained.

## 2.4 Molecular Mechanics Calculations

### a) *The Force Field*

Molecular mechanics calculations on alkali metal complexes of poly(oxyethylene) ligands were implemented on a version of MOLBLD-3 due to Boyd[50], modified to reproduce the united atom force-field AMBER[51]. AMBER has been used extensively to explain the properties of proteins[52], nucleic acids[53], the alkali metal complexes of spherands[54] and, appropriate to the present application, the alkali metal complexes of 18C6, a cyclic polyether[55]. AMBER uses a potential function of the form:

$$E = \sum_{\text{bonds}} k_b(r - r_0)^2 + \sum_{\text{angles}} k_\theta(\theta - \theta_0)^2 + \sum_{\text{dihedrals}} \frac{k_\phi}{2}[1 + \cos(n\phi - \gamma)] + \sum_{\text{nonbonded}} \left[ B_{ij} r_{ij}^{-12} - A_{ij} r_{ij}^{-6} + \frac{q_i q_j}{\epsilon r_{ij}} \right]$$

where the nonbonded terms are summed over all atom pairs separated by more than three bonds. A "united atom" approximation[56] was used, in which aliphatic $CH_2$ groups are represented as single atoms. This has the advantage of substantially reducing the number of interactions, and speeding up computer refinement. Van der Waals terms were input into the modified MOLBD3 as 12/6 Lennard Jones functions, $E_{NB} = A/r_{ij}^{12} - C/r_{ij}^{6}$, where the coefficents A and C were derived from group and atomic polarizabilities, effective united atom atomic numbers, and effective ionic radii by substitution into the Slater-Kirkwood equations as described by Scott and Sheraga[57]. Nonbonded parameters for the $CH_2$ group, the O atom and the $K^+$ and $Cs^+$ ions were taken from Wipff *et al*[55], and those for $Li^+$ were taken from Kollman *et al*[54]. Ethereal torsion parameters were taken from Wipff *et al*[55], and bond streching and angle banding parameters were taken from Kollman *et al*[53]. The partial atomic charge on complexed oxygen was taken by Wipff *et al*[55] to be - 0,6. Carbon atoms bonded to the oxygen had a compensating charge of +0,3 to maintain the ligand electrical neutrality. The cutoff distance for nonbonded interactions was set to 7 Å, as recommended by Brooks *et al*[58]; electrostatic terms were omitted if more than 9 Å separated the atoms[59]. All refinements were terminated when the rms shift in coordinates was less than 0,2 Å. The attenuation factor in MOLBLD3 was set to 9 for all calculations. Structures were generated using the molecular modelling package ALCHEMY (Tripos inc) and the refined structures were visualized using ALCHEMY.

*b) Conformations of Polyether in Organic Solvents*

Warshel[60] showed that the effective dielectric constant for short-range ionic interactions in water is considerably smaller than the bulk dielectric constant and increases roughly linearly with charge separation. This

model has been used successfully in molecular dynamics studies on proteins[61].

In the present study, a microscopic dielectric constant of $r_{ij}$ was used for the polyether in the least polar solvent. Since increased polarity of the solvent should quench the effects of partial atomic charges over distance, a microscopic dielectric constant of $4r_{ij}$ was chosen for the most polar solvent.

The polyether of the formula $CH_3-(CH_2-O-CH_2)_{12}-CH_3$ was constructed using ALCHEMY with the C-C-O-C-C-O units in the helical conformations adopted by the ligand in the crystal structure of complexes, and in a linear conformation.

Since the polar solvent is expected to quench the charges on the polyether, with which it directly interacts, but not the metal, which is embedded in the polyether, it was decided to attenuate intrapolyether interactions with a dielectric constant of $4r_{ij}$, and polyether-metal interactions by $2r_{ij}$.

## 2.5 Activated Carbon Elution Studies

### *a) Elution Mechanism Experiments*

For experiments on adsorption of sodium hydroxide and sodium cyanide onto carbon, 25,0 g of carbon was equilibrated in a magnetically-stirred vessel for 2 days with 250 ml of a solution containing sodium hydroxide at a concentration of 0,2 mol/l, or 0,1 mol/l plus sodium cyanide (0,1 mol/l). Carbon and solution were sampled periodically, and carbon was analysed for sodium and nitrogen as described above. Solution was analysed for hydroxide by titration with a standardized solution of hydrochloric acid (0,1000 mol/l), using phenolphthalein as

the indicator. The cyanide content of the solution was determined by titration with a solution of $AgNO_3$ (0,0255 mol/l), potassium iodide solution being added as indicator, and ammonia being added to solubilize the silver cyanide for a sharp end-point.

For experiments in which polymeric adsorbent resins were used, 1,0 g of dry resin was equilibrated in a rolling bottle for 20 hours with 50 ml of a solution containing 100 mg of gold, as well as 0,1 mol of sodium chloride or sodium hydroxide per litre. Solution was analysed for gold and resin for sodium, as described above.

*b) Kinetic Experiments*

Le Carbone G210 AS granular activated carbon, sized to between 2,07 and 1,16mm, was used. Cold water was used to thoroughly wash the carbon free of fines and soluble impurities before it was loaded with gold from a solution of potassium aurocyanide. The initial gold concentration on the carbon was about 1000 g/t, and was measured accurately as described earlier.

The majority of elution experiments were performed using the simple apparatus shown in Figure 2.5. A fluidized bed of carbon was located in a round-bottomed flask with heating mantle and reflux condenser. Fresh eluant solution was pumped into the reactor, which contained a fixed mass of carbon and volume of boiling solution. Eluate was removed by pumping from the top of the solution level at the same rate. Eluate portions were collected and analysed for gold content by atomic-absorption spectrophotometry, and the gold mass balance was checked periodically by analysis of gold on carbon by X-ray fluorescence spectrometry. Unless stated otherwise, the eluant solution contained 0,2 mol of sodium cyanide and 0,2 mol of sodium hydroxide per litre.

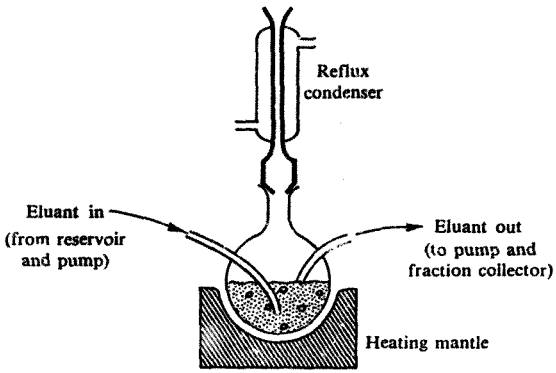


Fig. 2.5 Laboratory elution apparatus

Extraction of gold by an electrowinning cell having a single-pass extraction efficiency E was simulated as shown in Fig. 2 6. Outflow from the carbon bed, with a flowrate $V_1$ and gold concentration $S_{out}$, was diluted with fresh eluant pumped at a flowrate $V_2$. Both streams were mixed in a vessel, and the feed to the bed was pumped at the same flowrate ($V_1$) at which it was recovered from the bed. Solution was pumped from the mixing vessel at a flowrate equal to $V_2$ to maintain a constant volume in the vessel. Fractions were collected from this stream, and analysed. The single-pass extraction efficiency can be calculated from the flowrates as follows:

$$E = \frac{V_2}{V_1 + V_2} \qquad (2.3)$$

The concentration of gold in the feed to the carbon bed is then

$$S_{in} = S_{out} (1 - E) \qquad (2.4)$$

It is necessary to use this elaborate simulated electrowinning cell because in the case of an actual cell, physical sampling of eluant solution for analysis would require a large eluant reservoir. To calculate gold concentration on carbon, samples would have to be collected from three points at a time, as opposed to one in the system incorporating a simulated cell. Analysis involving a non-sampling technique such as UV spectrophotometry, which would also eliminate this problem, was also attempted. However, at the appropriate wavelength region of 240 nm, both hydroxide and cyanide absorb strongly, rendering the measurement inaccurate.

In experiments that employed a column rather than the round-bottomed flask used in the apparatus described above, carbon was placed in a jacketed column stoppered

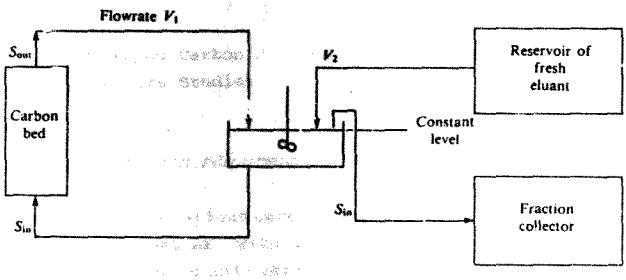


Fig. 2.6 **Simulation of the Zadra process by dilution**

with glass wool. Hot water was pumped through the jacket to attain a column temperature of 85°C. Eluant was pumped up through the carbon bed, and solution was removed from the top of the column at a rate equal to the inflow of solution. Fractions were collected and analysed for gold by atomic absorption spectrophotometry, as before.

## 2.6 Activated Carbon Surface Chemistry and Structure Studies

### *a) Carbons and Adsorbents Used*

The sources of the various carbons and adsorbents appear in Table 2.2, together with activation conditions of synthesized products and designated names. All commercial products were washed with copious amounts of cold de-ionized water to remove soluble impurities and fine particles, then oven-dried at 100°C, before use. All products were kept sealed in a desiccator.

### *b) Synthesis of Activated Carbons*

Samples of S-761 polymeric adsorbent were pyrolyzed under carefully controlled conditions similar to those described previously[62]. Samples of about 4 g were placed in porcelain boats and slid into a quartz tube, which in turn was inserted into a tubular furnace through which air, nitrogen, oxygen, steam or carbon dioxide was passed at a flowrate of 2 l/h. Temperature was controlled at all times by a programmable thermostat, as was the rate of temperature change. A typical pyrolysis programme is outlined below:

| | | | | | | | | |
|---|---|---|---|---|---|---|---|---|
| Time (h) | | 0,5 | | 0,5 | | 4 | final pyrolysis | |
| Temp (°C) | 25 | —> | 200 | —> | 200 | -> | temperature | |
| | | | | | | —> | 25 | |

**Table 2.2**

**Conditions of preparation of activated carbons studied**

| Carbon | Source | Supplier | Activation conditions | | |
|---|---|---|---|---|---|
| | | | Temperature | Atmosphere | Time,h |
| **Synthetic carbons** | | | | | |
| 25 | Pyrolysed S-761 Polymeric Adsorbent (phenyl-formalde-hyde matrix) | | 25 | air | 4 |
| 450 | | | 450 | | |
| 650 | | | 650 | | |
| 750 | | | 750 | | |
| 850 | | | 850 | | |
| 950 | | | 950 | | |
| 850/$H_2O$ | | | 850 | Steam | 1 |
| 850/$CO_2$ | | | 850 | $CO_2$ | |
| 850/$N_2$ | | | 850 | $N_2$ | |
| 850/1h | | | 850 | air | |
| **Commercial carbons** | | | | | |
| G210 | Coconut shell | Pica | H | | |
| RO3515 | Peat | Norit | H | | |
| AURC | Coal | Norit | H | | |
| Norit C | Wood | Norit | L | $H_3PO_4$ | |
| **Oxidized carbons** | | | | | |
| G210/$HNO_3$ | oxidized G210 | | H | | |
| G210/NaOCl | | | H | | |
| G210/$H_2O_2$ | | | H | | |
| G210/OX | | | H | | |
| Other | | | | | |
| Graphite | | Merck | H | | |
| XAD-8 | Acrylic polyester | Amberlite | L | | |
| S-761 | Phenol-formalde-hyde | Duolite | - | | |

As soon as the final pyrolysis temperature had been reached, the tube was taken out of the furnace and allowed to cool to room temperature, with the gas still flowing through. Pyrolysis products were stored in a desiccator.

*c) Oxidation of Activated Carbons*

Samples of G210 activated carbon were oxidized by four different techniques, as follows:

(i) **G210/$HNO_3$.** A 20 g sample of G210 was boiled for one hour in 250 ml of 1,0 M nitric acid, cooled and washed to neutrality with de-ionized water.

(ii) **G210/NaOCl.** A 20 g sample of G210 was boiled for one hour in 250 ml of 1,0 M NaOCl, cooled and washed to neutrality with de-ionized water.

(iii) **G210/OX.** A 20 g sample of G210 was boiled for two hours in 250 ml of 1:1 $HNO_3$(35%):$H_2SO_4$(99%), cooled and washed to neutrality with de-ionized water.

(iv) **G210/$H_2O_2$.** A 20 g sample of G210 was allowed to stand in 250 ml of a solution containing 20% (by mass) hydrogen peroxide, at ambient temperature (20°C) for one week.

*d) Synthesis of Polyxanthene and Polyquinone*

Polyxanthene was prepared using a method similar to that of McNeill and Weiss[63]. Phthalic anhydride (10 g), hydroquinone (7,432 g), pyromellitic dianhydride (14,723 g) and zinc chloride (9,199 g) were ground together to a fine powder and placed in a baffle furnace that was purged by nitrogen (2 l/h). The mixture was heated at 200°C for 48 hours and then at 250°C for 24 hours.

The product was ground and extracted with acetone in a Soxhlet extractor until the filtrate was colourless (10 days). Zinc was then leached out with 250 ml of a solution containing 4% (by mass) of hydrochloric acid for 24 hours. This was followed by Soxhlet extraction with water for six days, and drying at 60°C for 24 hours.

Polyquinone was prepared using a method similar to that of Pohl and Engelhardt[64]. Phthalic anhydride (10 g), anthracene (12,033 g) and zinc chloride (9,200 g) were ground together to a fine powder and placed in a baffle furnace that was purged with nitrogen (2 l/h). The mixture was heated at 200°C for 24 hours and then at 250°C for 24 hours.

The product was ground and extracted with ethanol in a Soxhlet extractor until the filtrate was colourless (6 days). Zinc was then leached out with 250 ml of a solution containing 4% (by mass) of hydrochloric acid for 24 hours. This was followed by Soxhlet extraction with water for three days and benzene for three days. The product was dried at 60°C for 24 hours.

*e) Adsorption of Aurocyanide*

A 0,25 g sample of adsorbent was contacted with 100 ml of a solution containing 300 mg of gold per litre, and either 0,033M $CaCl_2$, 0,1M HCl, or no additives. Adsorption took place in a rolling bottle for 20 hours. In the case of the acidic solutions for Norit RO3515 AURC and G210 granular carbons, the range of pyrolyzed S-761 carbons, as well as powdered graphite, Norit C, G210 and XAD-8, a 0,1 g sample was used so that a measurable amount of gold in solution could be obtained. Extraction efficiencies are reported for 0,1 g adsorbent throughout. Gold in solution was determined by atomic-absorption spectrophotometry (AAS).

*f) Techniques for the Characterization of Physical Properties*

Surface areas were measured by the $N_2$-BET method, and skeletal densities by helium pycnometry. Pore size distributions were measured by mercury displacement.

Conductivities of carbons and adsorbents were measured using a Hewlett-Packard 3478A multimeter connected to a conductivity cell constructed as shown in Figure 2.7. The cell consisted of two teflon cylinders, with copper disc electrodes (6 mm diameter) placed on male and female ends, as shown. Carbon was placed between the electrodes and a constant, accurately measured pressure of 500 N was placed on the cell using an Instron model 1175 press. The gap between the electrodes was typically between 2 and 4 mm, and was determined by the measurement of the distance x between the male and female parts of the cell in Figure 2.7, using a set of Vernier calipers. Measurement of this distance was made at three different points around the cell. Reported conductivities are the average of three separate determinations at different electrode gaps. The value obtained for graphite (603 S/cm) is somewhat lower than that reported in the literature[65] (727,3 S/cm). This is probably due to the fact that the literature measurements were made under much higher pressures[63,64], resulting in a greater degree of interparticle contact. Conductivities reported in this study are internally consistent and very reproducible, however, thereby allowing trends to be established.

X-ray diffractograms were obtained using a Philips PW1050/25 X-ray diffractometer with Cu $K_\alpha$ radiation.

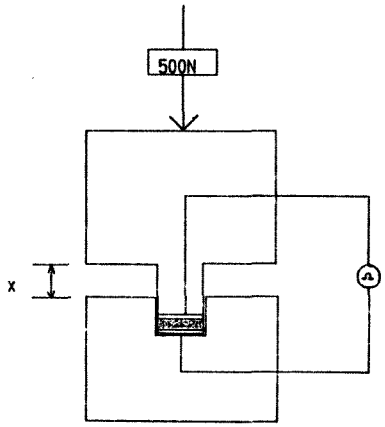


Fig. 2.7 Apparatus for the measurement of conductivity of carbons

g) *Techniques for the Characterization of Chemical Properties*

Infrared spectra of activated carbons, polymers and adsorbents were obtained using a Perkin-Elmer 1725X Fourier Transform Infrared Spectrophotometer. For each spectrum, 200 scans were made, at a resolution of 4 $cm^{-1}$.

Spectra of polymers and adsorbents were obtained using a diffuse reflectance (DRIFT) accessory. Vacuum-dried samples were pulverized for 5 minutes in a Spex 5100 Mixer/Mill before mixing 6 mg of adsorbent with 200 mg of dry KBr, by shaking manually for several seconds. Pure KBr was placed in the sample holder to obtain a background spectrum that was automatically subtracted, prior to obtaining spectra of the adsorbents.

Spectra of activated carbons were obtained using the instrument in the transmission mode, as described above. No mathematical smoothing functions were performed on the spectra.

The adsorption activities of activated carbons, polymers and adsorbents for phenol were determined using the method of Weber and Van Vliet[66]. A 0,1 g sample of adsorbent was placed in a rolling bottle for 20 hours with 100 ml of solution containing 0,5077 mM phenol in 0,005N $NaHCO_3$. Phenol was determined before and after contact by UV spectrophotometry at 268 nm, on a Beckman MIV Research ultraviolet-visible spectrophotometer.

Analysis of adsorbents for carbon and hydrogen were made using a Heraeus elemental analyser, and for oxygen using a Leco oxygen analyser.

Measurements of pH change in water were made using a Labion digital pH meter. A 0,1 g sample of adsorbent was contacted

with 10 ml of de-ionized water in a rolling bottle for twenty hours prior to re-measurement of pH.

Reduction potentials of activated carbons, polymers and adsorbents were determined by the method of McDougall *et al.*[32]. The carbon was immersed in a 0,01M NaCl solution which was kept at a pH of 5,0 for fifteen minutes. The potential was measured using a graphite rod electrode referenced against a saturated calomel electrode. The graphite rod electrode was contacted with the surface of a carbon particle and the potential measured. The average value for at least twenty particles was obtained in this manner.

## CHAPTER 3 THE MECHANISM OF ADSORPTION OF AUROCYANIDE ONTO ACTIVATED CARBON

The chemistry of adsorption of aurocyanide onto activated carbon has been the topic of much attention for seventy-five years but, despite the commercial importance of the process, no consensus has yet been reached regarding the mechanism of adsorption. These differences largely arise because activated carbon is not readily amenable to direct investigation by spectroscopic techniques. Thus, very little is known about surface properties of the adsorbent. For instance, identities of oxygen-containing organic functional groups formed on the carbon surface during activation remain uncertain, and the nature of the gold cyanide adsorbate has not been unequivocally established.

### 3.1 The Mechanism of Adsorption of Aurocyanide onto Activated Carbon - A Literature Review

The intention here is not to discuss the results of each of the relevant studies, but rather to summarize (i) the main observations that need to be explained, (ii) various theories that have been proposed to account for these observations, and (iii) to identify major inconsistencies present in current understanding of the system.

#### a) *Summary of Factors Influencing Adsorption of Aurocyanide onto Activated Carbon*

(i) As discussed earlier, activated carbons are popularly divided[24,29] into two groups : H or high-temperature carbons, formed at 700 to 1000°C, and L or low-

temperature carbons, formed at 300°C. Carbons useful for gold generally fall into the H category.

(ii) The extent of adsorption of aurocyanide onto carbon increases with increasing concentration of cations[32,62,67]. Cation type is also found[62] to influence the gold adsorption activity. Other factors that increase extent of extraction are low temperatures[32,62,67], and aeration of the solution[11].

(iii) The extent of adsorption of aurocyanide onto activated carbon is reduced with increasing concentration of anions[11] such as $CN^-$, $S^{2-}$, $SCN^-$ and $OH^-$. A neutral complex such as $Hg(CN)_2$ is found[32] to displace aurocyanide from activated carbon. A similar effect is found to occur with certain organic solvents[68] such as ethanol, acetone or acetonitrile.

(iv) The adsorption process is found[11] to be reversible; however, slow diffusion through the pore system of the carbon results in true equilibrium taking a long time (on the order of several months) to be reached. A pseudo-equilibrium, corresponding to adsorption in macropores and mesopores, is reached in about twenty-four hours. It is found[68] that adsorbed aurocyanide transfers spontaneously between activated carbon particles in contact with one another.

### b) *Summary of Mechanisms Postulated for Adsorption of Aurocyanide onto Activated Carbon*

A number of mechanisms have been proposed over the years, but all of them, in their simplest form, reduce to one of the following:

(i) adsorption of aurocyanide without chemical change[3,7,11,32,62,67-74]

(ii) adsorption of aurocyanide with decomposition of $Au(CN)_2^-$ to AuCN[3,73-75], or

(iii) adsorption of aurocyanide with reduction of gold(I) either to gold metal or to a partially reduced state between gold(I) and gold [32,76].

The first mechanism can be subdivided further into adsorption by simple coulombic ion exchange[69,70,72-75], or adsorption involving ion-pair formation[3,7,11,32,62,67,71]. In some cases a dual mechanism has been proposed, such as initial adsorption by ion-exchange interaction followed by decomposition to AuCN[73,74].

The literature pertaining to the subject was critically reviewed by McDougall and Hancock[77] in 1981 and, more recently, by McDougall and Fleming[11], who concluded that the most likely mechanism of gold loading under typical CIP operating conditions is the adsorption of aurocyanide without chemical change. Moreover, they suggested that adsorption probably occurred by a mechanism first proposed by Kuzminykh and Tyurin[71], which involved the extraction of ion pairs of the type $M^{n+}[Au(CN)_2^-]_n$, where $M^{n+}$ = $Na^+$, $K^+$, $Ca^{2+}$, $Mg^{2+}$, etc. at high pH values, and where $M^{n+} = H^+$ in acidic solution. Further evidence for this mechanism was provided by Adams[22,62].

c) *Summary of Major Inconsistencies Present in Modern Theories of Adsorption of Aurocyanide onto Activated Carbon*

A study of the relevant literature indicates that none of the theories proposed for the mechanism of adsorption of aurocyanide onto activated carbon are entirely consistant with all known facts. The nature of the adsorbed species has yet to be elucidated completely - for example, the

analysis of loaded carbons for cations, gold and nitrogen[32,75] are not always consistent with the simple ion-pair species discussed above. The possibility also exists that studies on different carbons under different conditions could result in various adsorption mechanisms holding under various conditions. It is a major challenge to explain all the observations in terms of a reasonable mechanism. Direct evidence from instrumental techniques would undoubtedly aid this task considerably.

The bonding mechanism between the adsorbed gold species and the activated carbon surface has been studied by direct techniques such as X-ray Photoelectron Spectroscopy (XPS)[32] and Electron Spin Resonance (ESR)[62] spectroscopy. The conclusions arrived at in general indicate some form of charge-transfer interaction between the gold species and the carbon surface[62]. This could be dependent on specific types of active sites being present. This aspect is important for an understanding of the process.

Other aspects of the chemistry involved in the adsorption process remain poorly understood. These include the effects of cations, oxygen bubbling, acid and base treatment, the various properties of the carbon, as well as the desorption of aurocyanide by various species.

The aim here is to provide a self-consistent adsorption mechanism that accounts for all observations presented in the literature. Interpretation of results in terms of preconceived ideas, and neglect of observations of other authors has greatly contributed to the current disagreement in the literature.

### 3.2 Novel Studies on the Nature of the Adsorbed Species

Recently, Adams and Fleming[76] showed from elemental analyses that the ion-pair species $K^+[Au(CN)_2^-]$ and

$Ca^{2+}[Au(CN)_2^-]_2$ are loaded from 0,5 M KCl and $CaCl_2$ solutions, respectively. Another experiment, by careful monitoring of $K^+$, $Au(CN)_2^-$, $H^+$ and $Cl^-$ concentrations in solution and on the carbon, suggested that under slightly acidic conditions (pH 3) from low ionic strength solutions (i.e., no supporting electrolyte added), gold is extracted by the following ion-pair mechanism:

$$Au(CN)_2^- (aq) + H^+ (aq) \rightleftharpoons HAu(CN)_2 (ads) \qquad (3.1)$$

$$Au(CN)_2^- (aq) + K^+ (aq) \rightleftharpoons K^+[Au(CN)_2^-] (ads) \qquad (3.2)$$

$$H^+Cl^- (ads) + Au(CN)_2^- (aq) \rightleftharpoons HAu(CN)_2 (aq) + Cl^- (aq) \qquad (3.3)$$

the possibility that other mechanisms may be prevalent under different conditions will be examined in this Chapter.

*a) Effect of Gold Concentration on the Carbon on the Nature of the Adsorbed Species*

McDougall *et al.*[32] based their suggestion that some decomposition of aurocyanide takes place at high loadings of gold on carbon, on nitrogen micro-analyses of carbons loaded in the presence of acid or cations. Table 3.1 presents results for potassium, gold, and nitrogen loaded onto carbons from 0,1 M potassium chloride, and 0,1 M hydrochloric acid solutions.

The stoichiometry conforms to that of $KAu(CN)_2$ for carbons loaded from 0,1 M potassium chloride solutions, even at high gold loadings. However, there is less nitrogen present on acid-loaded carbons, suggesting that decomposition of the $Au(CN)_2^-$ occurs to some extent, particularly at high gold loadings:

$$H^{+} + Au(CN)_2^{-} \rightarrow AuCN + HCN(\uparrow) \qquad (3.4)$$

Evidence for the presence of partially polymerized AuCN species on acid-treated carbons was recently[79] invoked from XPS studies.

**Table 3.1**
**Analysis for potassium, gold, and nitrogen on carbons loaded from 0,1M potassium chloride and 0,1M hydrochloric acid**

Conditions
Carbon mass 1,0 g
solution volume 400 ml
initial gold in solution 50 to 700 mg/l
time 72 h

| Gold on loaded carbon, wt % | Loading conditions | Elemental analysis, mmol/g K | Au | $\frac{1}{2}$N[a] |
|---|---|---|---|---|
| 2,02 | 0,1M KCl | 0,107 | 0,103 | 0,100 |
| 3,47 | | 0,146 | 0,176 | 0,196 |
| 5,25 | | 0,261 | 0,267 | 0,299 |
| 8,15 | | 0,488 | 0,414 | 0,471 |
| 8,95 | | 0,442 | 0,454 | 0,489 |
| 2,03 | 0,1M HCl | | 0,103 | 0,075 |
| 3,85 | | | 0,195 | 0,125 |
| 6,93 | | | 0,352 | 0,275 |
| 13,5 | | | 0,685 | 0,485 |
| 16,3 | | | 0,853 | 0,625 |

[a] Value for N is corrected for the nitrogen value of the non-loaded carbon (0,25 wt %; 0,178 mmol/g)

This explanation is substantiated by the strong smell of hydrocyanic acid exuded by the reaction bottles when gold was loaded to very high values from acid solution.

Moreover, previous[80] evidence obtained by X-Ray diffractometry (XRD) has shown that reaction (3.4) occurs to some extent when aurocyanide is adsorbed from acidic medium by polymeric adsorbent resins.

*b) Elution of Aurocyanide from Activated Carbon with Sodium Hydroxide*

Hydroxide ion does not form a stable complex with gold, so a sodium hydroxide solution would not be expected to elute from the carbon any gold that was present in the form of AuCN or metallic gold (or gold in a partially reduced state). Experiments were therefore carried out in which fresh sodium hydroxide solution was pumped continuously through a heated (90°C) column of loaded carbon until the concentration of gold in the spent eluate decreased below the detection limit (less than 0,1 mg/l). The results are presented in Table 3.2, which shows that gold can be eluted almost completely from carbon with a sodium hydroxide solution containing no cyanide. Moreover, this can be achieved with carbons loaded under both acidic and alkaline conditions, and with carbons loaded to very high gold concentrations.

Elution efficiencies for the carbons loaded from acidic solutions are somewhat lower than those loaded from potassium chloride solutions. This is consistent with the conclusions based on the micro-analysis data presented in Table 3.1. (Note that under typical plant conditions of a gold loading of 0,5 to 2 per cent from solutions of pH 10,5, the presence of AuCN on the carbon can be ruled out.)

**Table 3.2**
**Elution of aurocyanide from activated carbon with 0,1 M sodium hydroxide at 90°C**

Conditions
Carbon mass 1,0g
solution volume 400 ml
initial gold in solution 50 to 700 mg/l
time 72 h

| Gold on loaded carbon, % | Loading conditions | Elution efficiency % |
|---|---|---|
| 0,925 | 0,1M KCl | 97,6 |
| 3,71 | | 99,8 |
| 5,25 | | 98,5 |
| 8,15 | | 98,4 |
| 0,925 | 0,1M HCl | 96,8 |
| 6,93 | | 90,5 |
| 13,5 | | 87,3 |
| 16,8 | | 83,8 |

Two further batch elution experiments were carried out with 0,1 M sodium hydroxide, and the spent eluates were analysed for gold (by AAS) and for aurocyanide (by UV spectrophotometry). The results are presented in Table 3.3 and show that all the gold is present in the eluate as the aurocyanide ion, with the differences between the values obtained by the two methods being within the limits of accuracy of the techniques. Since there was no free cyanide present in the eluate, the eluted gold must have been loaded onto the carbon in the form of the aurocyanide ion. (The instance in which the loaded carbon was treated with boiling hydrochloric acid prior to elution will be discussed in detail in the following section.)

Table 3.3
Analyses of sodium hydroxide eluates
for $Au(CN)_2^-$ and Au after elution

Elution conditions:
0,2M NaOH, 95°C, 2 h

| Pre-treatment of loaded carbon | Analysis of eluate, mol/l | |
|---|---|---|
| | UV for $Au(CN)_2^-$ | AA for Au |
| None | $3,70 \times 10^{-4}$ | $4,15 \times 10^{-4}$ |
| | $3,78 \times 10^{-4}$ | $3,44 \times 10^{-4}$ |
| Washing with 1 M HCl at 95°C for 6 hours followed by washing with water | $5,10 \times 10^{-4}$ | $5,35 \times 10^{-4}$ |

These observations preclude the AuCN mechanism, but not the anion-exchange mechanism. Perhaps the most compelling evidence against the anion-exchange mechanism was the observation[32,80] that, while the presence of excess perchlorate anions was severely detrimental to the distribution of aurocyanide in the anion-exchange resin IRA-400 (as might be expected for the large, highly polarizable $ClO_4^-$ anion), only a slightly decreased distribution of aurocyanide was found for carbon[62].

In addition, the well-known effect of ionic strength on adsorption of aurocyanide onto activated carbon[21,57,68] and, in particular, the sensitivity of adsorption to type of cation in solution[62], are phenomena that can be explained more convincingly by the ion-pair mechanism than by an ion-exchange mechanism.

c) *Effect of the Treatment of Loaded Carbon with Hot Acid on the Nature of the Adsorbed Gold Species*

Periodic treatment of loaded carbon with hot acid solutions has been suggested by several workers as a procedure that enhances the gold-loading capabilities of carbon. Davidson and Veronese[81] proposed that, prior to elution, loaded carbon should be treated with acid to remove calcium carbonate, which is known to foul carbon in adsorption circuits, and which can have a deleterious effect on efficiency of elution. This procedure is currently in use on most CIP plants[1]. McDougall[82] patented a process whereby carbon is periodically removed from the adsorption circuit, treated with hot acid, and then returned to the adsorption circuit. It is claimed[82] that this treatment converts aurocyanide to the insoluble AuCN species, which is thereby excluded from the adsorption equilibrium, allowing the carbon to be loaded to higher gold values.

(i) SEM and XRD studies of gold species on carbons subjected to acid and base treatments

In the previous section (Table 3.3) it was shown that treatment of loaded carbon with hot hydrochloric acid (prior to elution with hot sodium hydroxide) had virtually no effect on the form of the aurocyanide complex eluted from the carbon. However, it can be seen from the results in Figure 3.1 that pre-treatment of the carbon with boiling hydrochloric acid for different lengths of time results in a progressive decrease in the efficiency of gold elution with hot sodium hydroxide, indicating that some of the gold on the carbon is converted to a species other than aurocyanide. Moreover, the loss in efficiency reaches a plateau after 2 hours, corresponding to 50 per cent elution efficiency. Even after prolonged treatment with boiling acid, it is still possible to elute 50 per cent of the gold

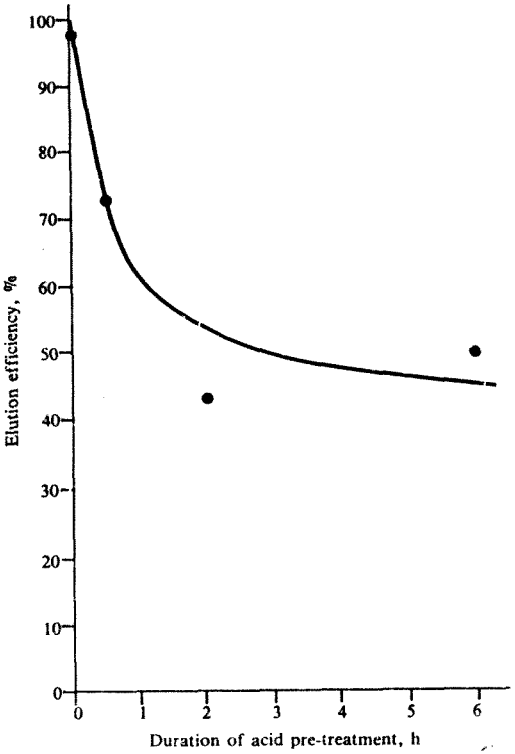


Fig. 3.1 Effect of duration of acid pre-treatment on the efficiency of the elution of gold from activated carbon with a sodium hydroxide solution
(Conditions: 4 per cent (m/m) hydrochloric acid pretreatment at 95°C followed by elution with 0,1 mol/l sodium hydroxide at 90°C)

with sodium hydroxide, and this appears in the eluate as the aurocyanide ion (Table 3.3).

These samples of carbon were examined by XRD and SEM after being boiled in acid, and again after subsequent elution with a hot caustic solution. It was found that no discrete particles or crystals of AuCN or metallic gold could be detected on the carbon surface after treatment with hot acid (Figure 3.2a). However, after the same carbon sample had been eluted with hot sodium hydroxide, metallic gold, in the form of large crystalline particles, was observed on the carbon surface (Figure 3.2b). The metallic nature of the particles was confirmed by XRD. Interestingly, many of the particles on the carbon that had been boiled in acid for only 30 minutes were larger (5μm, Figure 3.3a), than those on the carbon that had been boiled for 6 hours (1μm, Figure 3.2b). At even higher magnification (Figure 3.3b), the remarkable dendritic structure of the crystals can be clearly seen.

Another interesting difference between these carbons is evident from the micrographs in Figure 3.4. Gold crystals of uniform size are distributed fairly evenly throughout the particle of carbon that was acid-boiled for 6 hours (Figure 3.4a), whereas a preponderance of gold crystals is situated along the particle edge (Figure 3.4b) and around the major features (Figure 3.3a) of carbon that was boiled in acid for 30 minutes. Moreover, the crystals vary in size in this case.

These results can be rationalized by consideration of the values for standard reduction potentials, calculated from experimental equilibrium constants[83-85] (see Appendix 1):

$$AuCN + e^- \rightarrow Au^0 + CN^- \qquad (E^0 = -0,166V) \quad (3.5)$$

$$2AuCN + e^- \rightarrow Au^0 + Au(CN)_2^- \qquad (E^0 = 0,252V) \quad (3.6)$$

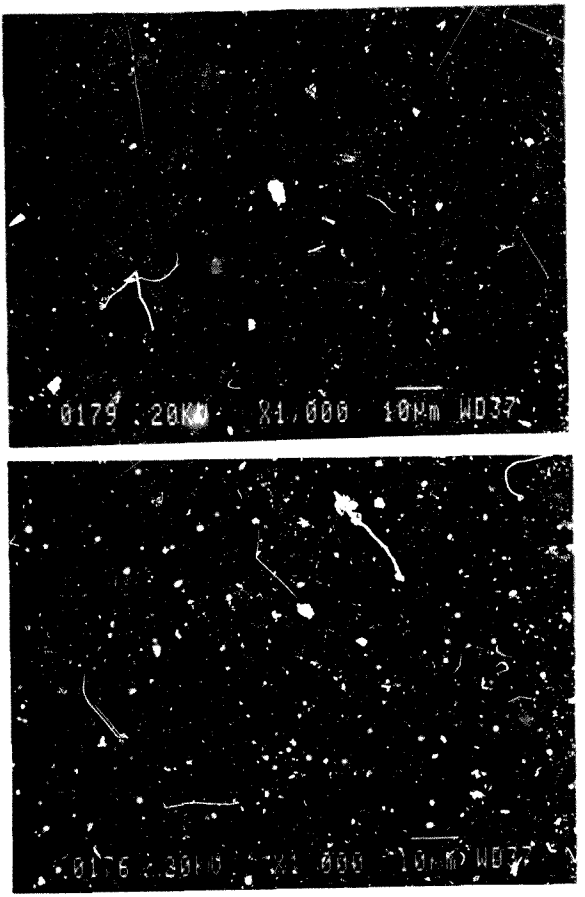


Fig. 3.2 SEM micrographs of activated carbon surfaces after

(a) acid pre-treatment for 6 hours (4 per cent hydrochloric acid at 95°C), and

(b) acid pre-treatment for 6 hours followed by elution with sodium hydroxide (0,1 mol/l) at 90°C

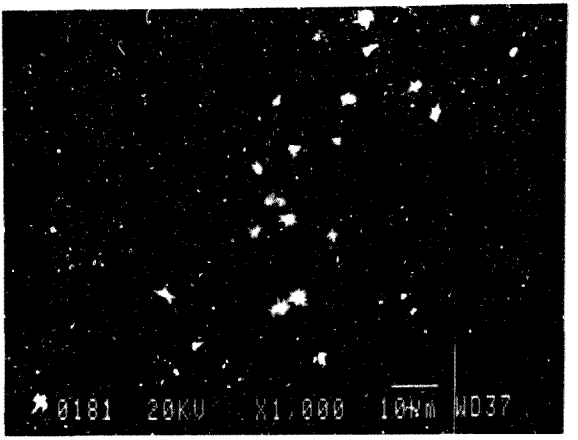


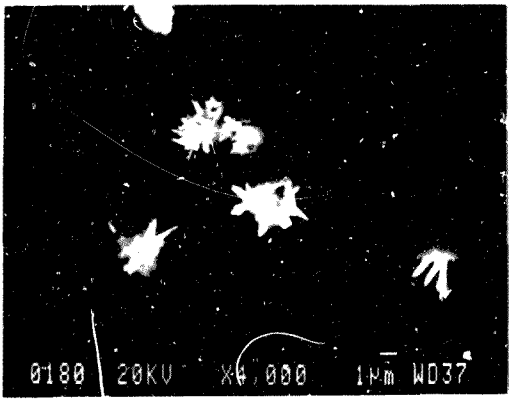


Fig. 3.3 SEM micrographs of activated carbon surfaces after pre-treatment for 30 minutes with 4 per cent hydrochloric acid at 95°C followed by elution with sodium hydroxide (0,1 mol/l) at 90°C

(a) Gold crystals concentrated in a macropore, and

(b) a magnified portion of (a), showing the dendritic structure of the crystals


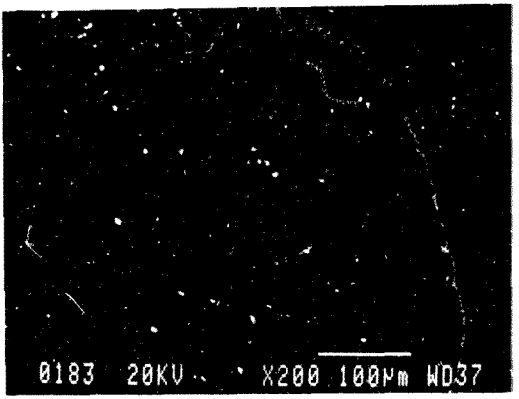


Fig. 3.4 SEM micrographs of activated carbon particles after

(a) pre-treatment for 6 hours with 4 per cent hydrochloric acid at 95°C followed by elution with sodium hydroxide (0,1 mol/l) at 90°C, and

(b) acid pre-treatment for 30 minutes followed by elution with sodium hydroxide

Activated carbons are known[32] to have reduction potentials between 0,40 and 0,08 V (versus SHE), so AuCN molecules in close proximity to one another on the carbon surface could theoretically be reduced in accordance with Equation (3.6). On that basis, it would be possible to strip only about 50 per cent of the gold from the carbon with sodium hydroxide (as confirmed by Figure 3.1), and the gold would appear in solution as the aurocyanide ion (as confirmed by Table 3.3). Moreover, the remaining 50 per cent of the gold would remain on the carbon in the form of the metal (as confirmed by Figure 3.2).

It is proposed, therefore, that aurocyanide on activated carbon is converted to AuCN (Equation 3.7) by boiling of the carbon in acid for about 2 hours.

$$Au(CN)_2^- \text{ (ads)} + H^+ \text{ (aq)} \rightarrow AuCN \text{ (ads)} + HCN \text{ (g)} \qquad (3.7)$$

The exact nature of the adsorbed AuCN is not clear at this stage, since no polymeric AuCN could be observed on the acid-boiled carbon by XRD or SEM (Figure 3.2a). This aspect will be addressed later in this Chapter.

When the carbon is subsequently treated with hot sodium hydroxide, the AuCN decomposes according to Equation (3.6). This reaction occurs only in alkaline solution and not after treatment with boiling acid, and moreover, the intensities of the X-ray diffraction peaks for metallic gold in carbon samples that had been boiled in sodium hydroxide (0,1 mol/l) for 2 hours, were very similar to those for carbon samples that had been washed at room temperature in sodium hydroxide solution overnight. In contrast, when the carbon was boiled in water instead of sodium hydroxide after the treatment with hot acid, no X-ray diffraction peaks for metallic gold were observed. This reaction is studied in more detail in the following section.

Further proof of a mechanism involving Equation (3.6) is found in a study of the rate of elution. Elution kinetics have been modelled in this Thesis (see Chapter 5), the elution rate being proportional to the concentration on the carbon of gold that can be eluted. Since AuCN and metallic gold cannot be eluted by hydroxide, a decrease in the elution rate could be ascribed to the presence of one of these species. The results presented in Table 3.4 show that the rate of elution is enhanced slightly when the loaded carbon is treated with cold hydrochloric acid prior to elution with sodium hydroxide. This gold, therefore, cannot be in the form of AuCN and must be present as $HAu(CN)_2$. However, the rate of elution is halved after the carbon has been boiled in acid prior to elution with sodium hydroxide, and this is consistent with the conversion of 50 per cent of the aurocyanide to the metal via reaction (3.6).

**Table 3.4**
**Effect of pre-treatment of carbon with hydrochloric acid on the rate of elution of gold with sodium hydroxide**

Elution conditions
0,2M NaOH, 95°C

| Pre-treatment | Rate of elution of gold mg/h |
|---|---|
| None | 1,47 |
| 0,1 M HCl, 25°C, 24h | 1,61 |
| 1 M HCl, 95°C, 1h | 0,79 |

(ii) Mössbauer spectroscopic study of gold species on carbons subjected to acid and base treatments

Gold-197 Mössbauer spectroscopy can provide detailed information regarding the oxidation state, bonding and electronic environment of gold atoms in a sample. Parameters for a range of gold compounds are plotted in Figure 2.3, and separate correlation bands for gold(I) and gold (III) compounds are evident. Cashion and co-workers[39,40] have made Mössbauer measurements of aurocyanide loaded onto activated carbon and found the characteristic quadrupole due to $Au(CN)_2^-$ to be present, adding weight to the theory that aurocyanide adsorbs onto activated carbon without chemical change.

Figure 3.5 shows the Mössbauer spectrum of a carbon that was loaded with aurocyanide to 5% gold (m/m) and subsequently boiled in 4% hydrochloric acid for three hours. The spectrum shows two distinct quadrupoles, with isomer shifts and quadrupole splittings that can be readily assigned to $Au(CN)_2^-$ and AuCN species (see Table 3.5).

With a knowledge of the Debye-Waller factors for adsorbed species, it is impossible to arrive at a quantitative description of the system; however, this assignment is entirely consistent with the conclusions of the previous section, i.e. that reaction (3.4) is occurring.

Klauber[79] has suggested from XPS studies that $Au_4(CN)_5^-$ oligomers are present on the carbon surface after acid washing. This suggestion is consistent with the fact that XRD peaks due to polymeric AuCN are absent from such carbons, and it is likely that $Au_4(CN)_5^-$ represents an average chain length, rather than an isolated species. It is possible that the microporosity of the carbon plays an

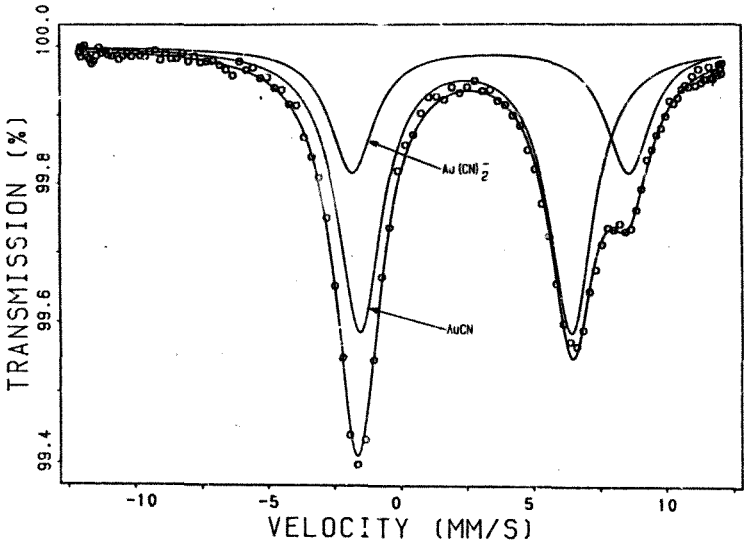


Fig. 3.5 $^{197}$Au Mössbauer spectrum of aurocyanide loaded onto carbon and subsequently boiled in 4% hydrochloric acid for 3 hours. Solid lines represent fitted curves

**Table 3.5**
**Mössbauer spectral parameters for gold species on activated carbons and gold compounds**

| Absorber | Isomer shift (IS) mm/s | Quadrupole splitting (QS) mm/s | Ref. |
|---|---|---|---|
| Carbon loaded with aurocyanide and subsequently boiled in 4% HCl for 3 hours. | 3,37 | 10,40 | |
| | 2,44 | 7,96 | |
| Above sample subsequently boiled in 0,1M NaOH for 3 hours. | 3,49 | 10,40 | |
| | -1,21 | 0,00 | |
| $KAu(CN)_2$ | 3,05 | 9,80 | 44 |
| | 3,23 | 10,21 | 44 |
| | 3,10 | 10,21 | 44 |
| | 3,12 | 10,21 | 44 |
| AuCN | 2,3 | 8,0 | 39 |
| Au | -1,23 | 0 | 39 |
| $HAuCl_4.4H_2O$ | 0,64 | 0,94 | 39 |
| AuCl | -1,4 | 4,5 | 39 |

important role in the reaction, by limiting the AuCN chain length within the micropore. The reaction could be represented thus:

$$(x+1)\ HAu(CN)_2 \rightleftharpoons HAu_{x+1}(CN)_{x+2} + x\ HCN(\uparrow) \qquad (3.8)$$

The Mössbauer spectrum of the resultant species in Equation (3.8) would be indistinguishable from separate $Au(CN)_2^-$ and AuCN species, since the NC-Au-CN and the CN-Au-CN electronic environments occur in both scenarios.

It is noteworthy that Mössbauer spectra of carbons loaded under acidic conditions and subjected to moderate drying, display an additional Mössbauer quadrupole that is attributed[86] to $Au(CN)_2Cl_2^-$. The reaction that evidently occurs under these conditions is the oxidation reaction

$$Au(CN)_2^- + 2Cl^- \rightleftharpoons Au(CN)_2Cl_2^- + 2e^- \qquad (3.9)$$

The standard reduction potential for this reaction can be calculated to be $E^0 = +0,97V$. The electrons could be provided by the reduction of oxygen (activated carbons contain both chemisorbed and physisorbed oxygen):

$$O_2\ (g) + 2H^+\ (aq) + 2e^- \rightleftharpoons 2H_2O \qquad (3.10)$$

$$(E^0 = 1,23\ V)$$

Activated carbons are known[87] to act as oxidation catalysts, and this factor may also play a role. Moreover, carbons that have been loaded with gold in the presence of an acid such as HCl, retain some adsorbed HCl[78], providing the proton in Equation (3.10). Both half-reactions (3.9) and (3.10) would benefit from an increase in HCl concentration in the carbon pores, such as would occur upon moderate drying. This could explain why the oxidation is only evident after some drying has occurred. The lack of such a species being evident in Figure 3.5 is probably a

manifestation of reaction (3.8) being driven nearly to completion by the evolution of gaseous HCN.

The Mössbauer spectrum of the carbon shown in Figure 3.5, subsequently boiled in sodium hydroxide solution (0,1 mol/l) for three hours, is shown in Figure 3.6. The spectral parameters appear in Table 3.5, and can be unequivocably assigned to metallic gold and $Au(CN)_2^-$, once again in agreement with Equation 3.6. As discussed earlier, the peak intensities are proportional not only to concentration of the particular species, but also to the Debye-Waller f-factor for the species. The Debye-Waller factors for several gold compounds appear in Table 3.6 below.

The f factor for metallic gold is an order of magnitude higher than that for $KAu(CN)_2$, suggesting that the ratio of Au to $Au(CN)_2^-$ is on the order of 1, as predicted by Equation (3.5). Figure 3.7 shows a scaled-up view of the $Au(CN)_2^-$ quadrupole in Figure 3.6, verifying the presence of this species.

Table 3.6
Debye-Waller factors for some gold compounds
(after Cohen *et al.*[88])

| Compound | f |
|---|---|
| Au | 0,19 |
| AuCN | 0,095 |
| $KAu(CN)_2$ | 0,015 |
| $KAu(CN)_4$ | 0,059 |

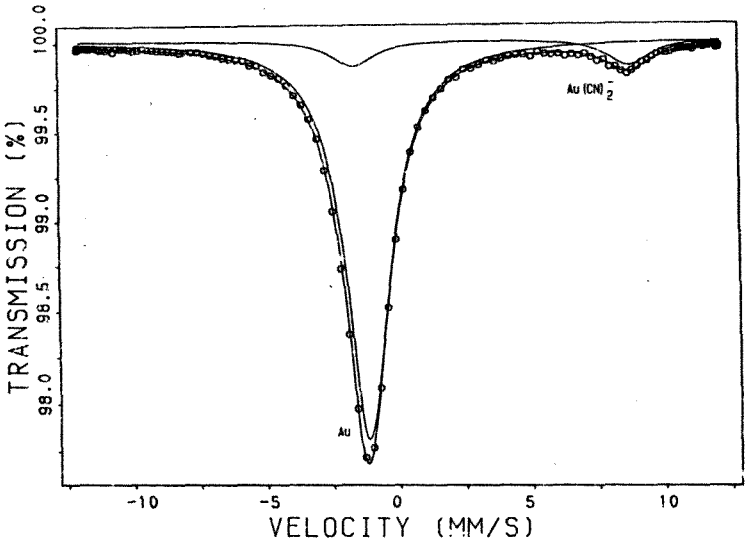


Fig. 3.6 $^{197}$Au Mössbauer spectrum of the activated carbon sample shown in Fig. 3.5 that was subsequently boiled in 0,1M sodium hydroxide solution for 5 hours

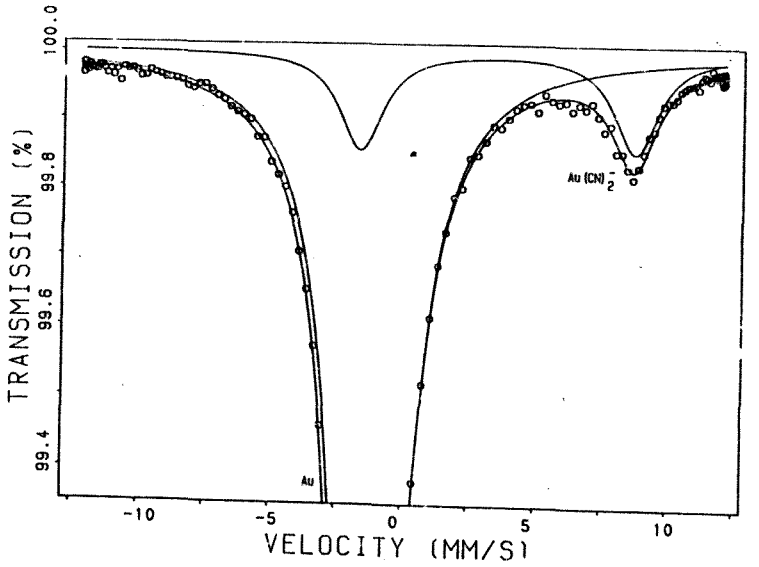


Fig. 3.7 $^{197}$Au Mössbauer spectrum shown in Fig. 3.6, showing detail of quadrupole assigned to $Au(CN)_2^-$

### (iii) Kinetics of AuCN precipitation from aqueous solution

In the previous section, it was suggested that reaction (3.6) had occurred to completion after about two hours of reaction. The work presented in the present section serves as a comparison between the kinetics of precipitation on the carbon surface and in aqueous solution, rather than a definitive study of the reaction. Figure 3.8 shows that at 95°C, complete precipitation of AuCN from a solution containing 0,005 mol/l $KAu(CN)_2$ in 0,1 mol/l HCl is attained in a similar time interval, providing additional evidence for the proposed reaction scheme. The kinetics were found to be first order, and rate constants were obtained from the slope of plots of ln $[Au(CN)_2^-]$ against time. Figure 3.9 shows an Arrhenius plot of the data, from which an activation energy $E_a$ = 72,5 kJ/mol can be calculated, via the Arrhenius equation

$$k = e^{-Ea/RT} \qquad (3.11)$$

where R is the gas constant, and T is the temperature.

### (iv) Decomposition of AuCN in aqueous solution

In section (ii), the observation was made that reaction (3.6) occurs not only on the carbon but also when solid polymeric AuCN is contacted with alkaline solution. This is interesting because, unlike the situation where activated carbon is present and acts as a reductant, there is no immediately obvious reducing agent present in the absence of carbon.

To explore this reaction further, AuCN was contacted with aqueous solutions varying in pH and temperature, that were analysed for gold, cyanide and cyanate. The results are

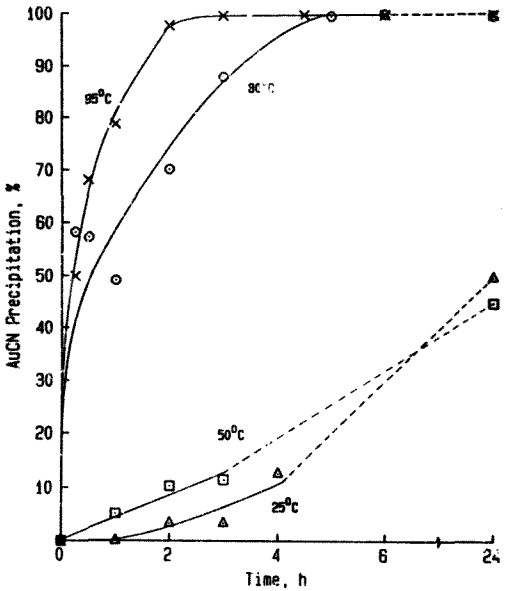


Fig. 3.8 **Kinetics of AuCN precipitation from aqueous solution at various temperatures**

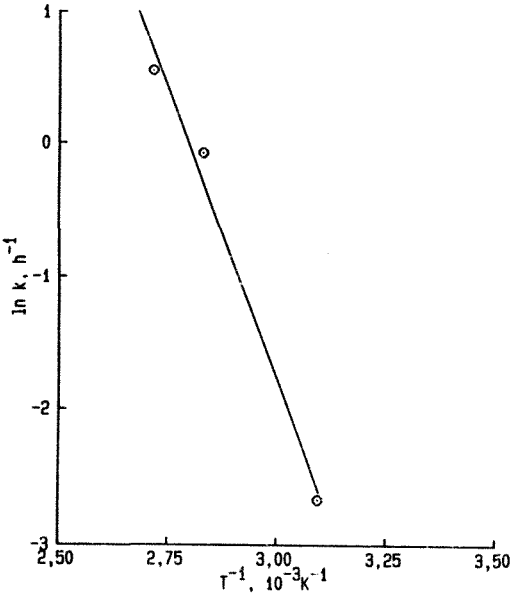


Fig. 3.9 **Arrhenius plot of data for the precipitation of AuCN from aqueous solution**

shown in Table 3.7. AuCN was found to be stable at 20°C at pH values of less than 12. Some gold was found to dissolve at a pH value of 13, and this amount increases dramatically at 95°C. The UV spectra of the resultant solutions are shown in Figure 3.10, which show the characteristic bands for $Au(CN)_2^-$ at 239 nm and 229 nm, confirming the fact that aurocyanide is one of the products.

**Table 3.7**
**Decomposition of AuCN in aqueous solution**

| pH | Temperature °C | Concentration, mmol/l | | |
|---|---|---|---|---|
| | | Au | $CN^-$ | $CNO^-$ |
| 1 | 20 | 0,003 | <0,02 | <0,02 |
| 3 | 20 | 0,001 | <0,02 | <0,02 |
| 5 | 20 | 0,004 | <0,02 | <0,02 |
| 7 | 20 | 0,005 | <0,02 | <0,02 |
| 9 | 20 | 0,005 | <0,02 | <0,02 |
| 11 | 20 | 0,010 | <0,02 | <0,02 |
| 13 | 20 | 1,428 | <0,02 | <0,02 |
| 13 | 95 | 2,215 | <0,02 | 0,428 |

The fact that, as well as $Au(CN)_2^-$, a substantial amount of cyanate was detected in the pH 13 solution that had been boiled is evidence that the oxidation half-reaction corresponding to the reduction reaction (3.6) is the oxidation of cyanide to cyanate:

$$CN^- + 2OH^- \rightleftharpoons CNO^- + H_2O + 2e^- \quad (E^0 = -0,97V) \qquad (3.12)$$

A comparison with the reduction potential for reaction (3.6) (i.e. $E^0 = 0,252V$), shows that this reaction scheme is thermodynamically feasible. The fact that the cyanate

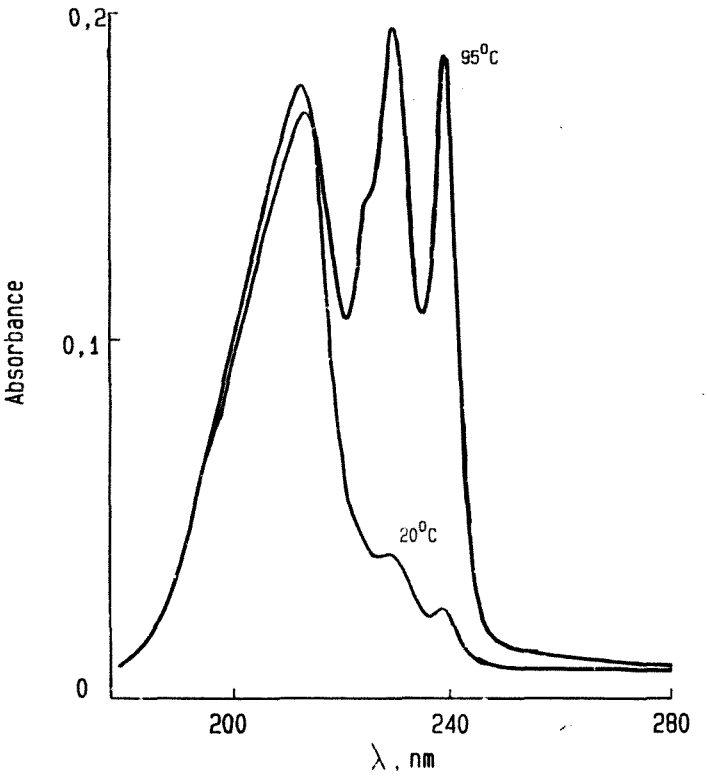


Fig. 3.10 **Ultraviolet spectra of aqueous solutions in contact with polymeric AuCN under various conditions**

concentration is markedly smaller than the gold concentration in this solution is probably due to the catalytic oxidation of cyanate to ammonia and carbon dioxide[89], particularly at high temperatures.

Further proof for these hypotheses is gained from an X-ray diffractometric examination of solid residues at the end of the reaction. Figure 3.11 shows the X-ray diffractograms of residues from the reactions at high pH values. At pH 11, the residue consists of AuCN, with only a negligible Au peak at a $2\theta$ value of 38°. The contribution due to metallic gold is somewhat higher at a pH value of 13, and upon boiling at pH 13, the majority of the AuCN is converted to the metallic form, with only a small AuCN peak remaining. From the solution gold concentration of 2,215 mmol/l, it can be calculated that 28 per cent of the gold, i.e. approximately one-third, had dissolved as $Au(CN)_2^-$. All of these facts are consistent with the following reaction scheme:

$$2AuCN + 2e^- \rightleftharpoons 2Au^0 + 2CN^- \qquad (E^0 = -0,166V) \quad (3.13)$$

$$CN^- + 2OH^- \rightleftharpoons CNO^- + H_2O + 2e^- \qquad (E^0 = -0,97V) \quad (3.14)$$

---

$$2AuCN + 2OH^- \rightleftharpoons 2Au^0 + CN^- + CNO^- + H_2O \qquad (3.15)$$

$$AuCN + CN^- \rightleftharpoons Au(CN)_2^- \qquad (3.16)$$

---

$$3AuCN + 2OH^- \rightleftharpoons 2Au^0 + Au(CN)_2^- + CNO^- + H_2O \qquad (3.17)$$

From a knowledge (see Appendix 1) of $K = 1,205 \times 10^7$ for reaction (3.16), the equilibrium constant for reaction (3.17) can be calculated to be $K = 4,02 \times 10^{13}$. Moreover, the equilibrium constant for the equivalent reaction in neutral solutions, i.e.

$$3AuCN + H_2O \rightleftharpoons 2Au^0 + Au(CN)_2^- + CNO^- + 2H^+ \qquad (3.18)$$

can be calculated to be $K = 0,402$. These values are a reflection of the fact that an increase in hydroxide concentration will push the equilibrium to the right. The

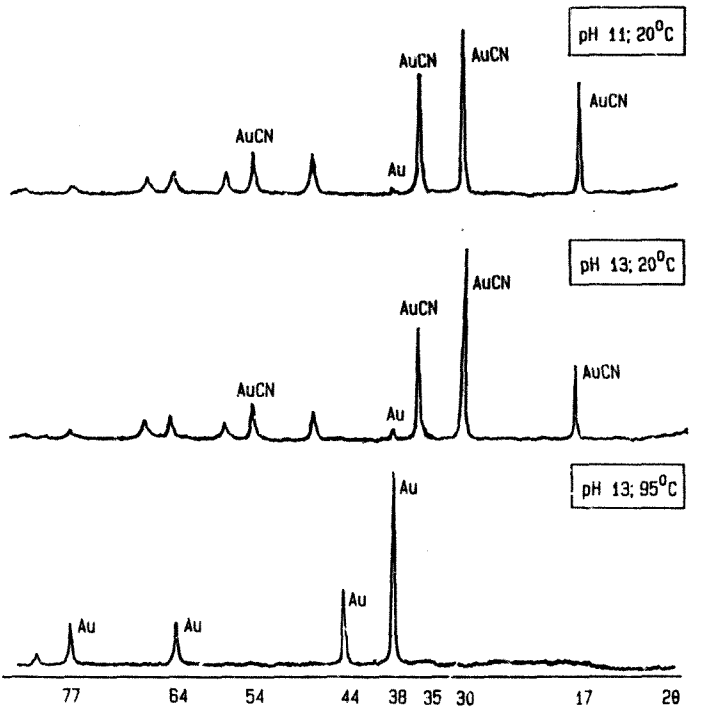


Fig. 3.11 X-ray diffractograms of solid residues resulting from the contact of polymeric AuCN with aqueous solutions under various conditions

calculated values of K indicate that the reaction should occur to a significant extent only in alkaline solutions, which is consistent with the experimental results shown in Table 3.7

The fact that about half of the gold could be eluted from the carbon as $Au(CN)_2^-$ does not seem to be consistent with the stoichiometry required for reaction (3.17), i.e. more $Au(CN)_2^-$ is forming than predicted. This observation is explicable in terms of the Mössbauer result (Figure 3.5), which indicated an apparent incomplete conversion of $Au(CN)_2^-$ to AuCN upon acid-boiling for three hours, due to the formation of short-chain oligomers such as $Au_4(CN)_5^-$, as proposed by Klauber[79]. This average chain-length is also consistent with the N/Au ratios presented in the following section. It is noteworthy that this average stoichiometry, when taken in conjunction with Equation (3.17), results in a final stoichiometry for $Au^0/Au(CN)_2^-$ of 1, which is the experimentally determined value. Therefore, the conclusion in the case of carbon is that Equation (3.6) is correct, but that the oxidation half-reaction is that of cyanide oxidation. No cyanate could be detected in the resultant alkaline solution after boiling the activated carbon; however, activated carbon is known[89] to catalyze the further oxidation of cyanate, even at ambient temperatures, which may account for this observation.

*d) Thermal Stability of Adsorbed Gold Species on Activated Carbon*

A study of the thermal stability of the adsorbed gold species may provide useful information regarding the adsorption mechanism. Moreover, the influence of drying on the nature of the adsorbate is an aspect that has thus far been neglected in most mechanistic studies of this system. It will be shown in the following section that the source of

the disagreement between workers is the differing conditions of ionic strength employed in the various investigations. It is possible that the chemical nature of the adsorbate changes with variation in the drying procedure employed. Moreover, recent results[86] indicate that a portion of the $Au(CN)_2^-$ is oxidized to $Au(CN)_2Cl_2^-$ upon vacuum drying of carbon loaded with aurocyanide from acidic media.

Finally, an understanding of the system at somewhat higher temperatures is useful in consideration of non-eluted gold that accompanies the carbon to the regeneration kiln (normal plant practice involves thermal regeneration of activated carbon at >600°C to remove adsorbed organics, prior to reintroduction into the adsorption vessels).

In the present work, three carbon samples were loaded with up to five per cent gold (by mass) under various conditions. The carbons were dried at different temperatures for 24 hours and analysed for gold and nitrogen. Table 3.8 shows analytical values for N/Au ratios on the carbons.

The stoichiometry of the adsorbed gold conforms with that of $Au(CN)_2^-$, when loaded from 0,1 M KCl or with no additives present. Table 3.8 shows that the ratio of nitrogen to gold remains unchanged at 2,0 even after the loaded carbon has been heated to temperatures as high as 240°C. This suggests that the aurocyanide remains stable on the carbon surface, even at high temperatures, an issue that has raised doubts in the past[39] regarding drying techniques. The ratio of nitrogen to gold is less than 2 when loaded from acidic solution, indicating that some decomposition to AuCN has occurred. It is significant that carbon loaded from aurocyanide solution containing no additives exhibited N/Au ratios of 2,0. This suggests that only a negligible amount of aurocyanide loaded under neutral conditions at low ionic strength is in a thermally unstable form such as $HAu(CN)_2$.

The N/Au ratio remains approximately 2 even at 270°C, but drops to about 1,5 when the carbon is heated to 300°C, indicating that some decomposition has occurred. Figure 3.12 shows X-ray diffractograms of aurocyanide-loaded carbons that were heated to various temperatures. Large peaks corresponding to metallic gold were observed after heating to 300°C or higher. Smaller peaks were observed in carbons heated to 270°C, and none on those heated to 240°C.

**Table 3.8**

**N/Au ratios for activated carbons loaded with aurocyanide under various conditions and dried at different temperatures**

Conditions:

Mass of carbon: 3,0g
Volume of solution: 30 ml
Initial gold in solution: 18000 mg/l
Time of constant 24 hrs
Drying time 24 hrs

| Drying temperature °C | No additives | 0,1M KCl | 0,1M HCl |
|---|---|---|---|
| 60 | 2,17 | 2,08 | 1,41 |
| 90 | 1,96 | 1,95 | 1,45 |
| 120 | 1,93 | 1,93 | 1,36 |
| 140 | 2,61 | 2,17 | 1,66 |
| 180 | 2,05 | 1,94 | 1,27 |
| 240 | 1,96 | 2,02 | 1,32 |
| 270 | 2,16 | 1,81 | 1,48 |
| 300 | 1,58 | 1,46 | 1,54 |

These results suggest that alkaline aurocyanide-loaded carbons exhibit a reasonable stability to thermal treatment at temperatures less than 270°C, whereupon

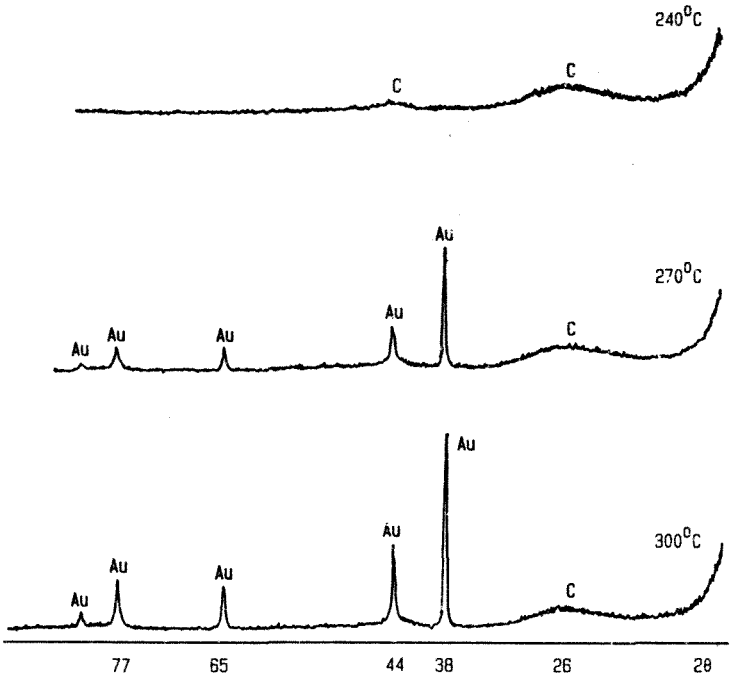


Fig. 3.12 **X-ray diffractograms of activated carbons loaded with aurocyanide in the presence of 0,1M KCl, after heating at various temperatures**

reductive decomposition to metallic gold begins to occur, being complete at about 300°C. These effects are confirmed by examination of the scanning electron micrographs of the surfaces of the 240°C, 270°C and 300°C heat carbons, shown in Figures 3.13, 3.14 and 3.15 respectively. Metallic gold particles appear white in the micrographs. No gold particles are evident on the carbon heated to 240°C, whereas 2μm particles are observed on the carbon heated to 270°C, and 7μm particles on the carbon heated to 300°C. Figure 3.16 shows that spherical particles are randomly distributed throughout the carbon heated to 300°C. This is in contrast to the dendritic gold particles formed in the pores of activated carbons by the reduction of AuCN. (See Figure 3.3).

It is noteworthy that large quantities of HCN gas have been found[90] to evolve from a carbon loaded with aurocyanide from 0,1 M KCl solution at a pH value of 10, upon heating to temperatures above about 300°C. This suggests that a reaction mechanism such as the following may be occurring at these temperatures:

$$Au(CN)_2^- + e^- \rightleftharpoons Au + 2CN^- \quad (E^0 = -0,611v) \qquad (3.19)$$

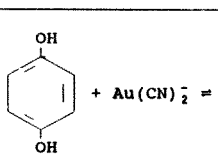


$$+ e^- + 2H^+ \quad (E^0 = +0,286V) \qquad (3.20)$$

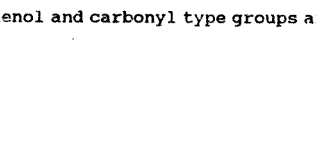


$$+ Au(CN)_2^- \rightleftharpoons + Au + 2HCN(\uparrow) \qquad (3.21)$$

Phenol and carbonyl type groups are known[24] to be present on


Fig. 3.13 SEM micrograph of an activated carbon surface loaded with aurocyanide in the presence of 0,1M KCl, after heating at 240 °C


Fig. 3.14 SEM micrograph of an activated carbon surface loaded with aurocyanide in the presence of 0,1M KCl, after heating at 270 °C

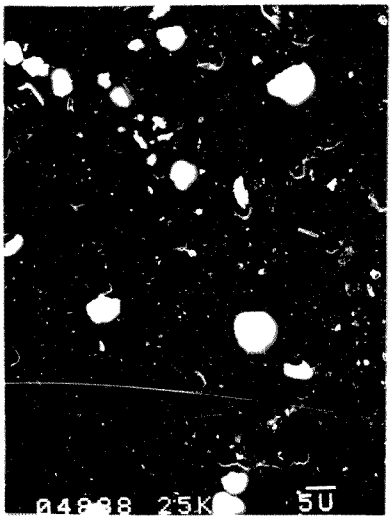


Fig. 3.15 SEM micrograph of an activated carbon surface loaded with aurocyanide in the presence of 0,1M KCl, after heating at 300 °C

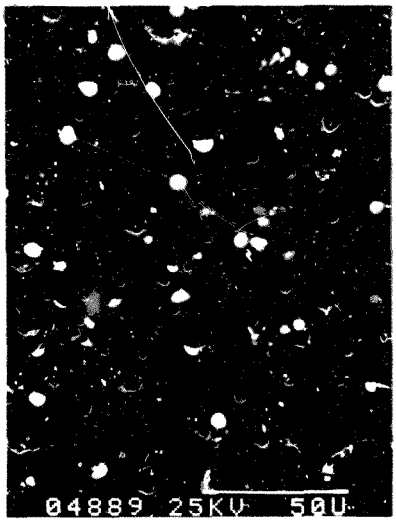


Fig. 3.16 SEM micrograph of the activated carbon surface shown in Fig. 3.15, showing the distribution of gold particles

activated carbon surfaces, and these would function as hydroquinone and quinone groups, due to the high degree of conjugation present in the graphitic microcrystallite. Moreover, the standard reduction potential for reaction (3.20) in alkaline solution ($E^0 = +0,286V$) conforms well to the typical value of about +0,24V found for activated carbons.

The carbon that was loaded in the presence of 0,1 M HCl showed N/Au ratios of about 1,5 (see Table 3.8), confirming that some degradation to AuCN occurs upon adsorption of aurocyanide from acidic solutions. No major changes in N/Au are observed upon heating. Figure 3.17 shows that similar changes in the X-ray diffractograms to the alkaline-loaded carbons occur, that are also consistent with the formation of metallic gold.

The large quantities of HCN gas that were found[91] to evolve upon heating loaded carbons, were evident at much lower temperatures (170 $^0$C) when the carbon was loaded with aurocyanide from 0,01M HCl solution (pH 2), than when a neutral solution was used (300 $^0$C). Moreover, it was shown earlier that reaction (3.22) occurs at room temperature to some extent:

$$Au(CN)_2^- + H^+ \rightarrow AuCN(\downarrow) + HCN(\uparrow) \qquad (3.22)$$

The present results confirm this inherent instability of aurocyanide loaded onto activated carbon from acidic solution. The fact that the N/Au ratio remains at about 1,3 even at 300°C indicates that the nitrogen is retained on the carbon. The marked increase in the intensity of the $Au^0$ XRD peaks for carbon heated to 300°C (Figures 3.12 and 3.17), suggests that this nitrogen is not bound to the gold.

Mössbauer spectra of the heated activated carbons are shown in Figures 3.18 and 3.19. A summary of the Mössbauer parameters for these spectra, along with

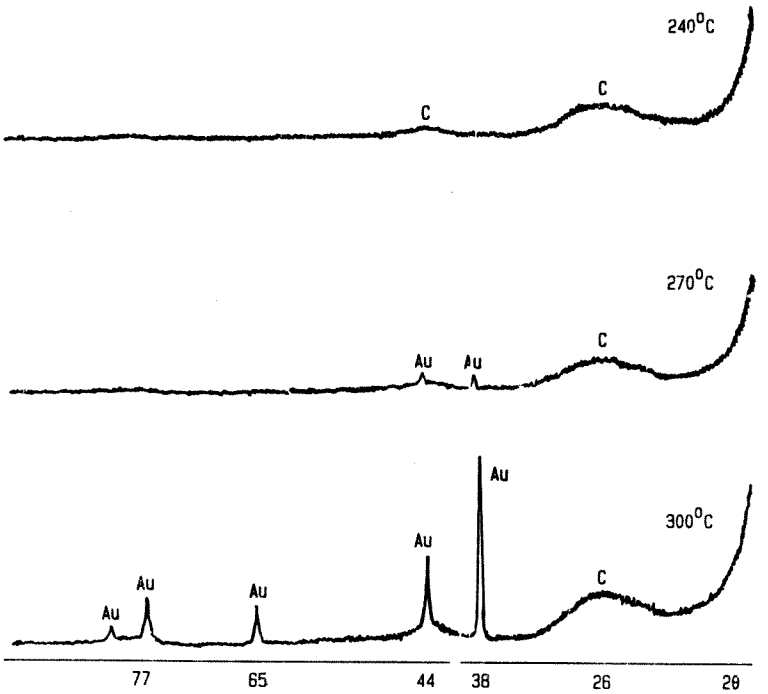


Fig. 3.17 **X-ray diffractograms of activated carbons loaded with aurocyanide in the presence of 0,1M HCl, after heating at various temperatures**

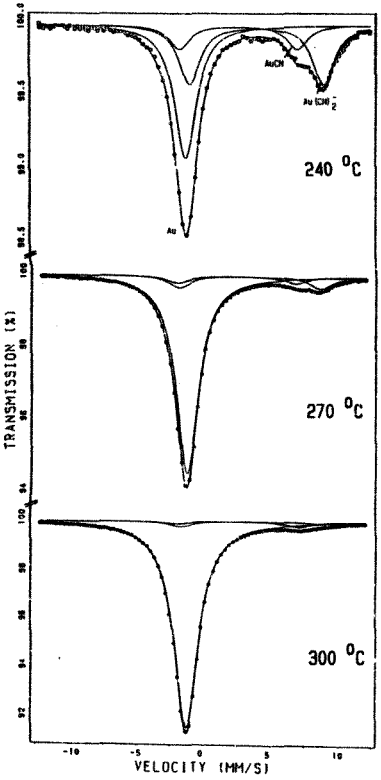


Fig. 3.18 $^{197}$Au Mössbauer spectra of activated carbon ·ded with aurocyanide in the presence of 0,1M KCl, and subsequently heated to various temperatures

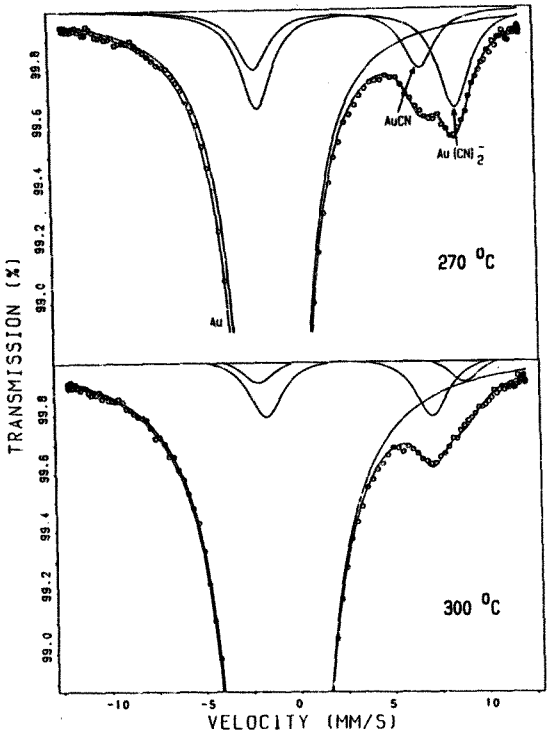


Fig. 3.19 Expanded view of $^{197}$Au Mössbauer spectra shown in Fig. 3.18, showing detail of peaks due to minor species

literature values for reference compounds, appears in Table 3.9.

The Mössbauer peaks indicate the presence of metallic gold, $KAu(CN)_2$ and an AuCN-type species, which is consistent with the occurrence of reaction (3.22). Equation (3.20) is a possible source of the acid that is required for this reaction.

**Table 3.9**
**Mössbauer spectral parameters for gold species on activated carbons and gold compounds**

| Compound | IS mm/s | QS mm/s | f | Ref. |
|---|---|---|---|---|
| Aurocyanide-loaded carbon heated to 240°C | -1,43<br>3,76<br>2,46 | 0,00<br>9,76<br>8,57 | | |
| Au | -1,23 | 0 | 0,19 | 39 |
| $KAu(CN)_2$ | 3,05<br>3,25<br>3,10<br>3,12 | 9,80<br>10,21<br>10,21<br>10,21 | 0,015 | 44<br>44<br>44<br>44 |
| AuCN | 2,3 | 8,0 | 0,095 | 39 |

An indication of the relative amounts of these three species on the carbon is gained by consideration of the recoil-free fractions, or Debye-Waller factors, f, for the corresponding gold compounds (see Table 3.9). Assuming that no change in the f factors occurrs upon adsorption onto carbon, it can be calculated that roughly two per cent of the adsorbed gold is in the metallic form. This is consistent with the SEM and XRD results, which suggested that the adsorbed aurocyanide species is comparatively stable to temperatures as high as 240°C.

The Mössbauer spectra shown in Figure 3.18 are consistent with the other data, in showing that most of the gold is present in the metallic form after heating at 270 °C, and this proportion is further increased when heated at 300 °C.

Figure 3.19 shows an expanded view of the minor components in the Mössbauer spectra of the carbons heated at higher temperatures. Further evidence for the proposed reaction mechanism is obtained by comparison of the relative ratios of $Au(CN)_2^-$ and AuCN-type species. At 270 °C and lower, $Au(CN)_2^-$ is predominant, whereas at 300 °C, AuCN is predominant. Reduction of AuCN to the metal is more favourable than reduction of $Au(CN)_2^-$ to the metal:

$$AuCN + e^- \rightleftharpoons Au + CN^- \qquad (E^0 = -0,166\ V) \qquad (3.23)$$

$$2AuCN + e^- \rightleftharpoons Au + Au(CN)_2^- \qquad (E^0 = 0,252\ V) \qquad (3.24)$$

$$Au(CN)_2^- + e^- \rightleftharpoons Au + 2CN^- \qquad (E^0 = -0,57\ V) \qquad (3.25)$$

The Mössbauer spectra provide strong evidence that reduction occurs via an intermediate AuCN-type species. The only other evidence for this type of species has been found when aurocyanide is loaded onto carbon under acidic conditions, as discussed earlier in this Chapter.

e) *Relation Between the Effects of Oxygen and Ionic Strength on the Adsorption of Aurocyanide onto Activated Carbon*

It is useful here to review the two schools of thought regarding the adsorption mechanism, evident from the most recent literature:

(1) adsorption of aurocyanide without chemical change[11,39,62,78,79], and

(2) adsorption of aurocyanide with decomposition of $Au(CN)_2^-$ to AuCN[73-75,91,92].

The consensus of opinion of most proponents[11,62,78,79] of mechanism (1) is that under normal plant conditions, aurocyanide is extracted in the form of an ion pair, $M^{n+}[Au(CN)_2^-]_n$. These conditions typically entail solutions of relatively high ionic strength. It is apparent, however, that all the investigations carried out by the proponents[73-75,91,92] of mechanism (2), without exception, employed conditions of low ionic strength, i.e. conditions atypical of those prevailing in a practical plant situation.

Results discussed earlier in this Chapter indicate that different adsorption mechanisms become operative under conditions of varying ionic strength. The present discussion aims to verify this hypothesis and explain this dichotomy in terms of one theory.

The influence of oxygen on the adsorption of aurocyanide onto activated carbon has been reported many times in the literature[11,73-75,77,91,92] and several studies have focussed on this aspect alone[74,91]. None of these studies have resulted in a complete understanding of all aspects of this effect, while all of them have contributed some useful observations. It is a further aim of the present work to explain this effect in terms of the above-mentioned theory, to explain its relationship to the ionic strength effect, and to demonstrate that oxygen has no effect under practical plant conditions.

The effect of oxygen on the system was first reported by Dixon, *et al*[93], who observed a reduction in the adsorption capacity of the carbon when nitrogen was bubbled through the solution. The effect was enhanced at higher temperatures. No explanation for the observation was profferred. Boehme and Potter[94] suggested that in the presence of oxygen an electrochemical reaction occurs, in which the carbon acquires a positive charge to which the

negativity-charged $Au(CN)_2^-$ ion is attracted. This is essentially the Frumkin[95] reaction, originally postulated to account for adsorption of acids onto activated carbon.

Tsuchida and Muir[74,75,96] proposed that the role of oxygen is to decompose some of the $Au(CN)_2^-$ to AuCN by the oxidation of one $CN^-$ to $CO_3^{2-}$ and $NH_3$. Cook[92] reported that the bubbling of oxygen through a solution containing gold-loaded carbon caused potassium ions to desorb and gold to adsorb, and postulated the same oxidative decomposition mechanism to account for the observations.

The most recent study, by Van der Merwe and Van Deventer[91] showed that oxygen is consumed during gold adsorption, but only a small amount of oxygen is consumed in the absence of gold. Once again, the mechanism postulated to account for these observations was the oxidative decomposition of $Au(CN)_2^-$ to AuCN.

(i) Adsorption of gold

Figure 3.20 shows the effects of bubbling oxygen and nitrogen through the solution, on the adsorption of aurocyanide onto activated carbon, from a low ionic strength solution (no additives). The presence of oxygen results in an increase in the amount of gold adsorbed, corroborating the results of previous workers[73,75,92].

Figure 3.21 shows the effect of bubbling the gases through the solution in the presence of 0,1M KCl (neutral solution). In this instance, there is only a slight enhancement in the rate of gold loading when oxygen is bubbled through the solution.

Figures 3.22 and 3.23 show the effects of bubbling the gases through the solution in the presence of 0,1M KOH and 0,1M HCl, respectively. In both cases, there is no enhancement

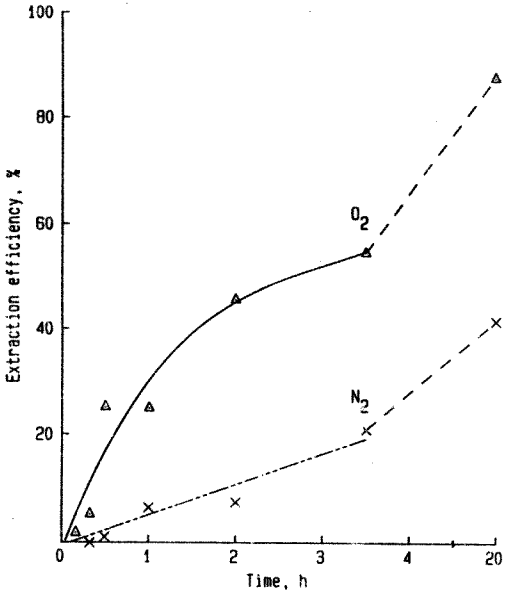


Fig. 3.20 Effects of oxygen and nitrogen bubbling on the adsorption of aurocyanide onto activated carbon from solution containing no additives. (Carbon mass 1,0g; solution volume 250 ml; initial gold concentration in solution 300 mg/l)

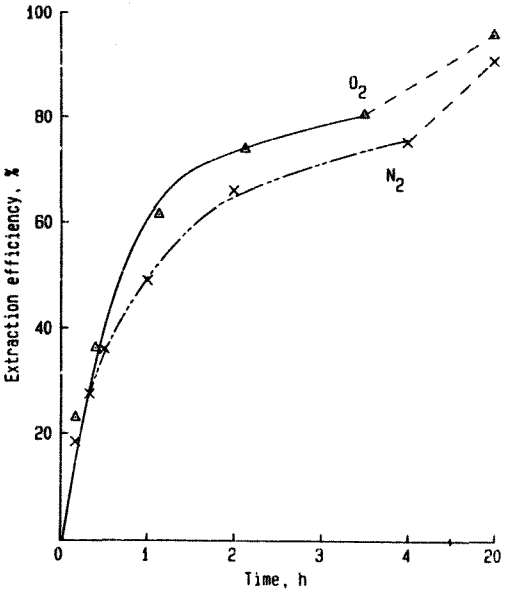


Fig. 3.21 Effects of oxygen and nitrogen bubbling on the adsorption of aurocyanide onto activated carbon from 0,1M KCl solution. (Carbon mass 1,0g; solution volume 250 ml; initial gold concentration in solution 300 mg/l)

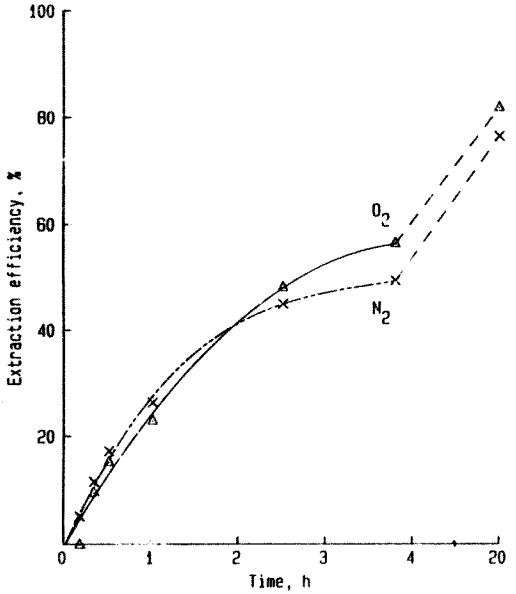


Fig. 3.22 Effects of oxygen and nitrogen bubbling on the adsorption of aurocyanide onto activated carbon from 0,1M KOH solution. (Carbon mass 1,0g; solution volume 250 ml; initial gold concentration in solution 300 mg/l)

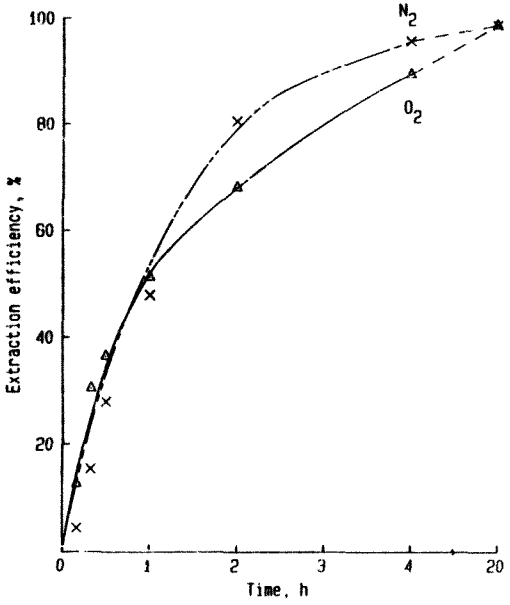


Fig. 3.23 *Effects of oxygen and nitrogen bubbling on* the adsorption of aurocyanide on activated carbon from 0,1M HCl solution. (Carbon mass 1,0g; solution volume 250 ml; initial gold concentration in solution 300 mg/l)

of gold loading in the presence of either gas, and the adsorption rates are very similar for both $O_2$ and $N_2$ over the entire 20 hour period.

(ii) Solution pH changes

Table 3.10 details the observed pH changes during the course of the above experiments. The pH values of the 0,1M HCl (pH 1) and 0,1M KOH (pH 13) solutions were found to remain constant throughout the experiment. The pH values of the neutral solutions were found to vary quite substantially, however. Larger increases in pH were observed in the presence of oxygen than in the presence of nitrogen, for both low (no additives) and high (0,1M KCl) ionic strength solutions. Only slight changes in pH (less than one pH unit) were observed in the 0,1M KCl solution, whereas more marked pH changes were observed when no additives were present.

**Table 3.10**
**Changes in solution pH during the adsorption of aurocyanide onto activated carbon under various conditions**

| Time h | Solution Conditions | pH in solution (ΔpH) | |
|---|---|---|---|
| | | $O_2$ | $N_2$ |
| 0 | No additives | 7,33 | 7,27 |
| 3,5 | | 8,06 (+0,73)[a] | 7,98 (+0,71) |
| 20,0 | | 10,25 (+2,92) | 8,80 (+1,53) |
| 0 | 0,1M KCl | 6,25 | 6,29 |
| 3,5 | | 6,79 (+0,54) | 6,73 (+0,44) |
| 20,0 | | 7,11 (+0,86) | 6,75 (+0,46) |

[a] Bracketed figures refer to changes in pH.

The observation that the pH of the solution increases upon adsorption of anions onto activated carbon is not restricted to aurocyanide ions, as shown in Table 3.11, for the adsorption of KCl onto activated carbon in the absence of aurocyanide. In the case of 0,1M KCl, the pH increases only in the presence of oxygen, and a slight decrease in pH was observed when nitrogen was bubbled through the solution.

**Table 3.11**
**Changes in pH of a 0,1M KCl solution in contact with activated carbon, in the absence of aurocyanide**

| Time h | pH in solution (ΔpH) | |
|---|---|---|
| | $O_2$ | $N_2$ |
| 0 | 7,34 | 7,34 |
| 4 | 8,11 (+0,77)[a] | 7,00 (-0,34) |
| 24 | 8,99 (+1,65) | 6,95 (-0,39) |

[a] Bracketed figures refer to changes in pH.

(iii) The nature of the adsorbed species

The concentrations of gold and nitrogen on the carbons at the end of the experiments reported in the previous section, are shown in Table 3.12.

For neutral and alkaline solutions, the ratio of nitrogen to gold on the carbon is approximately 2, corresponding to $Au(CN)_2^-$, whereas for 0,1M HCl solution, the ratio of nitrogen to gold is about 1,3, whether oxygen or nitrogen are bubbled through the solution.

The various solutions were analysed for $NH_4^+$, $HCO_3^-$ and

**Table 3.12**
**Concentrations of nitrogen and gold on carbons**

| Adsorption solution conditions | Concentration on carbon, mmol/g | | | |
|---|---|---|---|---|
| | $O_2$ bubbling | | $N_2$ bubbling | |
| | Au | ½N | Au | ½N |
| No additives | 0,171 | 0,174 | 0,150 | 0,142 |
| 0,1M HCl | 0,291 | 0,196 | 0,295 | 0,189 |
| 0,1M KOH | 0,232 | 0,206 | 0,237 | 0,210 |
| 0,1M KCl | 0,268 | 0,263 | 0,272 | 0,272 |

**Table 3.13**
**Concentrations of anions in gold adsorption solutions**

| Adsorption solution conditions | Concentration in solution, mmol/l | | | | | |
|---|---|---|---|---|---|---|
| | Before loading | | | After loading | | |
| | $NH_4^+$ | $HCO_3^-$ | $CNO^-$ | $NH_4^+$ | $HCO_3^-$ | $CNO^-$ |
| *$O_2$ bubbling* | | | | | | |
| No additive | 0,50 | 0,36 | 0,10 | <0,06 | 0,39 | 0,08 |
| 0,1M KOH | -[a] | 2,21 | - | - | 2,56 | - |
| 0,1M KCl | - | 0,16 | - | - | 0,25 | - |
| *$N_2$ bubbling* | | | | | | |
| No additive | | | | <0,06 | 0,26 | 0,10 |
| 0,1M KOH | | | | - | 1,67 | - |
| 0,1M KCl | | | | - | 0,20 | - |

[a] Not measurable due to high background electrolyte.

$CNO^-$ by ion chromatography both before and after adsorption. These results are presented in Table 3.13, and indicate that no build-up of oxidative decomposition products of $Au(CN)_2^-$ occurs in solution during the adsorption experiments.

(iv) Adsorption of chloride

The concentrations of chloride on the carbons, after the adsorption experiments, are shown in Table 3.14.

Table 3.14
Concentrations of chloride on carbons

| Adsorption solution conditions | Cl concentration on carbon, mmol/g | |
|---|---|---|
| | $O_2$ bubbling | $N_2$ bubbling |
| No additives | <0,0006 | <0,0006 |
| 0,1M KCl | 0,017 | <0,0006 |
| 0,1M KCl; no gold | 0,079 | 0,051 |

In the presence of aurocyanide, chloride was found to adsorb onto the carbon only when the solution was oxygenated. A greater amount of chloride was found to adsorb in the absence of aurocyanide and this occurred whether oxygen or nitrogen were bubbled through the solution.

(v) Discussion

The above results corroborate the results presented earlier, which indicated that different reaction mechanisms prevail in regions of low and high ionic

strength, and in regions of varying pH. The following discussion explains the results by consideration of these mechanisms and their sensitivity to different experimental conditions.

The results presented in Tables 3.12 and 3.13 indicate that the adsorbed species is present in the form of $Au(CN)_2^-$, when loaded from alkaline or neutral solutions. The N:Au stoichiometry is approximately 2 under these conditions. Moreover, the reaction products postulated[74,75] to arise from the oxidative decomposition of $Au(CN)_2^-$ to AuCN, viz. $NH_4^+$, $HCO_3^-$ and $CNO^-$, were not found to increase in concentration in the solution after gold adsorption. (Table 3.13). These facts suggest that no oxidative decomposition reaction of $Au(CN)_2^-$ occurs during adsorption from neutral or alkaline solution. Moreover, Tsuchida and Muir[73] failed to find any electrochemical evidence for such a reaction. Some formation of AuCN is evident when aurocyanide is loaded from 0,1M HCl solution, however, and this aspect was discussed in detail earlier.

*Mechanism of adsorption of aurocyanide onto activated carbon from solutions of low ionic strength.*

Low ionic strength solutions are not relevant to the conditions found in a practical situation. However, a study of the reaction occurring under these conditions was carried out in an attempt to explain the results of previous workers[73-75,91,92], who all investigated the adsorption of aurocyanide onto activated carbon from low ionic strength solutions.

Under conditions of low ionic strength, the bubbling of oxygen through the solution results in an enhancement in gold loading (Figure 3.20), and a larger pH shift (Table 3.10) than occurs with nitrogen bubbling through the

solution. Moreover, the phenomenon is not specific for potassium aurocyanide - the results in Tables 3.11 and 3.14 indicate that a significant amount of chloride adsorbs from a 0,1M KCl solution onto activated carbon, only in the presence of oxygen, and an upward shift in pH also occurs only in the presence of oxygen.

These observations are consistent with those reported[24] for the adsorption of acid onto activated carbon from low acid concentrations (<0,01N). In that study it was shown that no acid was adsorbed unless oxygen was purged through the system.

Bartell and Miller[97] observed upward pH shifts upon adsorption of various salts onto sugar charcoal, and postulated a hydrolytic theory of adsorption, which was further developed by Steenberg[29], who postulated the primary adsorption of protons, with secondary adsorption of anions.

More recently, Jankowska[98] has observed pH increases upon adsorption of halogen anions onto activated carbon, in the order

$$I^- > Br^- > Cl^- > F^-$$

This is the same order as that observed for the extent of loading of these species onto carbon.

The fact that oxygen and acid both play a role in hydrolytic adsorption of anions onto activated carbon is consistent with an electrochemical reaction of the type shown below, which involves reduction of oxygen at cathodic sites on carbon:

$$O_2 + 4e^- + 2H_2O \rightleftharpoons 4OH^- \qquad (E^0 = 0,401V) \qquad (3.26)$$

$$O_2 + 2e^- + 2H_2O \rightleftharpoons 2OH^- + H_2O_2 \qquad (E^0 = -0,146V) \qquad (3.27)$$

It is suggested that the other half of the electrochemical reaction involves oxidation of the carbon surface itself. Examples of such reactions previously postulated to occur on carbon are the quinone/hydroquinone type couple[99]:

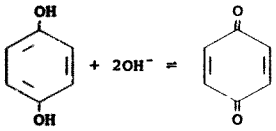


(3.28)

and the oxidation of the chromene group:

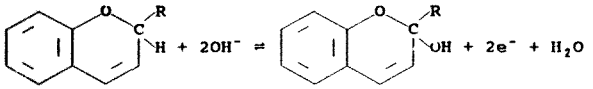


(3.29)

It has been suggested[69] that this structure can behave as an ion exchange site by virtue of formation of a carbonium ion:

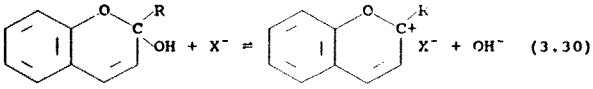


(3.30)

This carbonium ion will hydrolyze readily in alkaline solution to form the precursor chromenol group by reversal of the equilibrium shown in (3.30), the chromenol group being weakly basic[100].

The postulation that an electrochemical reaction such as that outlined in the above scheme occurs during adsorption

of anions onto carbon from low ionic strength solutions, is consistent with changes in potential that take place during adsorption, observed by Hughes, *et al*[96].

The equilibrium constant for a reaction such as that shown in Equation (3.30), i.e. formation of a carbonium ion from a precursor containing a chromenol group, has been reported[101] for pelargonidin 3-monoglucoside to be 955:

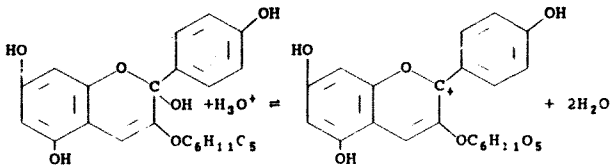


(3.31)

It is therefore proposed that two mechanisms are operative in the adsorption of aurocyanide from solutions of low ionic strength, and that relative contributions of the two pathways are influenced by the presence of oxygen in solution:

(1) adsorption of $M^{n+}[Au(CN)_2^-]_n$ ion pairs, which occurs to a greater extent in the absence of oxygen, and

(2) formation of ion-exchange sites in the presence of oxygen, which coordinate aurocyanide by simple electrostatic ion-exchange.

This mechanism is consistent with several previously published observations: Tsuchida and Muir[75] reported K/Au ratios of approximately 1 for deoxygenated carbons, and less than 1 when oxygen was present. Cook[92] observed desorption of $K^+$ ions from loaded carbon upon bubbling

oxygen through the solution. Van der Merwe and Van Deventer[91] observed that the amount of oxygen consumed varies with oxygen concentration in solution, rather than amount of gold loaded. They observed that no oxygen was consumed in the absence of anions, and that pre-treatment of carbon with oxygen or nitrogen did not result in any enhancement in loading upon contact of pre-treated carbon with aurocyanide solution. Both of these observations are manifestations of the inherent instability of a functional group such as the chromenol product from reaction (3.29). Finally, the 1:1 correlation between oxygen and acid consumptions observed[24] for adsorption of acids onto activated carbon from low ionic strength solutions, can be rationalized in terms of reactions (3.27), (3.29) and (3.30), which, upon addition, form the overall reaction:

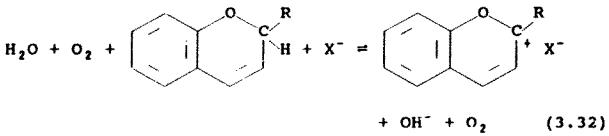


$$+ OH^- + O_2 \qquad (3.32)$$

*Mechanism of adsorption of aurocyanide onto activated carbon from solutions of high ionic strength*

High ionic strength conditions are those typically found in practical plant situations; thus it is the adsorption mechanism pertinent to these conditions that holds the most practical significance.

In the presence of 0,1M KCl (Figure 3.21), the rate of gold adsorption is only slightly faster in the presence of oxygen than when nitrogen is bubbling, in contrast to the large oxygen effects observed in low ionic strength solution.

Small upward pH changes are evident, both in the presence (Table 3.10) and absence (Table 3.11) of aurocyanide. It is noteworthy that chloride was only found to adsorb to a marked extent in the presence of oxygen, and to a much greater extent when no aurocyanide was present. These results suggest that, as for conventional ion-exchange processes[102], there is a high selectivity for aurocyanide over chloride. The smaller shift in pH that accompanies gold adsorption from high ionic strength solution is consistent with the fact that a much smaller oxygen effect is evident, and is also consistent with the results presented in section 3.2a, where elemental analyses of carbons loaded from high ionic strength solutions correlated well with the stoichiometry expected for adsorbed $KAu(CN)_2$ ion pairs.

The results in Tables 3.10, 3.11 and 3.14 suggest that from high ionic strength solution, only a small amount of ion-exchange sites are formed in the presence of oxygen and that virtually no ion-exchange sites are formed in the absence of oxygen. This is a small effect, however, and does not detract from the fact that *the mechanism of adsorption of aurocyanide from high ionic strength solution involves adsorption of* $M^{n+}[Au(CN)_2^-]_n$ *ion pairs*, with no significant contribution due to coordination by ion-exchange sites, and this is consistent with the mechanism proposed earlier.

In the presence of 0,1M KOH (Figure 3.22) or 0,1M HCl (Figure 3.23), no oxygen effect on the gold adsorption was observed, and no pH shifts were discernible. Under alkaline conditions, a reversal of an equilibrium such as that represented in Equation (3.29) would occur, thereby eliminating any ion-exchange sites.

The lack of an oxygen effect in the case of the acidic solution is consistent with the theory of adsorption of acids from high concentration solutions, which is

postulated[24] to occur predominantly by adsorption, rather than ion-exchange. This is also consistent with the conclusions arrived at previously[78], that aurocyanide adsorbs primarily as $HAu(CN)_2$ from acidic solutions, with some decomposition to AuCN also occurring.

*f) X-ray Photoelectron Spectroscopic Study of Adsorbed Gold Species on Activated Carbon*

In most previous work on the mechanism of adsorption, little attention has been given to the nature of the interaction between adsorbed gold species and activated carbon substrate. Adams *et al*[62] provided evidence from electron spin resonance (ESR) spectroscopy for a charge-transfer interaction between the highly delocalized carbon and vacant orbitals in the gold complex. The basis for this conclusion was reduction in total unpaired electron concentration with increasing gold loading. This postulation is consistent with the apparent reduction in oxidation state of the gold nucleus, as suggested from the results of X-ray photoelectron spectroscopic (XPS) studies[32,79,103], and also with the slight increase in charge density around the gold nucleus, as measured by Mössbauer spectroscopy. (See section 3.2c).

The nature of the bonding interaction also plays a significant role in activated carbon - supported gold chloride catalysts[104] for the hydrochlorination of acetylene. There is thus a need to establish the mechanism of bonding to carbon for each of the gold species $Au(CN)_2^-$, AuCN and $AuCl_4^-$. The aim of the present study was firstly to clarify this aspect, and secondly to elucidate the sources of the many inconsistencies in previous XPS studies[32,79,103,105-110] of gold species, which will be discussed in detail in this section.

(i) Inconsistencies in previous XPS investigations of gold compounds and adsorbed species

Table 3.15 shows results of previous XPS investigations of gold compounds and adsorbed species, together with the referencing method adopted by each group of researchers, where reported. In the majority of cases[32,79,103,111] the observed binding energy for adsorbed aurocyanide species is reported to lie between those of metallic gold (about 83,6 eV) and $KAu(CN)_2$ salt (about 85,3 eV); however, Cook *et al.*[110] report binding energies of between 85,6 and 86,0 eV for the adsorbed species, which lies outside the range mentioned above, indicating a gold oxidation state greater than 1,0. Moreover, the absolute values of binding energies in Table 3.15 are spread over a range of 0,7 eV, even for the crystalline compounds. The results of McDougall, *et al*[32] lie far out of the range of the other results. The reason for these discrepancies lies in the variation of the choice of referencing system adopted by different researchers. It is evident from Table 3.15 that despite the fact that there is general consensus that the spectra are referenced against the carbon (1s) peak, there is no consistency in the choice of either the source of carbon or the absolute value that is to be assigned to this peak. Sources of carbon used include activated carbon[110], teflon[107], "hydrocarbon oil contamination"[103,105] and the cyanide ligand[79]. The latter choice was not used in the present study, because the electron density around the cyanide carbon, and hence the binding energy (BE), is likely to be altered drastically upon adsorption by charge-transfer interaction, which is the adsorption mechanism advocated by several researchers[62,79].

The binding energy of the carbon (1s) peak is also dependent on the type of carbon present. For example, Konno[112] cites the C(1s) binding energy for hydrocarbon oil as 284,8 eV, for methyl carbon as 285,1 eV and for methylene carbon as

Table 3.15

Au ($4f\ ^{7}/_{2}$) binding energies (eV) of gold compounds and adsorbed species

| Gold Compounds | | | | Adsorbed species | | Referencing technique | Ref. |
|---|---|---|---|---|---|---|---|
| $Au^{o}$ | AuCN | $KAu(CN)_2$ | $KAuCl_4$ | AuCN | $Au(CN)_2^-$ | | |
| | 85,0 | 85,2 | | 84,7 | 84,7 | C(1s) in cyanide assigned to 285,5 eV (C(1s) in activated carbon measured 284,43 eV) | Klauber[79] |
| 83,6 | | 85,6 | | | 84,2 | C(1s) in hydrocarbon oil contamination assigned to 285,0 eV | Dudarenko et al[103] |
| 84,0 | 84,9 | 85,1 | | | 85,6-86,0 | C(1s) in activated carbon assigned to 283,0 eV. Referencing technique for pure gold compounds is not given | Cook et al[110] |
| 83,8 | | | 87,7 | | | C(1s) in hydrocarbon oil contamination assigned to 285,0 eV | Knecht et al[105] |
| 83,4 | | | | | 84,9 | Not given | Wenge and Xiaoxia[106] |
| 83,5 | | | 87,4 | | | C(1s) in teflon assigned to 284,5 eV | Bancroft and Jean[107] |
| 83,8-84,4 | | | | | | Not given | Fritsch and Légaré[108] |
| 84,0 | | | | | | C(1s) in activated carbon assigned to 284,6 eV | Haacke[109] |

284,0 eV. Haacke[109] reports a binding energy of 284,6 eV for the C(1s) peak for activated carbon. Cook *et al*[110] report a value of 284,5 eV for graphite, based on assigning a value of of 83,98 eV to Au(4f $^{7}/_{2}$) for metallic gold. A standard referencing technique should be used in order to eliminate these inconsistencies. In the present work, all spectra were referenced against a value of C(1s) of 284,4 eV for activated carbon, which is consistent with the measured value of Klauber[111], and is close to the values measured by Haacke[109] and Cook *et al*[110]. Table 3.16 shows the values obtained in the present study for the binding energies of $KAu(CN)_2$, $NaAu(CN)_2$, AuCN and $HAuCl_4$, adsorbed onto activated carbon as well as in the salt form. The salts were physically mixed with activated carbon for referencing purposes. Also shown are the results of Klauber normalized to C(1s) = 284,4 eV for activated carbon. On this basis, there is now a reasonable agreement between binding energies for similar samples. This results in a shift in binding energy of about 2 eV on comparing the adsorbed $Au(CN)_2^-$ species with the salt. This is considerably higher than the shift of about 0,5 eV that can be calculated from Klaubers'[113] unadjusted measurements. It is likely that the anomalous results reported by Cook *et al*[110] are also explicable in terms of referencing problems, with adsorbed species referenced against C(1s) in activated carbon, and crystalline gold cyanide compounds apparently referenced against C(1s) in the cyanide ligand. Adjustment of binding energies, taking into account this effect and the difference in absolute value chosen for C(1s), once again accounts for the inconsistency.

The trend apparent from the results in Table 3.16 is that binding energies for all the adsorbed gold species undergo a shift to lower binding energy on adsorption, as compared to the salt. This suggests that a similar type of charge-transfer interaction with the carbon is occurring for $Au(CN)_2^-$, AuCN and $AuCl_4^-$. The shift measured is not in the

**Table 3.15**

**Au(4f $^{7}/_{2}$) binding energies (eV) of gold compounds and adsorbed species with referencing normalized to C(1s) of activated carbon at 284,4eV**

| Gold Compounds | | | | | Adsorbed species | | | | | | Ref. |
|---|---|---|---|---|---|---|---|---|---|---|---|
| $Au^{o}$ | AuCN | $NaAu(CN)_2$ | $KAu(CN)_2$ | $HAuCl_4$ | AuCN | $LiAu(CN)_2$ | $NaAu(CN)_2$ | $KAu(CN)_2$ | $HAu(CN)_2$ | $HAuCl_4$ | |
| 83,6-83,9 | 85,6 | 86,8 | 87,1 | 88,2 | 84,8 | 85,3 | 84,9 | 85,1 | | 86,5 | This work |
| | 85,7* | | 85,9* | | 84,7 | | | 84,7 | 84,7 | | Klauber[79] |

*Corrected by 0,7 eV to account for difference between the C(1s) binding energy for adsorbed cyanide (285,5 eV) and cyanide in the salt (This work - 286,2 eV)

C(1s) binding energy of the activated carbon that may be postulated to arise from a gold-carbon interaction, because such an effect would be enhanced with increasing gold loading. The consistent chemical shift evident at different gold loadings reaffirms the postulate that the point of reference is invariant.

It is noteworthy that shifts in binding energies of Zn and Ni have been observed[114] on adsorption of their complex cyanides onto activated carbon. These results have also[114,115] been interpreted in terms of a charge-transfer interaction with the surface.

(ii) Mechanisms of adsorption of gold cyanides onto activated carbon

The binding energies for gold on carbons that were loaded from 0,1M cyanide solutions of lithium, sodium and potassium do not fall into a consistent trend, as shown in Table 3.16. However, previous work[92] has demonstrated that the type of cation present has a significant influence on extent of gold loading, and moreover, the trends observed in the adsorption of $M^{n+}[Au(CN)_2^-]_n$ salts onto activated carbon were very similar to those observed in the extraction of aurocyanide by polymeric adsorberts and solvents. Moreover, adsorption of aurocyanide and cations from high ionic strength solution was shown in section 3.2a to be stoichiometric, indicating adsorption of species such as $KAu(CN)_2$ and $Ca[Au(CN)_2]_2$.

The presence of discrete ion pairs would be expected to result in shifts in the Au(4f $^7/_2$) binding energies for different cations, which was not observed. Moreover, this configuration would result in an asymmetric surface binding state for nitrogen, which, as was pointed out by Jones *et al*[111], is not the case. It is possible that all of the above results can be explained in terms of the separate

adsorption of anion and cation, with the cation solvated by the oxygen - containing functional groups that line the pore, in a manner akin to the strong solvation of cations by crown ethers[116] and by poly(oxyethylene) chains (See section 4.6), as shown in Scheme 1.

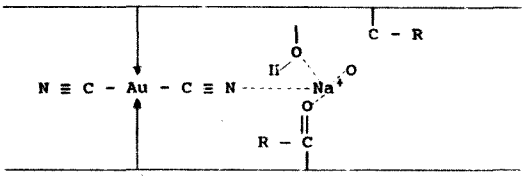


Scheme 1

It is also most likely that the Au ($4f^{7}/_{2}$) binding energy is not sufficiently sensitive to establish such subtle differences, given the fact the adsorbed $Au(CN)_2^-$ and AuCN species have such similar binding energies. (See Table 3.15).

The binding energy for gold on a carbon that had been boiled in hydrochloric acid (4 per cent by mass) for 5 hours had also decreased in relation to that of polymeric AuCN (Table 3.15). The Mössbauer spectroscopic study presented in section 3.2c suggested that much of the gold is in a N...Au - C electronic environment after this treatment, and the N binding energies of aurocyanide - loaded carbons subjected to room temperature acid treatment have shown[79] an asymmetry. This is consistent with the postulate of Klauber[79], that short-chain AuCN oligomers also adsorb onto the carbon surface by a charge-transfer interaction, as depicted in scheme 2.

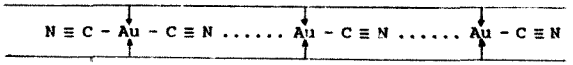


Scheme 2

A comparison of K(2p), Na(2p) and N(1s) binding energies between the adsorbed $KAu(CN)_2$ and $NaAu(CN)_2$, and their crystalline salts, appears in Table 3.17, together with data from the literature, corrected in a manner similar to that described earlier. The value of BE for K(2p) for adsorbed $KAu(CN)_2$ could not be obtained in the present work, due to its close proximity to the strong C(1s) peak.

It is evident from Tables 3.17 and 3.15 that all the atoms present in the adsorbed complexes, viz. Na, K, Au and N, undergo decreases in binding energy upon adsorption onto carbon, as compared with their crystalline salts. This is consistent with the mechanism schematically depicted above, with charge being transferred via the $\pi$ orbitals of the $Au(CN)_2^-$ complex. Metal-to-ligand change-transfer transitions (Au 5d $\rightarrow$ $\pi^*$ $CN^-$) have been shown to occur in $Au(CN)_2^-$, by electronic and Mössbauer spectroscopic measurements[117]. The bonding mechanism involves a d-orbital participation in Au-C $\sigma$-bonding, and in both $\pi$-donor and $\pi$-acceptor bonding with the $CN^-$ ligand. Moreover, weak Au....Au bonding has been shown[118] to occur between gold(I) atoms of $d^{10}$ configuration in certain mononuclear and polynuclear gold(I) compounds. The interaction

$$L - Au - L \; + \; L - Au - L \longleftrightarrow \begin{matrix} L - Au - L \\ \vdots \\ L - Au - L \end{matrix}$$

occurs perpendicular to the principal axis of the linearly coordinated gold(I) atoms. It is postulated that a similar interaction is occurring between $Au(CN)_2^-$ and activated carbon. It is also evident that sodium induces a greater shift in the N(1s) binding energy than does potassium, and this is consistent with the greater polarizing power of the smaller cation. The result is also consistent with the enhanced extraction[62] of $NaAu(CN)_2$ onto carbon, as compared with $KAu(CN)_2$. The fact that a cationic effect is observed on the N(1s) binding energy and

Table 3.17

Na(2p), K(2p) and N(1s) binding energies (eV) of gold compounds and adsorbed species with referencing normalized to C(1s) of activated carbon at 284,4 eV

| Na(2p) | | K(2p) | | N(1s) | | Ref. |
|---|---|---|---|---|---|---|
| $NaAu(CN)_2$ salt | $NaAu(CN)_2$ adsorbed on carbon | $KAu(CN)_2$ salt | $KAu(CN)_2$ adsorbed on carbon | $MAu(CN)_2$ salt | $MAu(CN)_2$ adsorbed on carbon | |
| 32,2 | 31,4 | 295,2 | - | 401,0 (K) | 400,1 (K)<br>399,4 (Na) | This work |
| - | - | 293,8 | 292,9 | 399,3 (K)<br>399,8 (AuCN) | 398,1 (K)<br>397,5 (H)<br>399,0 (AuCN) | Klauber[79] |

not the Au(4f $^{7}/_{2}$), is probably related to the fact that the interaction beteen cation and nitrogen is a direct one. The lack of asymmetry observed in the N(1s) spectrum could be due to the fact that the interaction is a weak one, as depicted by the long N...Na bond in Scheme 1 above. It is also explicable in terms of a scheme whereby both ends of the aurocyanide ion, on average, are coordinated to cations, resulting in a symmetrical configuration. An example of such a system is that deduced from the crystal structure[119] of $KAu(CN)_2$, in which the potassium cation is coordinated by the nitrogens of the cyano groups. Finally, it should be noted that the measurements reported in this section were all made under conditions of ultra-high vacuum, and it is uncertain whether this aspect has an effect on the results. The charge-transfer mechanism is independently supported, however, by the slight upward shift in the Mössbauer parameters of adsorbed aurocyanide species.

### (iii) Mechanism of adsorption of gold chloride onto activated carbon

The Au(4f $^{7}/_{2}$) binding energy for adsorbed $AuCl_4^-$ species on activated carbon is once again lower than that for the crystalline salt. A charge-transfer interaction between carbon surface and gold atom is possible because $AuCl_4^-$ has a square planar conformation, and can therefore adsorb essentially flat on the surface.

An interesting difference arises when $AuCl_4^-$ is adsorbed from an oxidizing medium (aqua regia), as opposed to a non-oxidizing medium (1,0M HCl), as is evident from a comparison of the Au(4f $^{7}/_{2}$) X-ray photoelectron spectra, shown in Figure 3.24. The $AuCl_4^-$ that was loaded under oxidizing conditions shows only one, well-defined, oxidation state, whereas that loaded from 1,0M HCl solution shows two oxidation states, one of which is consistent with

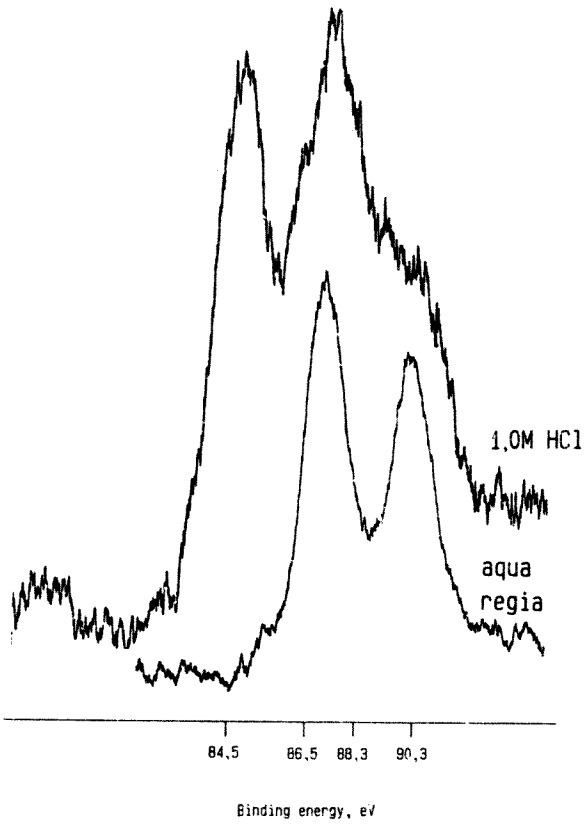


Fig. 3.24 Au(4f) photoelectron spectrum of gold species on activated carbon contacted with a solution of $AuCl_4^-$

metallic gold.

The reduction of $AuCl_4^-$ to metallic gold by activated carbon is a well known phenomenon[120,121]. However, Mössbauer spectroscopic studies presented later in this Thesis show the presence of some adsorbed $AuCl_4^-$ species. The fact that it is possible to adsorb $AuCl_4^-$ onto activated carbon with no reduction to the metal is a novel result that has significance in the above-mentioned catalytic process, where it is the gold in the higher oxidation state that has been postulated[104] to give rise to the active species. The relevant reduction half-reactions are shown below, and confirm that reduction to the metal, rather than to $AuCl_2^-$, is likely to be effected by a typical activated carbon ($E^0$ ~0,24 V, versus the standard hydrogen electrode)[32]:

$$AuCl_4^- + 3e^- = Au^0 + 4Cl^- \qquad (E^0 = 1,0V) \quad (3.33)$$

$$AuCl_4^- + 2e^- = AuCl_2^- + 2Cl^- \qquad (E^0 = 0,0V) \quad (3.34)$$

$$AuCl_2^- + e^- = Au^0 + 2Cl^- \qquad (E^0 = 1,0V) \quad (3.35)$$

It is of interest to compare the binding energy of gold foil reference material (84,2 eV) with that of the metallic gold component loaded onto carbon (84,6 eV). Fritsch[108] has noted an increase in binding energy of metallic gold with decreasing particle size, and the present results are consistent with this explanation.

Finally, there are some interesting effects present in the spectrum of the $HAuCl_4$ salt. The salt was mixed physically with activated carbon for the purpose of referencing, as described earlier. The Au($4f\ ^7/_2$) spectrum is shown in Figure 3.25, and shows that both $HAuCl_4$ (BE = 88,2 eV) and metallic gold (BE = 84,6 eV) are present. The relatively high binding energy of the latter is consistent with the presence of very small gold particles[108]. The fact that the yellow salt was still visible confirms that the higher binding energy peaks are attributable to the crystalline salt itself, rather than the adsorbed species. The sample

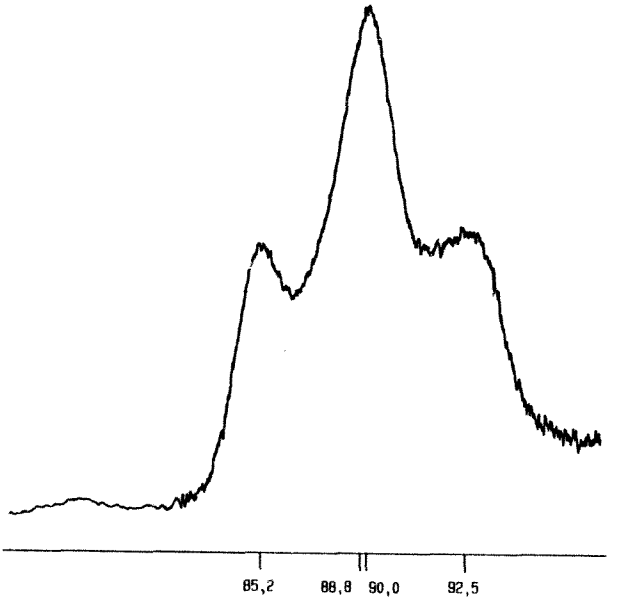


Fig. 3.25 Au(4f) photoelectron spectrum of $HAuCl_4$ salt in physical contact with activated carbon

appeared to be stable under the conditions of UHV as compared with a similar sample which when exposed to the atmosphere, rapidly blackened, indicating reduction to the metal.

Another aspect of the reduction reaction under conditions of UHV is evident from the XPS spectra shown in Figures 3.26 and 3.27. Figure 3.26 shows the C(1s) spectra for the physical mixture of $HAuCl_4$, the adsorbed $AuCl_4^-/Au^0$, and an unreacted carbon sample. The physically mixed sample shows the presence of two types of carbon on the surface, whereas the adsorbed sample remains unchanged, as compared with the blank carbon. Figure 3.27 shows that the concentration of oxygen peak on the surface of the carbon, as measured by the intensity of the O(1s) peak, is much depleted, whereas that of the adsorbed sample is much the same as for the unreacted carbon. It is suggested that under UHV conditions, it is the chemisorbed oxygen on the carbon surface that reacts with the gold chloride, resulting in a reduced form of carbon also being evident from the XPS measurement.

g) *Fourier Transform Infrared Spectroscopic Study of Adsorbed Aurocyanide Species on Activated Carbon*

The only other reported infrared spectroscopic study of gold-loaded carbons[91] suffered from the fact that the spectrum of the virgin carbon[122] was inconsistent and could thus not be used as a baseline. The assignments of $\nu$(CN) bands in that work to $Au(CN)_2^-$ and AuCN are therefore dubious, being lower in intensity than most of the background peaks.

Clark *et al*[123] reported $\nu$(CN) for CuCN-loaded carbons at very high concentrations, and concluded that the species was present in the form of a surface-stabilized $Cu^+Cu(CN)_2^-$

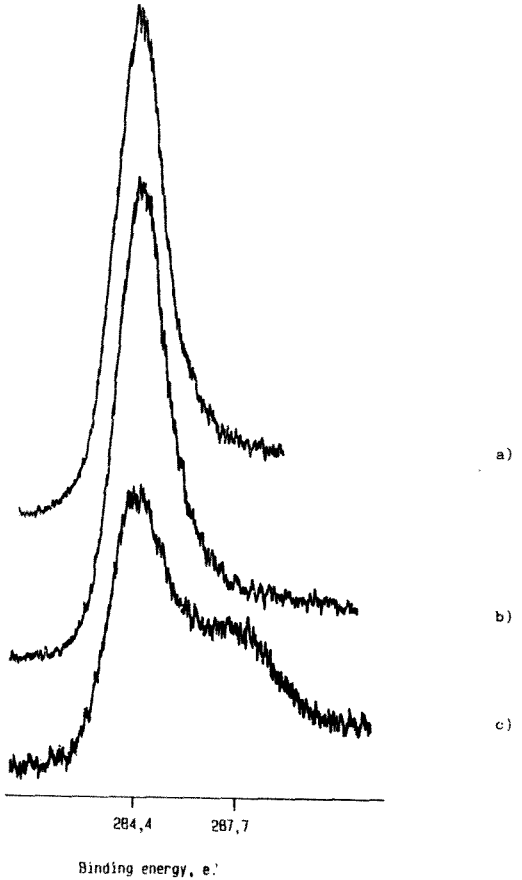


Fig. 3.26 C(1s) photoelectron spectra of
a) G210 activated carbon,
b) activated carbon contacted with a solution of $AuCl_4^-$ in 1,0M HCl, and
c) activated carbon in physical contact with $HAuCl_4$ salt

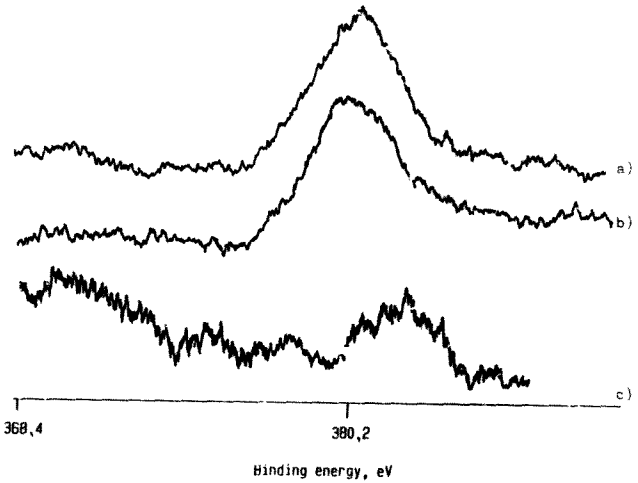


Fig. 3.27 O(1s) photoelectron spectra of

a) G210 activated carbon
b) activated carbon contacted with a solution of $AuCl_4^-$ in 1,0M HCl, and
c) activated carbon in physical contact with $HAuCl_4$ salt

species.

This section aims at presenting the results of the first self-consistent infrared spectroscopic study of aurocyanide-loaded activated carbon, and at contributing to further clarification of the adsorption mechanism.

To obtain absorption bands with significantly high signal-to-noise ratios, it proved necessary to load carbons up to somewhat higher levels (10 to 20 per cent Au) than those normally achieved in practice (1 to 2 per cent Au). Jones *et al*[111] have shown that a consistent adsorption isotherm is obtained over a range of between 2 and 60 per cent Au, that covers both of these concentration ranges. This suggests that the present results have general application. Moreover, the XPS studies presented in the previous section and elsewhere[79] have also examined this wide range of concentration, and it is of interest to compare the results of the two techniques.

(i) Effect of gold concentration on the carbon

The infrared spectra of carbons loaded from $KAu(CN)_2$ solution in the presence of excess KCl, are shown in Figure 3.28. The background spectrum of virgin carbon is clearly evident in the spectra of the loaded carbons. The presence of a band at about 2140 $cm^{-1}$ provides unequivocal evidence for the presence of $Au(CN)_2^-$, and the absence of any band in the 2250 to 2200 $cm^{-1}$ region suggests that no AuCN is present, as shown by comparison of $\nu$(CN) bands in Tables 3.18, 3.19 and 3.20. Both spectra are consistent with the presence of two distinct species, that adsorb at about 2138 $cm^{-1}$ and 2142 $cm^{-1}$, respectively. Moreover, it is evident that similar spectra are obtained over this range of loading concentrations.

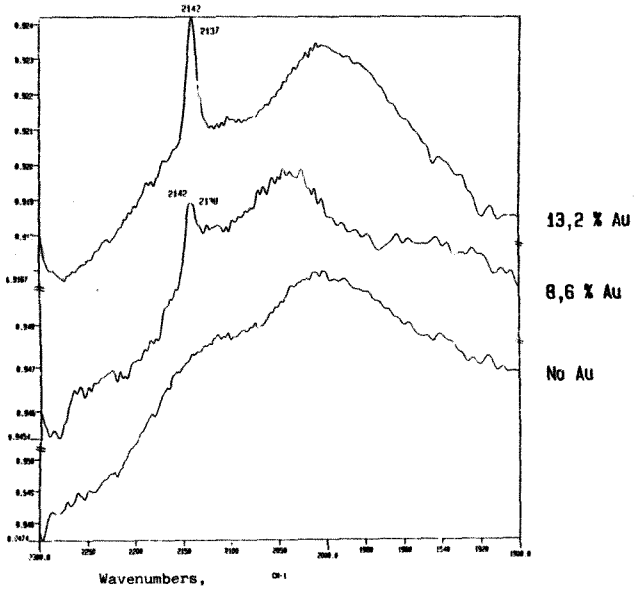


Fig. 3.28 Infrared spectra showing the CN stretch bands of $KAu(CN)_2$ on activated carbon at various concentrations. (Drying conditions : 25°C, *in vacuo*)

Table 3.18

**Infrared spectral data for solid aurocyanide salts**

| Salt | $\nu$(CN), $cm^{-1}$ | Ref. |
|---|---|---|
| $HAu(CN)_2$ | 2146 | 124 |
| | 2212 | 125 |
| $LiAu(CN)_2$ | 2152 | 126 |
| | 2159 | 90 |
| $NaAu(CN)_2$ | 2154 | 126,90 |
| $KAu(CN)_2$ | 2140 | 126 |
| | 2141 | 127 |
| | 2142 | 90 |
| $CsAu(CN)_2$ | 2159 | 90 |
| $NH_4Au(CN)_2$ | 2134 | 90 |
| | 2139 | 126 |
| $Bu_4Au(CN)_2$ | 2140 | 90 |
| $Be[Au(CN)_2]_2$ | 2165 | 90 |
| $Ca[Au(CN)_2]_2$ | 2162 | 90 |
| | 2142 | |
| AuCN | 2239 | 128 |
| $AgAu(CN)_2$ | 2209 | 126 |
| $TlAu(CN)_2$ | 2143 | 126 |
| | 2136 | |
| | 2125 | |

Table 3.19
Infrared spectral data for aurocyanide species in solution and adsorbed on ion-exchange resins

| Condition | ν(CN), $cm^{-1}$ | Ref. |
|---|---|---|
| Aqueous solution | | |
| $HAu(CN)_2$ | 2147 | 124 |
| $KAu(CN)_2$ | 2147 | 127 |
| Methyl ethyl ketone (MEK) solution | | |
| $LiAu(CN)_2$ | 2145<br>2152<br>2172<br>2177 | Chapter 4 |
| $NBu_4Au(CN)_2$ | 2145 | Chapter 4 |
| 1-Methyl-2-pyrrolidinone solution | | |
| $NaAu(CN)_2$ | 2143 | 126 |
| $KAu(CN)_2$ | 2142 | 126 |
| Adsorbed on ion-exchange resins | | |
| Dowex A-1 + $Au(CN)_2^-$ | 2138 | 127 |
| IRA-400 + $Au(CN)_2^-$ | 2142 | 90 |
| DOW XF-4149 + $Au(CN)_2^-$ | 2142 | 90 |

Table 3.20

**Infrared spectral data for aurocyanide species adsorbed on activated carbon**

| Cation | Gold on loaded carbon, % | Drying conditions (24h) | ν(CN), $cm^{-1}$ |
|---|---|---|---|
| $K^+$ | 13,2 | 25°C, *in vacuo* | 2142<br>2137 |
| $K^+$ | 8,6 | 25°C, *in vacuo* | 2142<br>2138 |
| $Cs^+$ | 18,9 | 25°C | 2140<br>2156 |
| | | 25°C, *in vacuo* | 2140 |
| | | 120°C | 2141<br>2156 |
| | 9,2 | 25°C, *in vacuo* | 2140 |
| | | 120°C | 2142 |
| $Ca^{2+}$ | 21,8 | 25°C | 2156 (s)<br>2141 (m) |
| | | 25°C, *in vacuo* | 2143 (s)<br>2162 (sh)<br>2152 (sh)<br>2167 (sh) |
| | | 120°C | 2143 (s)<br>2163 (sh)<br>2151 (sh)<br>2169 (sh) |
| $Li^+$ | 19,7 | 25°C | 2142 (s)<br>2157 (s)<br>2168 (m) |
| | | 25°C, *in vacuo* | 2142 (s)<br>2152 (sh)<br>2168 (sh) |
| | | 120°C | 2143 (s)<br>2151 (sh)<br>2170 (m) |
| | 9,3 | 25°C, *in vacuo* | 2142 (s)<br>2160 (sh)<br>2169 (m) |

### (ii) Effects of cation and drying conditions

Infrared spectra of an activated carbon loaded with aurocyanide from $Cs^+$ solution and dried under various conditions are shown in Figure 3.29. The strong band at 2140 $cm^{-1}$ that is evident after drying at 25°C decreases in intensity with relation to the band at 2156 $cm^{-1}$ as the carbon is dried at higher temperatures. The 2156 $cm^{-1}$ band is assigned to the solid $CsAu(CN)_2$ salt (see Table 3.18). The reason why only one band is observed in the case of $KAu(CN)_2$ (Figure 3.28) is that the $KAu(CN)_2$ salt absorbs at a very similar frequency (2141 $cm^{-1}$) to that of the free $Au(CN)_2^-$ (2142-2147 $cm^{-1}$) and to that of $Au(CN)_2^-$ loaded onto anion-exchange resins (2142 $cm^{-1}$).

Neither $K^+$ nor $Cs^+$ have sufficient polarizing power to significantly perturb the bonding within the aurocyanide anion. It is only small cations such as $Li^+$ that undergo a sufficiently high degree of orbital overlap with $Au(CN)_2^-$ to result in shifts in $\nu(CN)$, as evidenced by the spectra of LiNCS in organic solvents[129]. The present results are thus also consistent with the presence of $K^+Au(CN)_2^-$ and $Cs^+Au(CN)_2^-$ ion pairs on the wet activated carbon surface.

Figure 3.30 shows that at a somewhat lower concentration of gold on the carbon, only one band, at 2140 $cm^{-1}$, is observed, even after drying the carbon at 120°C for 24 hours. This is consistent with the assignment of the 2156 $cm^{-1}$ band to solid $CsAu(CN)_2$ salt, which evidently only occurs at very high gold loadings, and only on dry carbons.

Infrared spectra of an activated carbon loaded with aurocyanide (19,7 per cent Au) from $Li^+$ solution and dried under various conditions are shown in Figure 3.31. A strong band at 2142 $cm^{-1}$ is evident in all of the spectra. However, under drier conditions, the additional bands at 2154 $cm^{-1}$ and 2170 $cm^{-1}$ become more evident. Figure 3.32 shows that a similar spectrum is obtained even at a much

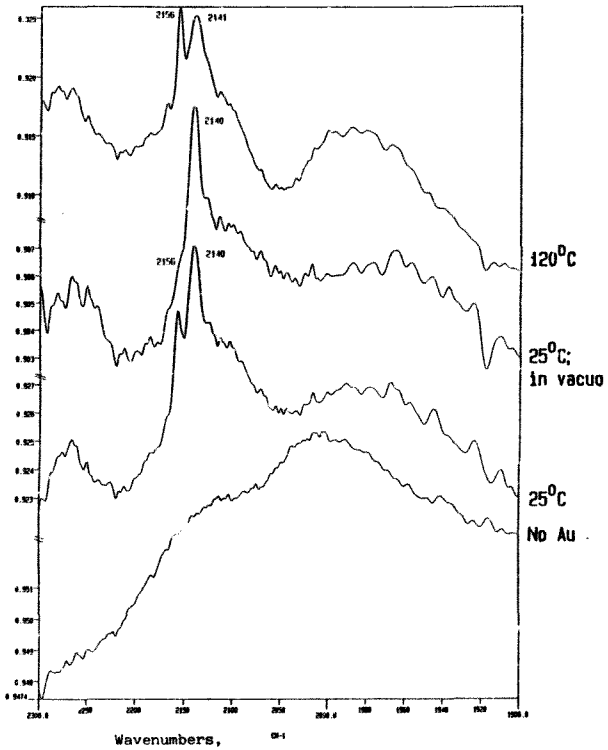


Fig. 3.29 Infrared spectra showing the CN stretch bands of $CsAu(CN)_2$ on activated carbon after drying under various conditions. (18,9 per cent Au on carbon)

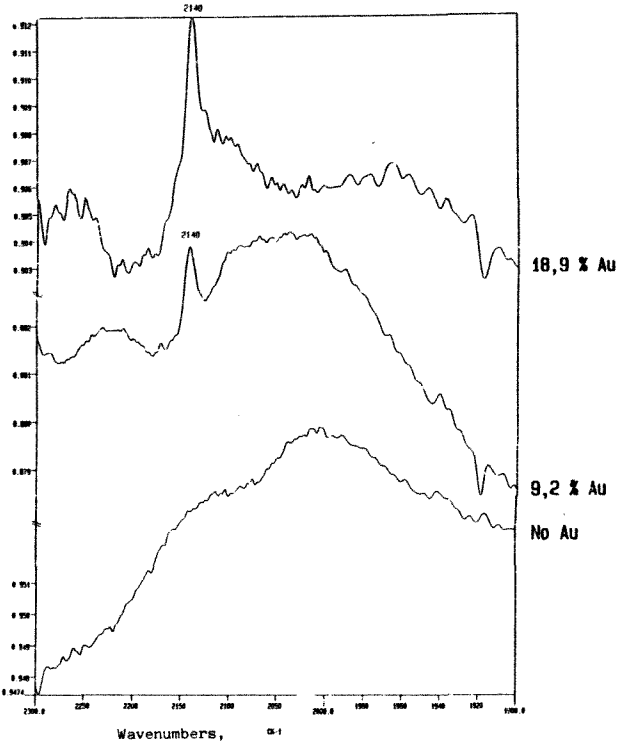


Fig. 3.30 Infrared spectra showing the CN stretch bands of $CsAu(CN)_2$ on activated carbon at various concentrations.

a) Dried at 25°C, *in vacuo*

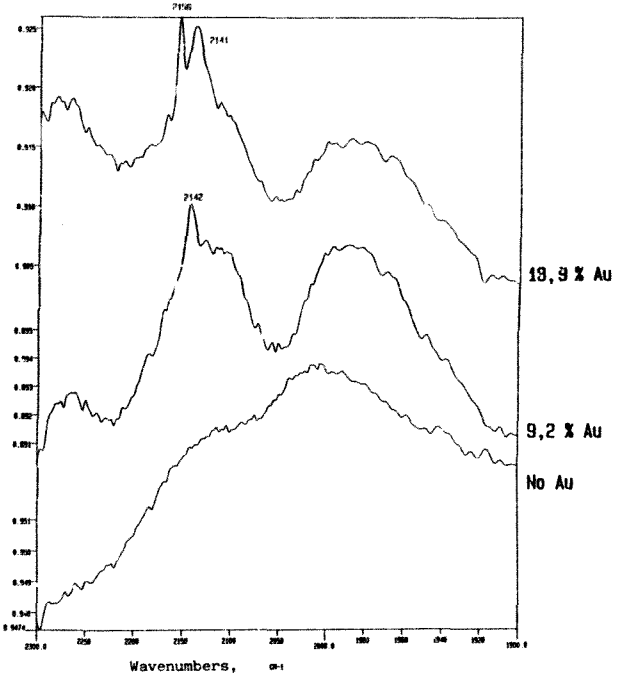


Fig. 3.30 Infrared spectra showing the CN stretch bands of $CsAu(CN)_2$ on activated carbon at various concentrations.

b) Dried at 120°C

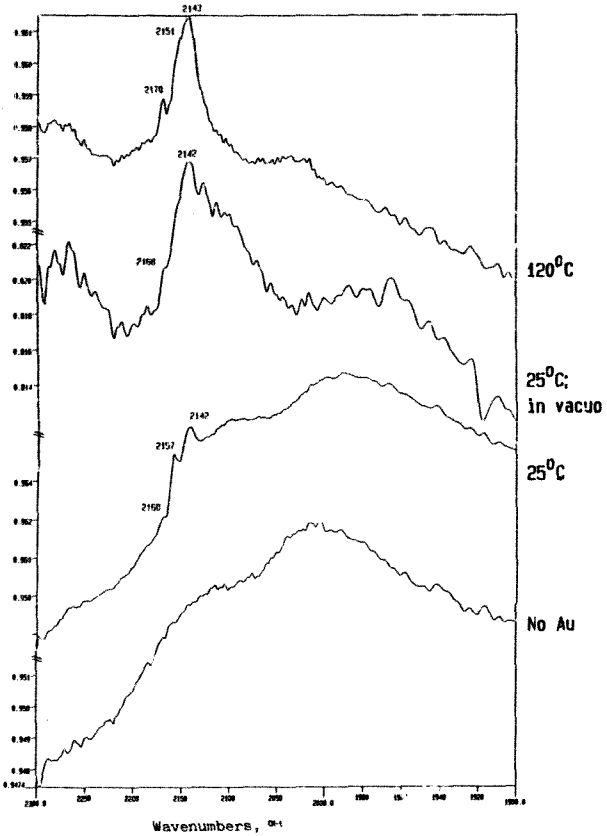


Fig. 3.31 Infrared spectra showing the CN stretch bands of $LiAu(CN)_2$ on activated carbon after drying with various conditions. (19,7 per cent Au on carbon)

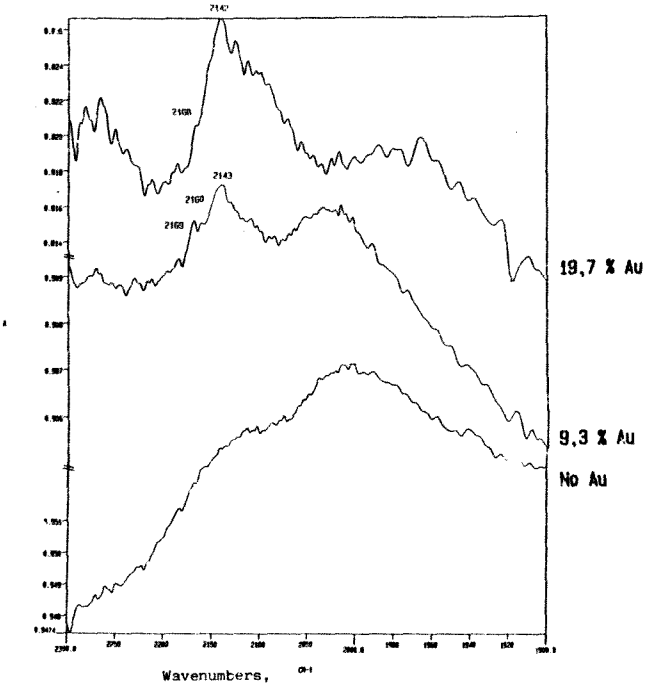


Fig. 3.32 Infrared spectrum showing the CN stretch bands of $LiAu(CN)_2$ on activated carbon at various concentrations. (Drying conditions : 25°C, *in vacuo*)

lower loading of gold on the carbon (9,3 per cent Au). Work to be presented in Chapter 4 shows that a similar pattern of $\nu$(CN) bands arise from solutions of $LiAu(CN)_2$ in certain organic solvents, as shown in Figure 3.33 for $LiAu(CN)_2$ in methyl ethyl ketone. In this instance, the bands are assigned (see Chapter 4) to the free ion or solvent-separated ion pair (2145 $cm^{-1}$), contact ion pair (2152 and 2177 $cm^{-1}$) and contact dimer (2172 $cm^{-1}$). The spectra in Figure 3.30 for $LiAu(CN)_2$ on activated carbon are not easily attributable to the formation of the solid $LiAu(CN)_2$ salt, since this would not explain the marked enhancement in the 2170 $cm^{-1}$ peak intensity under drier conditions. Moreover, $LiAu(CN)_2$ is soluble[130] to the order of 7 mol/l in water, and is very hygroscopic. The effect of drying on the spectrum is thus postulated to be due to more favourable conditions for ion association when less water is present, rather than to the precipitation of solid $LiAu(CN)_2$ salt, and the fact that the spectrum remains unchanged at lower gold loadings, in contrast to the situation with $CsAu(CN)_2$, is also consistent with this suggestion. Moreover, activated carbons tend to rapidly adsorb atmosphere moisture[24]. High-temperature activated carbons are well known[24,131] to contain a preponderance of oxygen-containing functional groups such as phenols and carbonyls and these would undoubtedly be able to solvate species such as $LiAu(CN)_2$ in a manner akin to that of solvents such as methyl ethyl ketone.

Infrared spectra of an activated carbon loaded with aurocyanide from $Ca^{2+}$ solution and dried under various conditions are shown in Figure 3.34. The spectra are complex, with bands at 2143, 2153, 2162 and 2168 $cm^{-1}$ being present in the dried carbons. The bands at 2143 and 2162 $cm^{-1}$ are assigned to the solid $Ca[Au(CN)_2]_2$ salt, and those at 2153 and 2168 $cm^{-1}$ are possibly manifestations of ion association effects. The 2143 $cm^{-1}$ band probably also contains a component due to free $Au(CN)_2^-$ ions. The fact that the 2162 and 2168 $cm^{-1}$ bands are absent in the spectrum

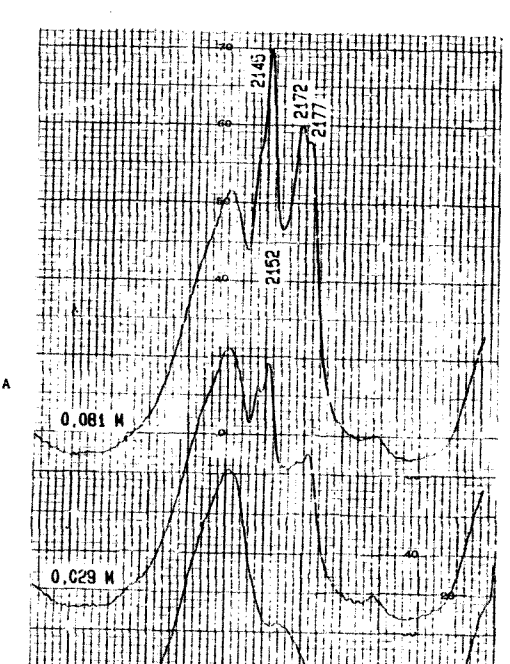


Fig. 3.33 Infrared spectra showing the CN stretch bands of $LiAu(CN)_2$ in methyl ethyl ketone at various concentrations

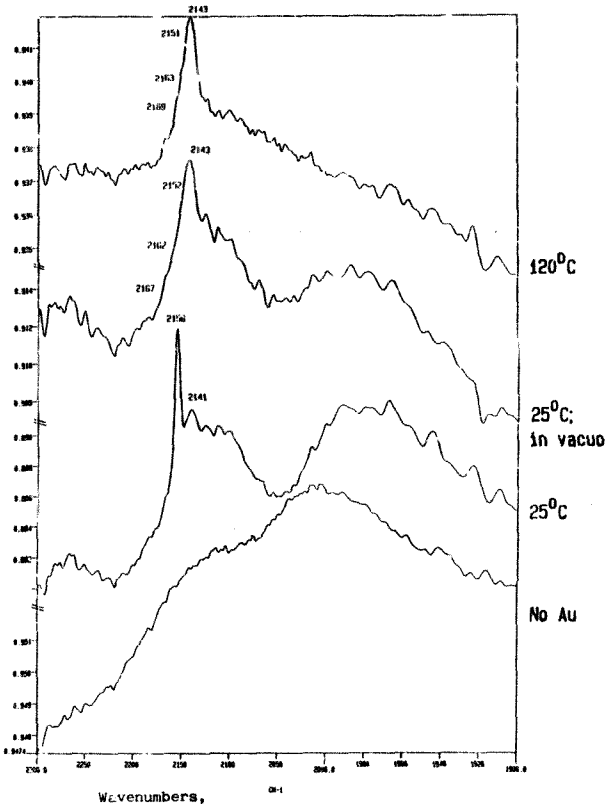


Fig. 3.34 Infrared spectra showing the CN stretch bands of $Ca[Au(CN)_2]_2$ on activated carbon after drying under various conditions. (21,8 per cent Au on carbon).

of the carbon dried at 25°C, is consistent with this assignment.

## 3.3 Mechanisms of Adsorption of Other Complex Metal-ion Species onto Activated Carbon

An important test of the ion-pair mechanism of adsorption of aurocyanide species onto activated carbon is its applicability to other adsorption processes, as well as to the adsorption of other complex metal-ion species onto carbon. In previous work[80,132,133], aurocyanide was proposed to be adsorbed onto polymeric adsorbents by a similar mechanism, and more recently[134] onto certain weak-base ion-exchange resins from alkaline solution by an ion-pair mechanism. In studies of adsorption of the complexes of gold with thiourea[135] and thiocyanate[136] onto activated carbon, the evidence indicates that both species are adsorbed as ion pairs. This conclusion is particularly interesting in the case of the gold thiourea complex, which is positively-charged, having the form $Au(SC(NH_2)_2)_2^+$.

### a) *The Mechanism of Adsorption of $Au(CN)_4^-$ onto Activated Carbon*

The adsorption of the gold (III) cyanide species, $Au(CN)_4^-$, onto activated carbon, has thus far never been reported. This species is not normally present in gold plant leach liquors, but a study of the adsorption of $Au(CN)_4^-$ onto carbon was undertaken to obtain further insight into the mechanism of adsorption of $Au(CN)_2^-$ onto carbon, and to explain the high degree of selectivity of $Au(CN)_2^-$ over other anions.

(i) Adsorption of $Au(CN)_2^-$ and $Au(CN)_4^-$ onto activated carbon

Extraction efficiencies of the two species by activated carbon in the presence of various cations, are shown in Table 3.21.

Effects of cation type and ionic strength on extraction of $Au(CN)_4^-$ closely parallel those for $Au(CN)_2^-$, and are also consistent with the adsorption of an ion-pair species:

$$M^{n+} (aq) + n\ Au(CN)_4^- (aq) \rightleftharpoons M^{n+}[Au(CN)_4^-]_n (ads) \quad (3.36)$$

**Table 3.21**
**Extraction of $Au(CN)_2^-$ and $Au(CN)_4^-$ by activated carbon**

Conditions: Carbon mass 0,25g
Solution volume 100 ml
Initial gold in solution 300 mg/ℓ
Ionic strength 0,1 mol/kg

| Loading Conditions | Extraction Efficiency, % (/0,1 g) | | | |
|---|---|---|---|---|
| | After 1 hour | | After 20 hours | |
| | $Au(CN)_2^-$ | $Au(CN)_4^-$ | $Au(CN)_2^-$ | $Au(CN)_4^-$ |
| No Additives | 8,3 | 8,8 | 16,4 | 26,8 |
| 0,1 M KCl | 13,2 | 13,3 | 27,8 | 32,1 |
| 0,033 M $CaCl_2$ | 17,4 | 15,9 | 32,7 | 35,8 |
| 0,1 M HCl | 35,1 | 53,1 | 79,4 | 99,3 |

At increased $M^{n+}$ concentrations, the equilibrium is shifted to the right, resulting in enhanced adsorption. The trend of increasing adsorption in the sequence,

$$\text{no additive} < K^{+} < Ca^{2+} < H^{+}$$

is also consistent with an ion-pair mechanism, as discussed previously[62].

Extraction efficiencies for $Au(CN)_4^-$ are consistently higher than those for $Au(CN)_2^-$, both after one hour and twenty hours. This is once again consistent with the ion-pair mechanism[62], because larger ions, such as $Au(CN)_4^-$, tend to be less hydrated and more polarizable, and both of these factors impart a greater affinity for ion-pair extraction into a hydrophobic phase. A similar enhancement of $Au(CN)_4^-$ extraction over $Au(CN)_2^-$ extraction, as an ion pair of tetrahexylammonium into hexone, is demonstrated in Table 3.22. In fact, the sequence of extraction

$$Au(CN)_2^- > Ag(CN)_2^- > Zn(CN)_4^{2-} > Ni(CN)_4^{2-}$$

is also similar to that reported[11] for the adsorption of these ions onto activated carbon.

**Table 3.22**
**Extraction constants for complex cyanides from aqueous solution at 25°C by tetrahexylammonium erdmannate in hexone**
**(After Irving and Damodaran[137])**

| Anion, $X^-$ | Extraction constant $K_{X^-}$ |
|---|---|
| $Au(CN)_4^-$ | 165 |
| $Au(CN)_2^-$ | 15,8 |
| $Ag(CN)_2^-$ | 0,38 |
| $Zn(CN)_4^{2-}$ | $4,5 \times 10^{-4}$ |
| $Ni(CN)_4^{2-}$ | $0,11 \times 10^{-4}$ |

### (ii) Nature of the adsorbed species

The $Au(CN)_4^-$ ion has a formation constant $\beta_4 \sim 10^{56}$ and is thus exceedingly stable. From basic thermodynamic data, the following standard reduction potentials can be calculated:

$$Au(CN)_4^- + 3e^- \rightleftharpoons Au + 4CN^- \qquad (E^\circ = -1,81V) \qquad (3.37)$$

$$Au(CN)_4^- + 2e^- \rightleftharpoons Au(CN)_2^- + 2CN^- \qquad (E^\circ = -1,24V) \qquad (3.38)$$

These values can be compared with that for the $Au(CN)_2^-$ ion,

$$Au(CN)_2^- + e^- \rightleftharpoons Au + 2CN^- \qquad (E^\circ = -0,61V) \qquad (3.39)$$

as well as the value of $E^\circ \sim 0,24$ V found[32] for typical activated carbons. It is therefore unlikely that reduction of adsorbed $Au(CN)_4^-$ species occurs.

Analyses of carbons loaded with $Au(CN)_4^-$ under neutral and alkaline conditions for potassium, gold and nitrogen are shown in Table 3.23 below:

**Table 3.23**
**Analyses of $Au(CN)_4^-$ loaded carbons**

| Loading Conditions | Concentration, mmol/g | | |
|---|---|---|---|
| | K | Au | N/4 |
| 0,1M KCl | 0,307 | 0,219 | 0,224 |
| 0,1M HCl | - | 0,194 | 0,183 |

Adsorption of chemically unchanged $KAu(CN)_4$ and $HAu(CN)_4$ species is indicated from these results. This is consistent with the ion-pair mechanism, shown in Equation (3.36).

**Table 3.24**

**Values of isomer shift (IS) and quadrupole splitting (QS) for Mössbauer spectra of gold samples**

| Absorber | IS mm/s | QS mm/s | Ref. |
|---|---|---|---|
| *Carbons* | | | |
| Carbon loaded with $Au(CN)_4^-$ from 0,1M KCl | 4,03 | 7,18 | This work |
| Carbon loaded with $Au(CN)_4^-$ from 0,1M HCl | 4,10 | 7,02 | This work |
| Sample 1, boiled in 4% HCl for 4 hours | 3,30<br>2,73<br>3,48 | 9,93<br>8,78<br>5,90 | This work |
| *Reference spectra* | | | |
| $KAu(CN)_4$ | 4,2 | 6,9 | 42 |
| $KAu(CN)_2$ | 3,05<br>3,23<br>3,10<br>3,12 | 9,80<br>10,21<br>10,21<br>10,21 | 44 |
| AuCN | 2,3 | 8,0 | 39 |
| $KAu(CN)_2Cl_2$ | 2,56 | 5,26 | 42 |
| $KAuCl_4$ | 2,05<br>2,02<br>1,65 | 1,26<br>1,11<br>1,27 | 42<br><br>44 |
| $HAuCl_4.4H_2O$ | 1,87 | 0,94 | 42 |
| Au | -1,23 | 0 | 39 |

Mössbauer spectra of the samples appearing in Table 3.23, viz., loaded from 0,1M KCl and 0,1M HCl solutions, are shown

in Figures 3.35 and 3.36 respectively. Values of IS and QS for these spectra, together with some relevant literature values, are shown in Table 3.24.

Comparison with literature values for the Mössbauer parameters of crystalline $KAu(CN)_4$ provides further evidence that the only adsorbed species is in the form of $Au(CN)_4^-$, when loaded from both neutral and alkaline solution. The slight asymmetry can possibly be explained by the adsorption of the species over a range of active sites on the carbon surfaces.

Additional information can be obtained from the Mössbauer spectrum of a carbon loaded with $Au(CN)_4^-$ that was subsequently boiled in 4% HCl (See Figure 3.37). At least three sets of quadrupoles were required to fit the spectrum satisfactorily. The most intense quadrupole has values of IS and QS that lie between those for $Au(CN)_4^-$ and $Au(CN)_2Cl_2^-$ (See Table 3.24) and it is likely that a better fit would be obtained if both of these quadrupoles were assigned to it. The two less intense quadrupole splittings have parameters that correlate well with those for crystalline $KAu(CN)_2$ and AuCN. The acid treatment thus results in a complex mixture of gold(III) and gold(I) species, viz $Au(CN)_2Cl_2^-$, $Au(CN)_4^-$, $Au(CN)_2^-$ and AuCN, the relative amounts of which are uncertain, due to uncertainties in Debye-Waller factors of adsorbed species. The following set of reactions could account for this observation:

$$Au(CN)_4^- + 2H^+ + 2Cl^- \rightarrow Au(CN)_2Cl_2^- + 2HCN(\uparrow) \qquad (3.40)$$

$$Au(CN)_2Cl_2^- + 2e^- \rightleftharpoons Au(CN)_2^- + 2Cl^- \qquad (3.41)$$

$$Au(CN)_2^- + H^+ \rightleftharpoons AuCN + HCN\ (\uparrow) \qquad (3.42)$$

The ratio of nitrogen to gold on the acid-boiled carbon was

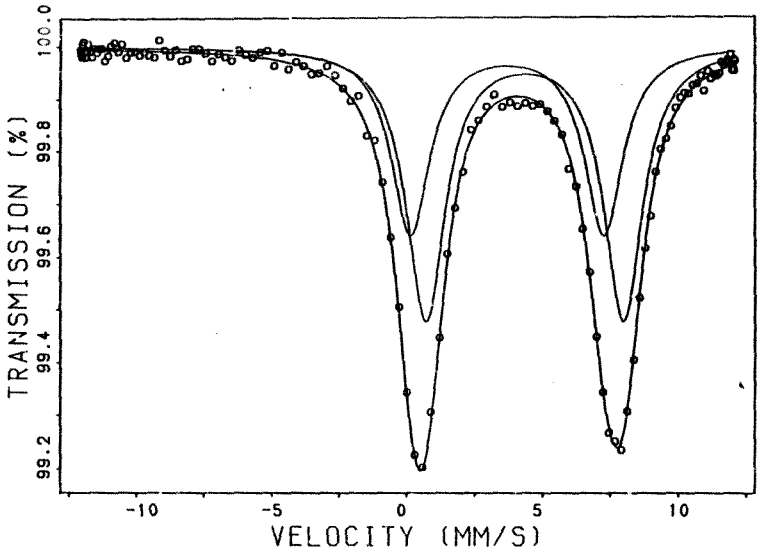


Fig. 3.35 $^{197}$Au Mössbauer spectrum of activated carbon loaded from $Au(CN)_4^-$ solution containing 0,1M KCl

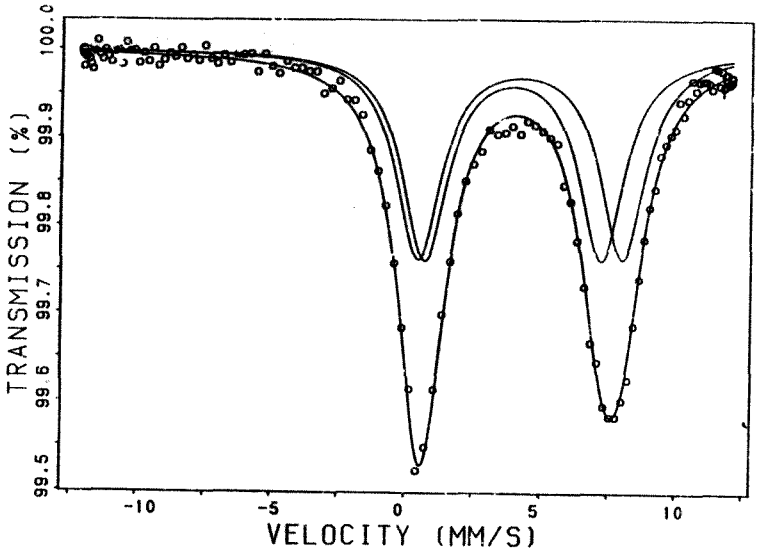


Fig. 3.36 $^{197}$Au Mössbauer spectrum of activated carbon loaded from $Au(CN)_4^-$ solution containing 0,1M HCl

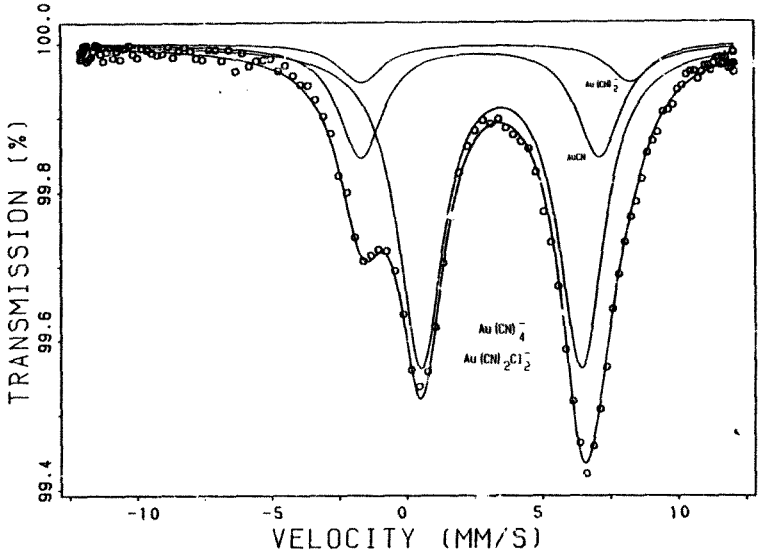


Fig. 3.37 $^{197}$Au Mössbauer spectrum of activated carbon loaded from $Au(CN)_4^-$ solution and subsequently boiled in 4% hydrochloric acid for four hours

measured by elemental analysis, and found to be N/Au = 1,95. This is consistent with the reaction scheme presented above, assuming $Au(CN)_2Cl_2^-$ and $Au(CN)_2^-$ to be the predominant species present.

*b) The Mechanisms of Adsorption of $Ag(CN)_2^-$ and $Ag^+$ onto Activated Carbon*

Adsorption of silver species onto activated carbons finds application in two main areas: (i) recovery of silver by adsorption of $Ag(CN)_2^-$ onto activated carbon from cyanide leach liquors and pulps, and (ii) preparation of carbon-supported metal catalysts. The recovery of silver by activated carbon normally occurs together with that of gold in the carbon-in-pulp process.

The mechanism of adsorption of silver onto activated carbon from cyanide solution is a topic that has not received much attention recently, unlike the preponderance of literature that has been published on the mechanism of adsorption of gold onto activated carbon from cyanide solution. The disagreement between researchers regarding this topic[73,74,91] is added incentive for the study of $Ag(CN)_2^-$ adsorption onto activated carbon, by affording a useful comparison with $Au(CN)_2^-$ adsorption.

In the first studies of the adsorption of $Ag(CN)_2^-$ onto activated carbon[138,139], a parallel behaviour to the $Au(CN)_2^-$ adsorption was discovered, and this was subsequently confirmed more recently by Tsuchida and Muir[73,74], who suggested adsorption by ion exchange onto oxygen-containing surface functional groups, followed by oxidative decomposition to AgCN. In the most recent work, Ibrado and Fuerstenau[140] postulate that silver adsorbs as the negatively-charged complex $Ag(CN)_2^-$ without being chemically bound to the co-adsorbed cation, without attempting to explain the adsorption mechanism *per se*.

Carbon-supported silver catalysts have been investigated[141] as potential catalysts for the hydrochlorination of acetylene in the production of vinyl chloride monomer (VCM). Moreover, silver nitrate has been used in metal-impregnated activated carbons for the adsorption of toxic gases[142,143] such as cyanogen chloride and hydrocyanic acid.

The mechanism of adsorption of silver onto activated carbon from nitrate[144] or ammonia[145,146] solutions is a less controversial topic than that from cyanide solutions. In these instances, the silver is postulated to be present as a mixture of silver metal and $AgNO_3$ or $Ag(NH_3)_2NO_3$. The nature of the adsorbates and of the reactions involved have not been dealt with in any detail, however.

The aim of the present section is to elucidate the mechanisms of adsorption of silver onto activated carbon from cyanide and nitrate solutions, so that an improved understanding of all the above-mentioned processes can be attained.

(i) Mechanism of adsorption of $Ag(CN)_2^-$ onto activated carbon

Stoichiometry of the adsorbate

Silver was loaded onto activated carbon from $KAg(CN)_2$ solutions of two different ionic strengths. The carbons were subsequently analysed for potassium, silver and nitrogen, and the results are shown in Table 3.25.

The stoichiometry of the adsorbed species corresponds to that required for the presence of $KAg(CN)_2$, when loaded from both high and low ionic strength solutions. Moreover, the increase in loading achieved at the higher potassium

concentration is consistent with a forward shift in the equilibrium

$$K^+ (aq) + Ag(CN)_2^- (aq) \rightleftharpoons K^+Ag(CN)_2^- (ads) \qquad (3.43)$$

These results parallel those for the adsorption of $Au(CN)_2^-$ onto activated carbon, and suggest that an ion-pair adsorption mechanism also prevails for $Ag(CN)_2^-$ adsorption. This is also consistent with previous work[62,138] on the effect of ionic strength on the adsorption of $Ag(CN)_2^-$ onto carbon.

Table 3.25
**Analyses of K, Ag and N on activated carbon loaded with silver from $KAg(CN)_2$ solution.**

| Loading conditions | Concentration, mmol/g | | |
|---|---|---|---|
| | K | Ag | ½N |
| No additives | 0,102 | 0,138 | 0,104 |
| 0,1 M KCl | 0,192 | 0,210 | 0,255 |

A value of $E^0 = -0,382$ V can be calculated for the standard reduction potential (as measured against the Standard Hydrogen Electrode (SHE), for the reduction of $Ag(CN)_2^-$:

$$Ag(CN)_2^- + e^- \rightleftharpoons Ag^0 + 2CN^- \qquad (3.44)$$

(This value was calculated from the value[147] of $\beta_2 = 10^{20}$ for $Ag(CN)_2^-$ and the standard reduction potential of $Ag^+$ (0,800V)[146]). Reduction potentials of activated carbons have been found[32] to lie between 0,40 and 0,08V, so argentocyanide would not be expected to be reduced by activated carbon, and this is consistent with the results shown in Table 3.25. It is also noteworthy that no metallic

silver, AgCN or AgCl could be detected on these carbons by XRD.

### Infrared spectrophotometric study of adsorbed $Ag(CN)_2^-$ species

Infrared spectra showing the $\nu$(CN) stretching frequencies for $Ag(CN)_2^-$ loaded carbons that were dried under various conditions, are shown in Figure 3.38. Observed values for adsorbed species are compared with those for free species in Table 3.26.

Table 3.26
$\nu$(CN) stretching frequencies for silver cyanide species

| Species | Drying conditions | $\nu$(CN), $cm^{-1}$ | Ref. |
|---|---|---|---|
| Carbon contacted with $KAg(CN)_2$ solution | 25°C; 24 h | 2089 | This work |
| | 120°C; 24 h | 2090<br>2170 | |
| | 180°C; vacuum dried 24h | 2170<br>2090 | |
| AgCN (s) | | 2164<br>2178 | 126<br>148 |
| $KAg(CN)_2$ (s) | | 2139 | 126 |
| $K_3Ag(CN)_4$ (s) | | 2097 | 126 |
| $Ag(CN)_2^-$ (aq) | | 2135 | 126 |
| $Ag(CN)_3^{2-}$ (aq) | | 2105 | 126 |
| $Ag(CN)_4^{3-}$ (aq) | | 2092 | 126 |

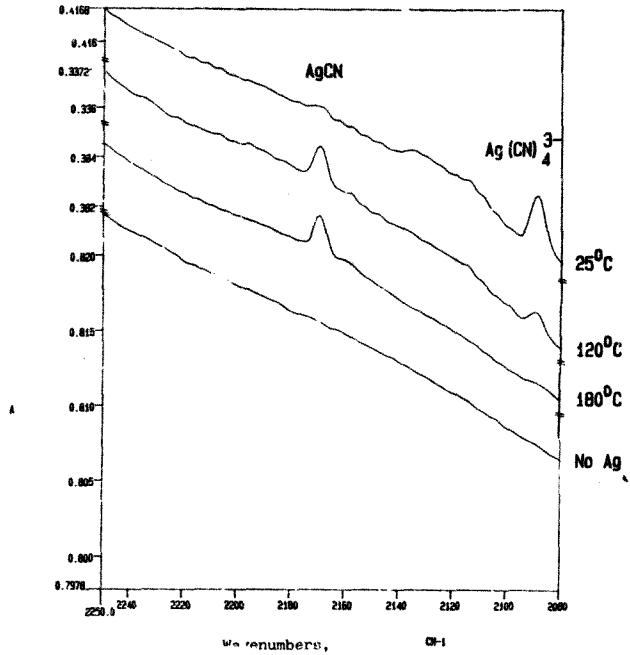


Fig. 3.38 Infrared spectra showing ν(CN) for silver cyanide species adsorbed on activated carbons from 0,1M KCl solution after various drying treatments

In the present work, a $\nu$(CN) band was observed at 2089 $cm^{-1}$ on carbons loaded with $KAg(CN)_2$ solution and left to dry at room temperature. This band is attributable to the $Ag(CN)_4^{3-}$ species. No band due to $Ag(CN)_2^-$ is evident. A possible explanation for this strange result is that the following reaction occurs on the carbon surface:

$$2Ag(CN)_2^- \rightleftharpoons Ag^+ + Ag(CN)_4^{3-} \qquad (3.45)$$

Clark *et al*[123] provide IR spectroscopic evidence for a similar reaction occurring when CuCN is adsorbed onto activated carbons at high loadings:

$$2CuCN \rightleftharpoons Cu^+ + Cu(CN)_2^- \qquad (3.46)$$

They postulate the individual ions to be "trapped on the surface of the support where they are effectively individually complexed (and hence stabilized) by surface -OH groups".

The driving force for reaction (3.45) is possibly surface complexation of $Ag^+$ ions or precipitation of AgCl. It is also possible that the driving force is reduction of $Ag^+$ to metallic silver, as occurs when $AgNO_3$ is contacted with carbon. It is not possible on the basis of the current results to unequivocally prove one of these reactions due to the absence of peaks in the X-ray diffractogram, which could be indicative of the presence of very small particles.

At increasingly high drying temperatures, an additional band at 2170 $cm^{-1}$ species appears, that is attributable to solid AgCN. This species presumably results from the loss of cyanide as HCN,

$$Ag^+ + Ag(CN)_4^{3-} + 2H_2O \xrightarrow{\Delta} 2AgCN(\downarrow) + 2HCN(\uparrow) + 2OH^- \qquad (3.47)$$

This reaction is similar to the one discussed in section 3.2d, in the case of $Au(CN)_2^-$ loaded carbons that are heated to somewhat higher temperatures of about 250°C, i.e.

$$Au(CN)_2^- + H_2O \xrightarrow{\Delta} AuCN(\downarrow) + HCN(\uparrow) + OH^- \qquad (3.48)$$

The $Au(CN)_2^-$ species is more stable than the silver cyanide complexes, which explains its higher thermal stability.

Effect of cyanide concentration

The effect of increasing cyanide concentration on extraction of silver is shown in Figure 3.39.

Extraction of silver from the solution steadily drops from 86% when no extra cyanide is added, to only 5% in the presence of 1,0 mol/l $CN^-$. An explanation for this effect is obtained by a comparison of Figure 3.39 with Figure 3.40, which shows distribution of silver cyanide species with increasing cyanide concentration, calculated using the HALTAFALL[149] program on an IBM PC II personal computer. The similarity between the curve for the $Ag(CN)_2^-$ species in Figure 3.40 and that for extraction of silver by activated carbon in Figure 3.39 is further evidence that silver is adsorbed as $Ag(CN)_2^-$ from cyanide solution, even when high concentrations of free cyanide are present. Lorado and Fuerstenau[140] have previously postulated that $Ag(CN)_2^-$ is the adsorbed species, on the basis that $Ag(CN)_2^-$ was calculated to be the predominant solution species in their experiment. The present work corroberates their work and moreover, provides a sounder correlation, since the $Ag(CN)_3^{2-}$ and $Ag(CN)_4^{3-}$ complexes were also present in substantial proportions in the present experiments.

The fact that the doubly negatively-charged $Ag(CN)_3^{2-}$ and triply negatively-charged $Ag(CN)_4^{3-}$ species are not adsorbed onto activated carbon to any significant extent,

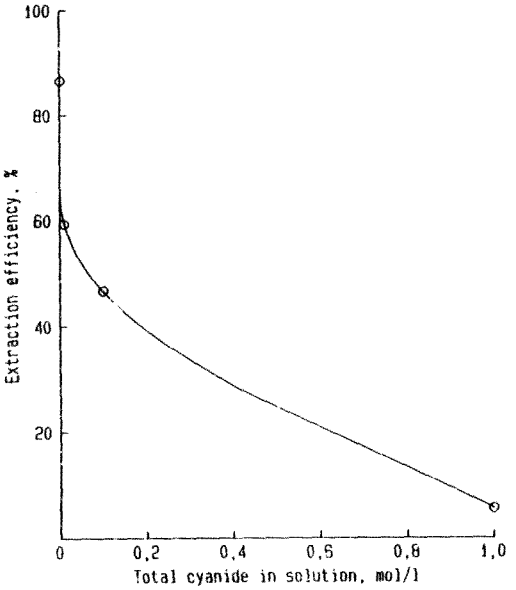


Fig. 3.39 Effect of cyanide concentration on the extraction efficiency of activated carbon for silver

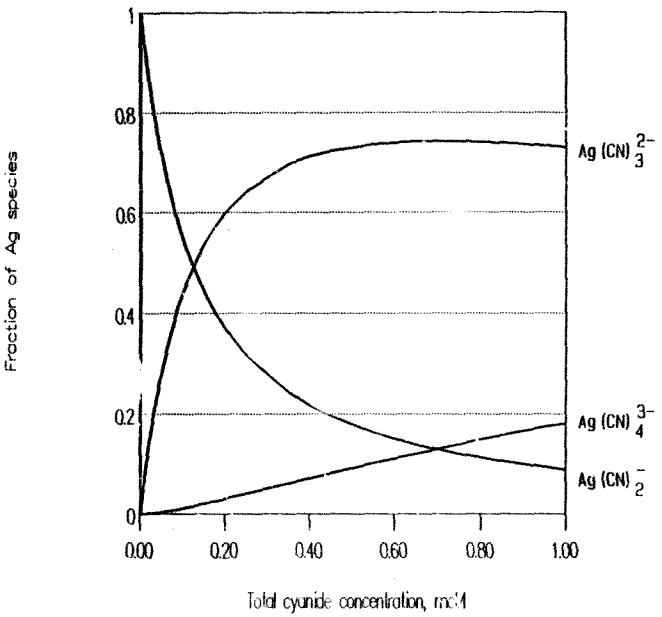


**Fig. 3.40** **Distribution of silver species in cyanide solution with increasing total cyanide concentration. (pH ~ 11; unadjusted)**

is consistent with the current theory of ion-pair adsorption. Multiply-charged anions are hydrated to a much greater extent, resulting in a lower affinity for a hydrophobic phase such as activated carbon[146,150].

These results are an apparent contradiction of the infrared spectrophotometric results, which suggested that $Ag(CN)_2^-$ anions may be adsorbed as $Ag^+$ and $Ag(CN)_4^{3-}$ - the latter species has just been shown to be poorly adsorbed. This anomaly could be explained by the fact that $Ag^+$ ions are complexed far more strongly by oxygen donor ligands such as poly(oxyethylene) groups[151] than are $K^+$ ions. This means that surface-complexed $Ag^+$ ions provide effective anion-exchange sites for the $Ag(CN)_4^{3-}$, which will thus be strongly bound to the carbon in the presence of $Ag^+$ ions, but not in their absence. Poly(oxyethylene) ligands coordinate cations by wrapping around the ion in a helical fashion (see Section 4.6), and it is considered that a similar situation occurs within the micropores of activated carbon, which contain a preponderance of oxygen-containing functional groups. Alternatively, the effect may result from the drying process.

Effect of acid and base treatments

The results in Section 3.2c indicated that boiling aurocyanide-loaded carbon in 4% HCl for several hours resulted in the conversion of aurocyanide to the insoluble AuCN polymer in some or other form:

$$Au(CN)_2^- \text{ (ads)} + H^+ \text{ (aq)} \rightarrow AuCN \text{ (ads)} + HCN(\uparrow) \quad (3.49)$$

Subsequent treatment of this carbon with boiling 0,1 M sodium hydroxide solution resulted in the reduction of the AuCN, forming $Au(CN)_2^-$ and metallic gold, e.g.:

$$2AuCN + e^- \rightarrow Au + Au(CN)_2^- \quad (3.50)$$